AD-A095 170 ACUREX CORP/AEROTHERM MOUNTAIN VIEW CA AEROSPACE SY--ETC F/G 18/3
SUMMARY REPORT. HYBLA GOLD EVENT.(U)
NOV 79 J R STOCKTON
UNCLASSIFIED ACUREX-FR-79-15-/AS(6988) DNA-5107F DNA001-79-C-0404 NL

1 OF 2
AD A095170

DNA 5107F

SUMMARY REPORT
HYBLA GOLD EVENT

Acurex Corporation
485 Clyde Avenue
Mountain View, California 94042

1 November 1979

Final Report for Period 7 July 1979—1 September 1979

CONTRACT No. DNA 001-79-C-0404

APPROVED FOR PUBLIC RELEASE;
DISTRIBUTION UNLIMITED.

THIS WORK SPONSORED BY THE DEFENSE NUCLEAR AGENCY
UNDER RDT&E RMSS CODE B345079462 J24AAXYX96006 H2590D.

Prepared for
Director
DEFENSE NUCLEAR AGENCY
Washington, D. C. 20305

Destroy this report when it is no longer needed. Do not return to sender.

PLEASE NOTIFY THE DEFENSE NUCLEAR AGENCY, ATTN: STTI, WASHINGTON, D.C. 20305, IF YOUR ADDRESS IS INCORRECT, IF YOU WISH TO BE DELETED FROM THE DISTRIBUTION LIST, OR IF THE ADDRESSEE IS NO LONGER EMPLOYED BY YOUR ORGANIZATION.

UNCLASSIFIED

SECURITY CLASSIFICATION OF THIS PAGE *(When Data Entered)*

19 REPORT DOCUMENTATION PAGE		READ INSTRUCTIONS BEFORE COMPLETING FORM
1. REPORT NUMBER DNA 5107F	2. GOVT ACCESSION NO. AD-A095	3. RECIPIENT'S CATALOG NUMBER 470
4. TITLE *(and Subtitle)* SUMMARY REPORT. HYBLA GOLD EVENT.		5. TYPE OF REPORT & PERIOD COVERED Final Report for Period 7 Jul 79—1 Sep 79
		6. PERFORMING ORG. REPORT NUMBER FR-79-15/ASY, Project 6988
7. AUTHOR(s) Jerry R. Stockton		8. CONTRACT OR GRANT NUMBER(s) DNA 001-79-C-0404
9. PERFORMING ORGANIZATION NAME AND ADDRESS Acurex Corporation 485 Clyde Avenue Mountain View, California 94042		10. PROGRAM ELEMENT, PROJECT, TASK AREA & WORK UNIT NUMBERS Subtask J24AAXYX960-06
11. CONTROLLING OFFICE NAME AND ADDRESS Director Defense Nuclear Agency Washington, D.C. 20305		12. REPORT DATE 1 November 1979 13. NUMBER OF PAGES 154
14. MONITORING AGENCY NAME & ADDRESS *(if different from Controlling Office)* 14 AC [illegible] X-F[illegible]-79-[illegible]		15. SECURITY CLASS *(of this report)* UNCLASSIFIED 15a. DECLASSIFICATION/DOWNGRADING SCHEDULE N/A

16. DISTRIBUTION STATEMENT *(of this Report)*

Approved for public release; distribution unlimited.

17. DISTRIBUTION STATEMENT *(of the abstract entered in Block 20, if different from Report)*

18. SUPPLEMENTARY NOTES

This work sponsored by the Defense Nuclear Agency under RDT&E RMSS Code B345079462 J24AAXYX96006 H2590D.

19. KEY WORDS *(Continue on reverse side if necessary and identify by block number)*

Instrumentation	UGT
Radiation	MX Trench
Blast and Shock	Plasma Flow
HYBLA GOLD	Nuclear Shock Tube

20. ABSTRACT *(Continue on reverse side if necessary and identify by block number)*

The HYBLA GOLD experiment was designed to increase our understanding of the phenomenology of the MX in-trench environment and to improve our confidence in making predictions of this environment.

The HYBLA GOLD experiment satisfied most of the original objectives. Useful data was obtained for the purpose of developing and validating instrumentation which might be required in future underground nuclear tests. In general,

DD FORM 1 JAN 73 1473 EDITION OF 1 NOV 65 IS OBSOLETE

UNCLASSIFIED

SECURITY CLASSIFICATION OF THIS PAGE *(When Data Entered)*

A 10134

20. ABSTRACT (Continued)

the instrumentation fielded to measure shock time-of-arrival, plasma static pressure versus time, and the shock front profile were successful. Although the wall ablation information obtained is somewhat difficult to interpret, it did provide sufficient data to establish upper bounds. The instrumentation systems designed to provide pipe wall expansion versus time were the least successful.

The data obtained in the HYBLA GOLD experiment has already been used to develop new empirical models of the plasma flow. These models have been used in the current assessment of the survivability and vulnerability of the MX continuous buried trench concept. Specifically, a new empirical ablation model has been formulated.

The effectiveness of ribs and alternate ablators was qualitatively evaluated. The test results indicate that the rib-wall pipe and water pipe were more effective flow attenuators than the smooth-wall pipe at pressures less than 5 kb. Examination of the available time-of-arrival data in the 0.3 m pipes indicates that the water pipe was the most effective attenuator and the smooth-wall pipe was the least effective attenuator.

The results of HYBLA GOLD were inconclusive regarding the scaling issue. The pressure attenuation in the 0.3 m and 0.91 m smooth-wall pipes appears to scale in a reasonable manner for L/D < 100. This does not imply that scaling laws will be valid for much larger diameter pipes (i.e., the MX trench) at distances greater than those observed.

These conclusions have been based primarily on peak pressure and time-of-arrival data without addressing some problems that exist in the data interpretation. The most outstanding unresolved discrepancy is the plasma pressure profile (S' bar gage) and the resulting pressure pulses (SIR and SLA) measured at the pipe wall-grout interface.

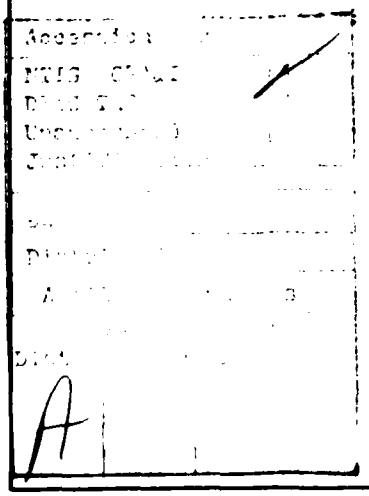

TABLE OF CONTENTS

TABLE OF CONTENTS (Concluded)

LIST OF ILLUSTRATIONS

LIST OF ILLUSTRATIONS (Continued)

LIST OF ILLUSTRATIONS (Concluded)

LIST OF TABLES

LIST OF TABLES (Concluded)

SECTION 1

INTRODUCTION

The basic purpose of the HYBLA GOLD underground nuclear test was to increase our understanding of the MX in-trench environment phenomenology and to improve our confidence in making predictions of this environment. This report describes the design of the nuclear test, summarizes the results and conclusions of the test, and finally, gives a proposed scaled simulation experiment which could prompt a thorough investigation of the trench environment problem. The remainder of this section discusses the reasons for nuclear testing, and the interaction of this nuclear test program with a complementary high-explosive test program.

1.1 REASONS FOR NUCLEAR TESTING

1.1.1 Background

There are two classes of attack: the relatively large Circular Error Probability (CEP) attack, and the small CEP attack, sometimes known as the zero CEP case (although zero clearly implies a finite miss distance). In the large CEP class, nearly all the bursts will land at relatively long distances from the trench. This situation does not appear to present a significant new threat to the trench design. The in-trench blast environment appears to be similar to the surface blast environment. While some issues have not been clearly resolved, it is believed that high-explosive testing is adequate.

For the small CEP class, there are some additional questions. Here, reference is made to bursts which land less than a few tens of meters from the trench. For this situation, very high pressures are developed inside the trench near the burst point. Associated with these high pressures are very high temperatures which can cause material to be ablated from the wall. Thus, it is necessary to account for both blast and fireball effects in evaluating the environment which might exist at much larger distances. These effects, as well as the question of the extended range of the shock environment in the trench, are some of the reasons for conducting this nuclear test.

Figure 1-1 shows the probability of one out of a number of weapons landing in the 4 m diameter of the trench as a function of CEP (Reference 1). It can be seen that an attacker must have a CEP of better than 10 m to 20 m to be highly confident that a significant number of weapons will be in the trench.

These small CEPs require advanced terminal guidance that may not exist now, but which might be developed if needed. Even if such a guidance system does not exist, it may be possible to design a basing system which is insensitive to future technological advances. For this reason, there is concern about the small CEP threat.

1.1.2 In-Trench Environment

The data from previous experiments which can be used to help understand the MX environment are exceedingly limited. In particular, only time-of-arrival (TOA) data, inadequate for developing empirical models, are available. First principle calculations from TOA data are beyond the state-of-the-art; the ablation and wall interaction processes must be treated by semi-empirical models which couple with radiation

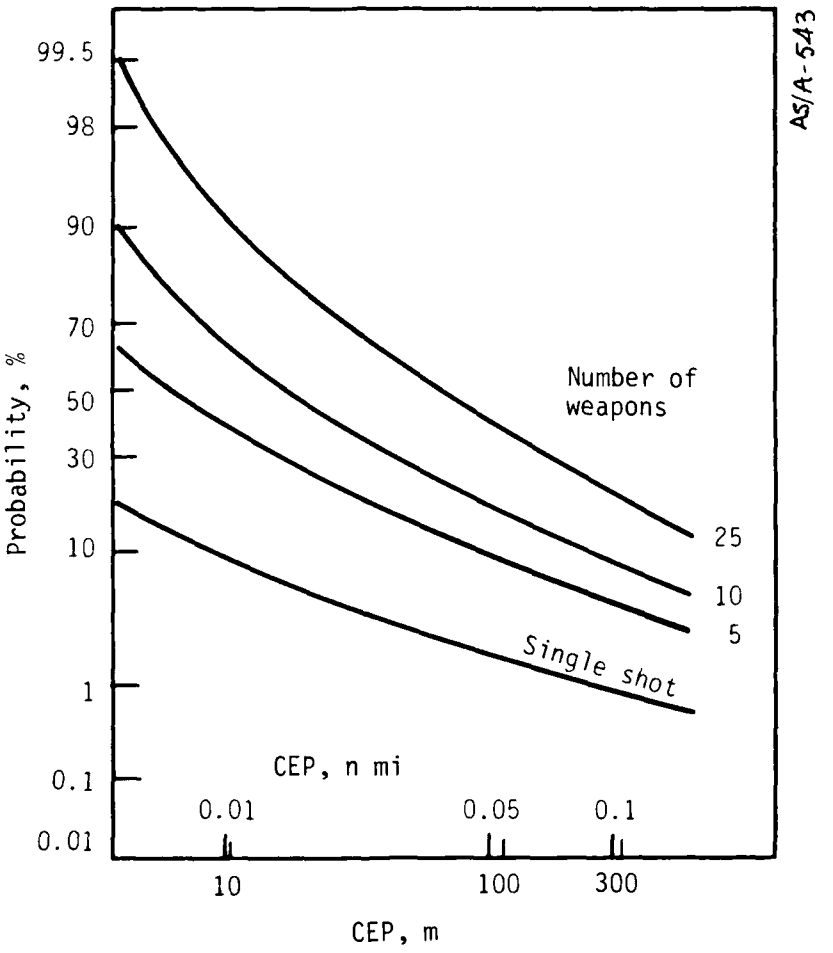

Figure 1-1. Probability of one weapon exploding inside a 4 m diameter trench.

hydrodynamic computer codes to provide estimates of the environment. The information available prior to HYBLA GOLD indicated that the in-trench environment (measured in terms of peak overpressure) may be approximately equivalent to that from a surface burst. That is, the available information indicated that the current trench design may not provide any unique environments. It is important to keep in mind that these early predictions were quite uncertain.

1.1.3 Prediction of the In-Trench Environment

These early calculations suggest that the attenuation of the blast environment is strongly governed by venting and ablation; thus, we will now explore the impact of these loss mechanisms.

Figure 1-2 shows the early calculations performed to analyze the MARVEL experiment (Reference 1). This was a nuclear shock tube experiment, conducted by the Lawrence Livermore Laboratory, in which only TOA data, as a function of distance, were obtained. It is quite evident that the no-loss case leads to a rather slow pressure attenuation. The addition of expansion in the modeling increases the attenuation rate somewhat; however, the attenuation in this calculation was strongly governed by the ablation modeling.

The range of uncertainty in the data, as depicted in Figure 1-2, is substantial. The modeling, at that time, agreed with the center of the data band, but by no means was this result unique.

Furthermore, and most important, no capability existed to bound the impact of ablation at this point other than the MARVEL experiment. The band in the theoretical calculations shown simply indicates what was considered to be reasonable. Later calculations, in support of the nuclear test design, will be discussed in a subsequent section.

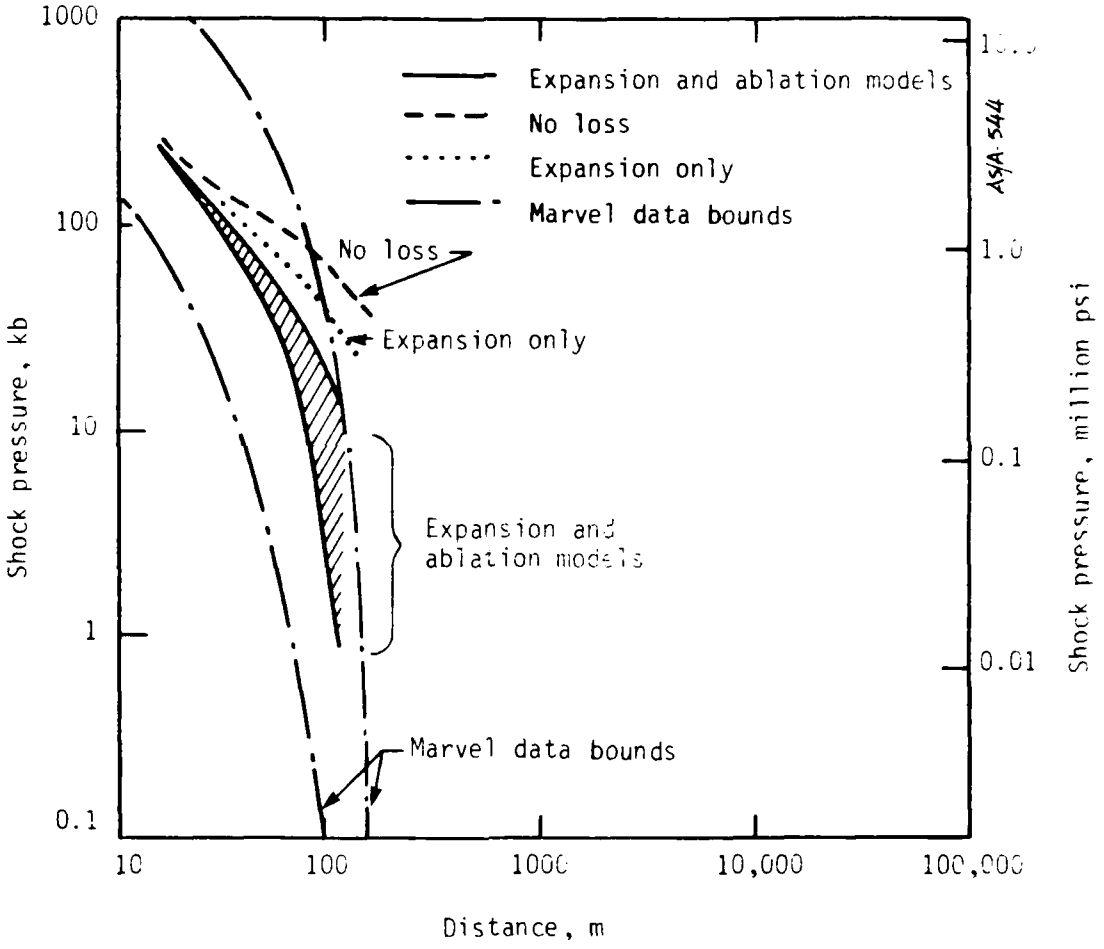

Figure 1-2. Impact of ablation and expansion models for the MARVEL experiment.

Because of this uncertainty, and because of the requirements of empirical modeling and the limited data base, it was thought that additional data which could help to improve our understanding of the ablation mechanisms would be highly significant.

1.2 INTERACTION WITH HIGH-EXPLOSIVE TESTING

Recognizing that both ablation and venting are potentially quite significant in attenuating the in-trench blast environment, the Defense Nuclear Agency embarked on a combined high-explosive and underground nuclear test program. The details of the high-explosive program will not be discussed in this report. However, it should be mentioned that the planned test program relies on high-explosive testing to understand the venting process. Because of the energy densities required, one can only study ablation in very small-scale, high-explosive experiments of about an inch in diameter. The serious concern of scaling to much larger diameters, as well as our basic lack of understanding of the physics involved, led to the development of an underground nuclear test to improve our understanding of ablation. During the early phases of the program, it was believed that the frictional wall interaction was less important than ablation in attenuating the flow down to the hundreds of psi range. For the longer distance cases where attenuation to the tens of psi range are concerned, the frictional wall interaction was thought to be much more significant.

In summary, an initial test program was developed in which venting and ablation are investigated through separate decoupled experiments. It was recognized that this was not entirely satisfactory and that there might be a nonlinear interaction between venting and ablation which could change the phenomena of flow attenuation. This resulted in an

investigation of a simulation experiment that might be conducted in a later phase of the program when all the blast and shock phenomenology of the actual trench environment would be reproduced in a scaled experiment.

SECTION 2

UNDERGROUND NUCLEAR TEST PROGRAM OBJECTIVES

In the initial test, a combined physics and instrumentation development experiment, no attempt was made to reproduce in detail the expected environment for the actual full-scale trench case. Rather, the aim was to design a physics experiment which would be easier to analyze and which could help improve understanding of the physics of wall ablation. Since there was concern about the potential utility of a larger scale simulation experiment, instrumentation was also developed and validated on this test to be used in a later underground nuclear test.

In this initial experiment, the investigation of venting was separated from that of ablation, partly as a matter of expediency; duplicating the venting process is a rather expensive and time-consuming process to reproduce in an underground test. More important, however, is that because of the uncertainty in the ablation modeling, it was more practical initially to have a simpler experiment which would be easier to analyze. By separating venting and ablation, the risk of mixing results from the two attenuation mechanisms in modeling would be reduced.

Experimental data were expected to provide an improved ablation model which is considerably more advanced than existing models. Also, there was concern about the scaling laws; since a full-scale, free-surface experiment

can never be accomplished, reliance on theoretical understanding is necessary to extrapolate smaller scale results.

The effectiveness of ridges (ribs) and alternative ablators were also investigated in this experiment to give a clearer picture of the utility of additional attenuation mechanisms. Finally, the data from this experiment, along with theoretical calculations, would be used to provide upper bound estimates of attenuation in the sense that they would not include the effect of the free surface. Again, the free-surface modeling would be accomplished by using data from high-explosive testing. The venting and ablation losses could then be combined by theoretical-empirical calculations.

SECTION 3

HYBLA GOLD EXPERIMENT DESIGN

This section discusses the experiment design, including design philosophy, test configuration and schedule.

3.1 DESIGN PHILOSOPHY

Basically, the HYBLA GOLD experiment was a nuclear driven shock tube. That is, there was a driver section driven by a nuclear source producing a shock wave in the experimental pipes running outward from the driver. Figure 3-1 shows the phenomena occurring in an ideal shock tube. If one starts with a high-pressure, high-temperature driver gas, and it comes in contact with the driven gas, it produces a shock running outward from the original contact surface (or contact region) which separates the driver gas from the driven gas. Across this contact surface, the pressure will be continuous, but the temperature and density will be discontinuous. An expansion wave will run backward into the driver gas causing a decreased pressure and temperature in the expanded driver gas, as shown in Figure 3-1.

3.2 DESIGN CONSIDERATIONS

A number of considerations which led to the experiment design will be discussed in the following subsections.

3.2.1 Maximum Data Return

Because underground nuclear experiments are expensive, complicated, and time-consuming, it is very important to maximize the information

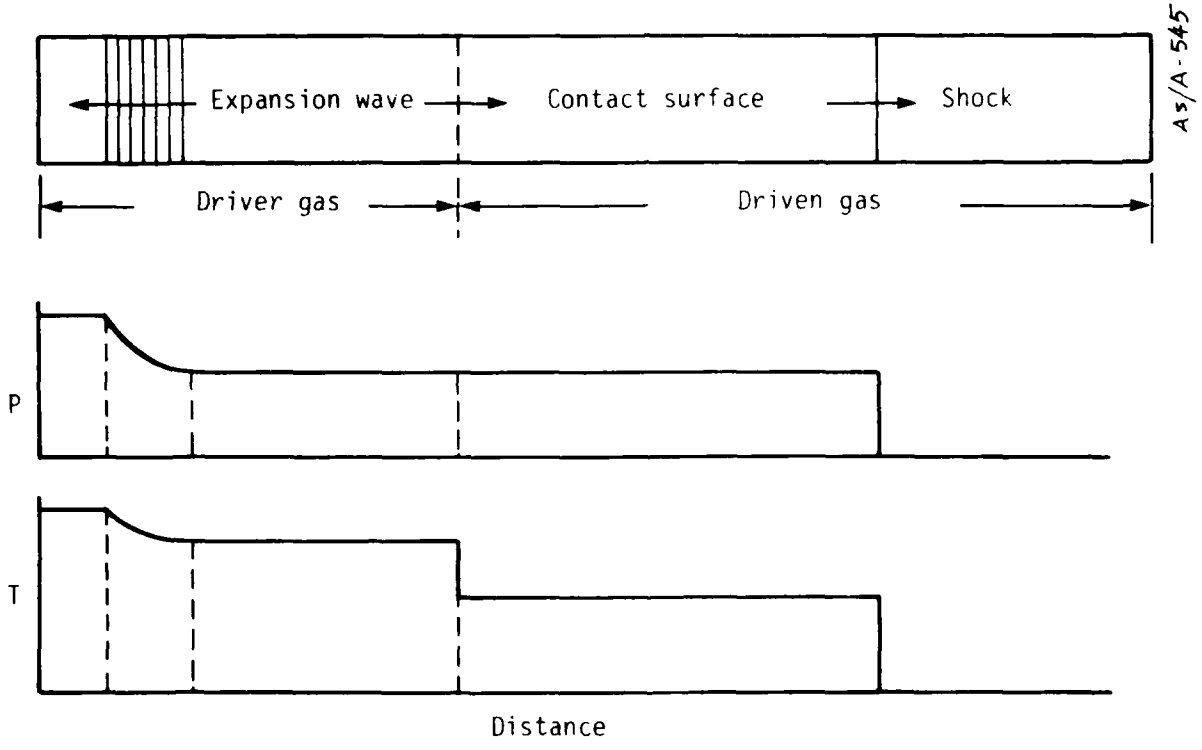

Figure 3-1. Example of a nuclear test condition, assuming an ideal shock tube.

return from a single experiment. It was attempted, therefore, to try to accommodate several experimental pipes. Also, it was desirable to have a length-to-diameter ratio (L/D) for each experimental pipe that was sufficient to exercise the boundary layer physics; therefore, an L/D of approximately a hundred was chosen so that attenuation could be looked at all along the pipe. To investigate the diameter scaling issue, three different pipes were necessary. Another objective was to examine the effectiveness of ridges and alternative ablators; hence, several wall materials and/or ablators and wall roughnesses were considered.

3.2.2 Minimum Front End-Complexity

It was desirable to minimize the complexity of the front-end driver section, (the region where the nuclear device is detonated and is the source of the high-energy gas) so that it was a reasonably calculable simple geometry. The mass of the device needed to be small compared to the mass of the driver gas to ensure uniformity of the driver gas and to keep the device debris out of the experimental pipes during the test time. The mass of the driver gas should be significantly greater than the mass of the driven gas in the experimental pipes so that the pulse duration will be as long as possible, and so that the driven gas did not drain out of the reservoir too early causing the driving pressure to attenuate too rapidly. Most significantly, negligible involvement of the driver section wall was desired. That is, since the concern was for understanding of ablation phenomena, it was not desirable for the mass in the driver section to be dominated by the amount of material that is ablated off the reservoir walls.

All of these conditions led to a rather large mass of air or driver gas material in the front-end section. For reference, about one metric ton of gas was considered in the driver section.

3.2.3 Duplicate Relevant Physics

It was important to duplicate the relevant ablation physics to accomplish the original objectives. In that regard, it was necessary to ensure that the pipe diameter was significantly greater than a Rosseland mean-free path so that the radiation transfer from the gas to the pipe wall would be duplicated in the experiment. In addition, the pipe diameter had to be much greater than the initial blowoff displacement so that the blowoff material did not immediately interact with the blowoff from the opposite wall. Finally, the flow conditions in general (the timing of the pulse, etc.) had to be approximately equivalent to the full-scale case. All of these conditions led to pipe diameters greater than several inches and, preferably, up to a meter or so.

3.2.4 Investigate Scaling Issues

To investigate the scaling phenomena as previously noted, three pipes were used. These pipes ranged in size from about 0.15 m to 1.0 m in diameter, roughly a factor of six in range. It was important to have the initial (or driving) conditions for each pipe to be roughly equivalent.

3.2.5 Minimum Test Pipe Complexity

Similar to the consideration for minimizing the complexity of the front-end driver section, it was necessary to minimize the complexity of the experimental pipe sections, although care was taken not to make the pipe sections so simple as to be irrelevant; therefore, an axisymmetric geometry was planned for the test pipe configuration. To achieve this, it was necessary to minimize significant hydrodynamic interaction or cross-talk between pipes to avoid discontinuities in stemming around the pipes, and to eliminate the hydrodynamic discontinuity across the contact surface (Section 3-1). The latter discontinuity could be eliminated by

adjusting the driver gas density. It was necessary to minimize the EMP interference with the instrumentation; hence, the unified grounding and shielding scheme was adopted, which is described in a later section.

3.2.6 Containable Design

Finally, it was necessary to ensure that the HYBLA GOLD design was containable leading to a minimum yield and certain other containment aspects that this report does not discuss in detail. The containment question was by no means trivial. HYBLA GOLD was a new kind of test which would highlight a major containment question; namely, the safe separation distance between successive working points, and the possibility of reusing an old working point for a future test.

The predictions for HYBLA GOLD were much less certain than those for normal underground nuclear tests (horizontal line-of-sight, or LOS, tests). Containment diagnostics for HYBLA GOLD would be very important because the test would provide a source of new information for the design of future underground nuclear tests. It was an opportunity to obtain new information related to LOS pipe flow, peculiar cavity formation, and it was a test near an old chimney.

3.3 TEST CONFIGURATION

The following subsections outline the proposed HYBLA GOLD test configuration, the options available, and the actual test configuration and test conditions that were chosen; not discussed is all the planning necessary to arrive at the final configuration. In addition to the design considerations, cost considerations were a major factor in the final decision.

3.3.1 Optional Test Configurations

The most promising options available are depicted in Figures 3-2 through 3-4 (Reference 1). A yield of about 1 kt contained in a reservoir of approximately 20 m^3 in volume (Figure 3-2) was considered as a starting point with several test pipes emerging from the reservoir, each approximately 100 m long, and ranging in size from 15 cm to about 1 m in diameter. The pipes would be arrayed in either a single drift (Figure 3-3) containing five test pipes, or two drifts (Figure 3-4) which would accommodate six test pipes. The drifts would be about 3 m by 4 m in cross-section, and would be filled with a rock matching grout stemming. The two drift option would minimize the hydrodynamic interaction between adjacent pipes and would allow increased pipe separation for instrumentation emplacement. The major advantage was the cost of the single drift configuration.

Tne preliminary layout of the experiment is shown in Figure 3-5. For the blast and shock experiment, a two drift configuration to accommodate the ablation pipes is shown. There was, as shown, a proposed EMP add-on experiment to the HYBLA GOLD ablation test. To minimize both the EMP and hydrodynamic interaction between the two experiments, a third drift was proposed which would contain a single 1 m diameter pipe for an EMP investigation. This pipe would face the nuclear source directly; hence, it would have a much higher prompt neutron and prompt gamma ray backgound than would be expected in the ablation pipes.

All the drifts would be approximately 100 m long and refilled with rock-matching grout. There would also be a stemming plug at the end of the pipes to seal off the high cavity pressure from the remaining outside drifts.

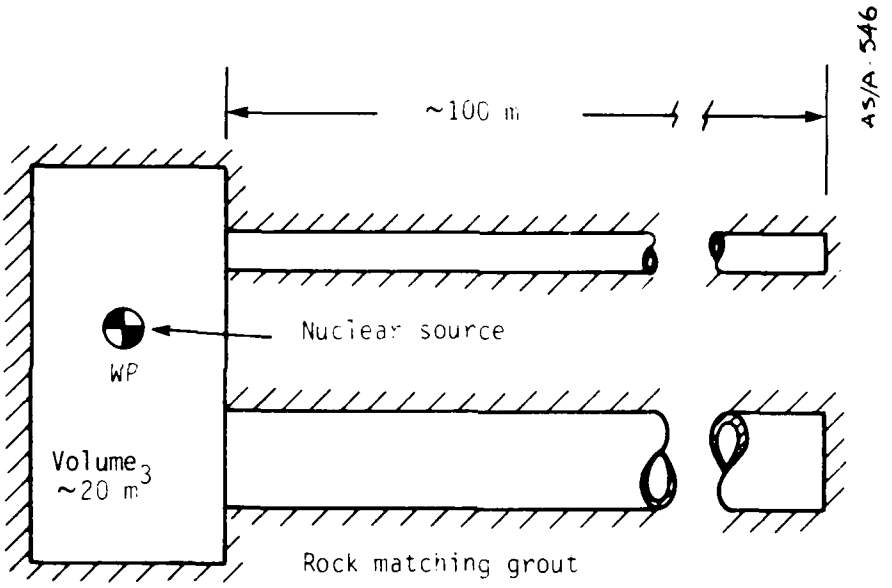

Figure 3-2. Proposed HYBLA GOLD reservoir configuration.

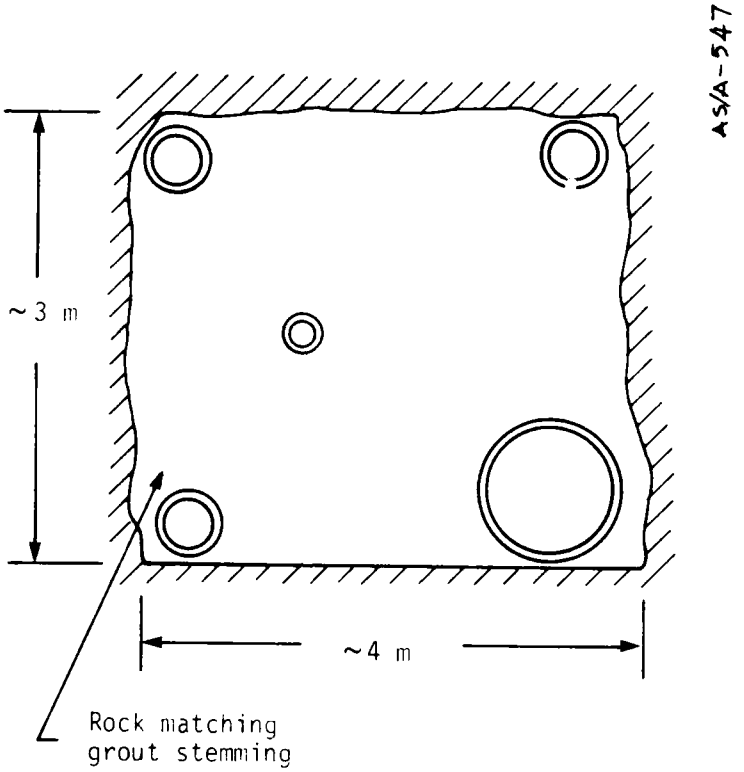

Figure 3-3. Proposed HYBLA GOLD test configuration, single drift option.

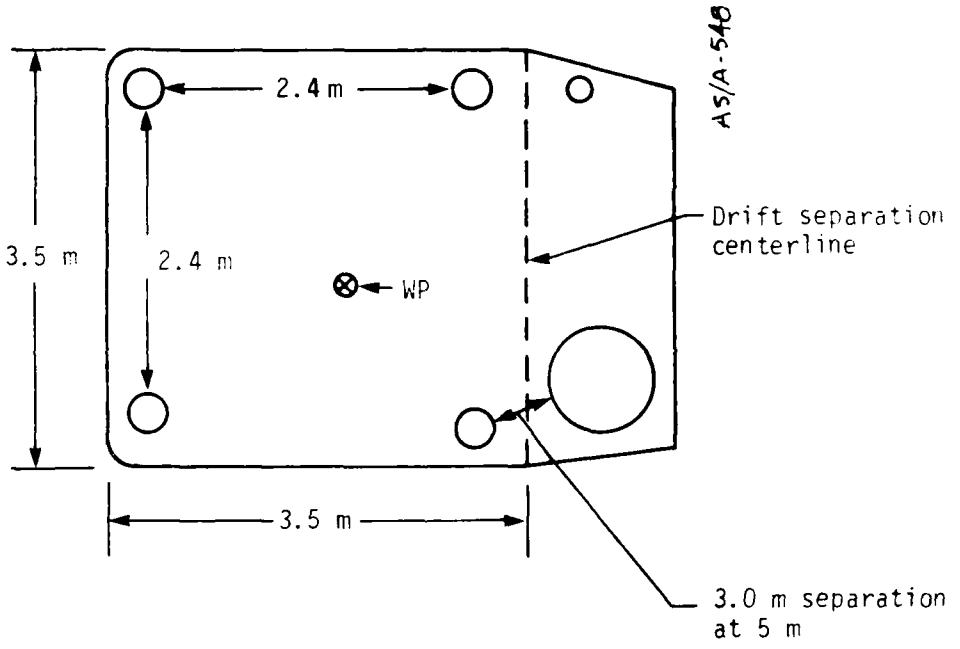

Figure 3-4. Proposed HYBLA GOLD test configuration, two drift option.

AS/A-549

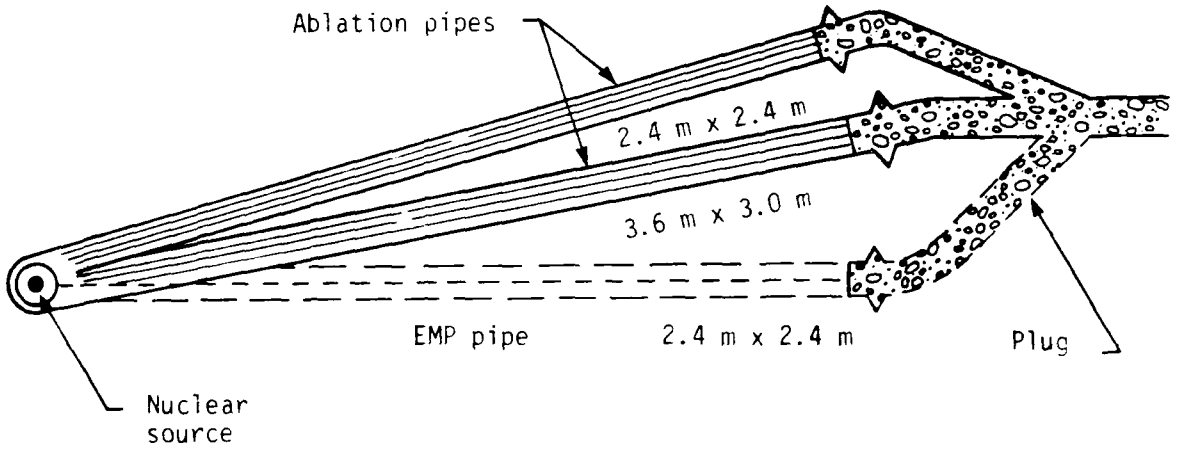

Figure 3-5. HYBLA GOLD preliminary layout, two drift option.

3.3.2 Initial Design

The major design criteria for the HYBLA GOLD event were as follows (Reference 2):

- Cost constraints limiting the test bed
- Desire to accommodate as many experiment pipes as possible, including an EMP pipe, if required
- Uncomplicated zero room (driver reservoir) with a volume of 25 m^3
- Minimum centerline spacing of 2.1 m pipe-to-pipe and pipe-to-cable run

The minimum pipe-to-pipe spacing requirement was needed to reduce hydrodynamic interaction between the test pipes. The calculations leading to this minimum spacing were performed by Lawrence Livermore Laboratories and are not discussed in this report (Reference 3). Maintaining this separation and restricting the mining effort to minimize costs dictated a design which would use two experiment drifts. Due to interaction problems along the entire pipe length, it seemed prudent to keep all the 30 cm diameter pipes in one drift and all other ablation pipes in the second drift.

The volume of the reservoir (zero room) was increased from 20 m^3 to 25 m^3 to maintain an axisymmetric configuration, to maintain a relatively simple geometrical shape, and to provide a zero room that could accommodate a separate EMP experiment drift, if required.

These criteria led to the design shown in Figure 3-6 (Reference 2). One drift (the main drift) would be constructed 3.0 m wide by 3.5 m wide for the first 35 meters, and 3.0 m by 2.7 m for the balance up to 100 m. This drift would contain one 0.91 m diameter pipe, approximately 100 m long and

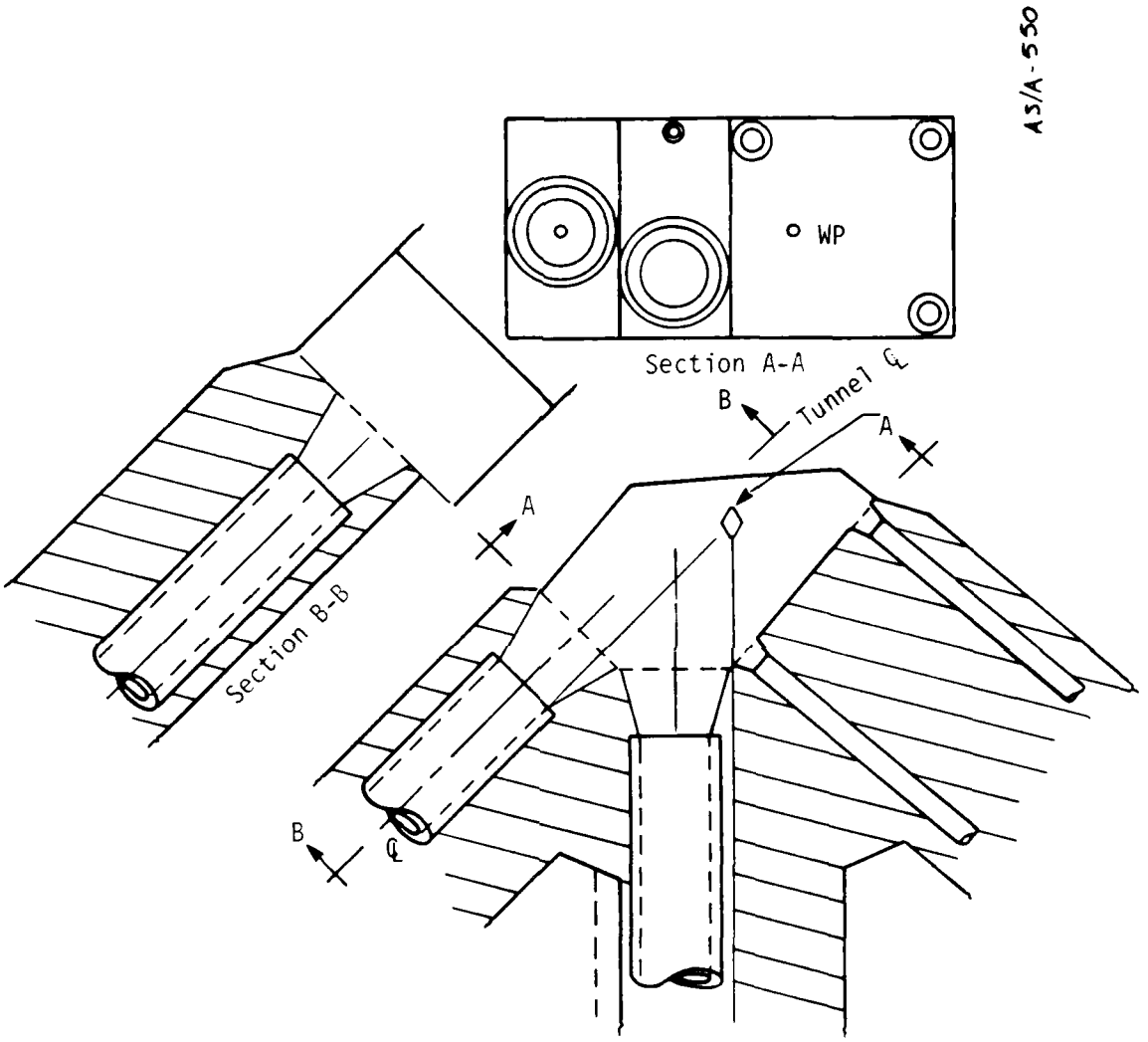

Figure 3-6. HYBLA GOLD zero room configuration, three drift option.

one 0.15 m diameter pipe, about 30 m long. This would yield length-to-diameter ratios of 100 and 200, respectively. The cross-talk between the pipes precluded obtaining useful information from the 0.15-m diameter pipe beyond 30 meters, thus leading to the shortened pipe.

The second drift (the auxiliary drift), 4.0 m wide by 3.5 m high, would extend for 65 meters and be constructed at an angle to the right of the first drift. This drift would contain three 0.3-m diameter pipes, about 64 meters long.

The third drift, if required, would be identical in size to the main drift and contain a 0.91-m diameter pipe.

The advantages of this design were: (1) good separation between pipes, (2) maintenance of an acceptable zero room volume, and (3) minimum mining costs. The major disadvantages are: (1) the loss of a 0.3-m diameter ablation study pipe, (2) a shortening of the remaining 0.3-m and 0.15-m diameter pipes, and (3) limiting the maximum L/D (L/D = 100) available for the 0.91-m ablation pipe. This was considered to be an acceptable compromise since it still provided for a scaling study using a 0.91-m, 0.3-m and 0.15-m pipe matrix, plus a choice of two of the three proposed pipes for studying the effectiveness of ridges and alternative ablators.

3.3.3 Final Design

The elimination of the EMP add-on experiment reduced the number of experiment drifts required to the two ablation pipe drifts. Figure 3-7 depicts the final HYBLA GOLD zero room configuration (Reference 4). This configuration permitted continued investigation regarding which type of 30 cm diameter pipe would be placed in each location in the auxiliary drift.

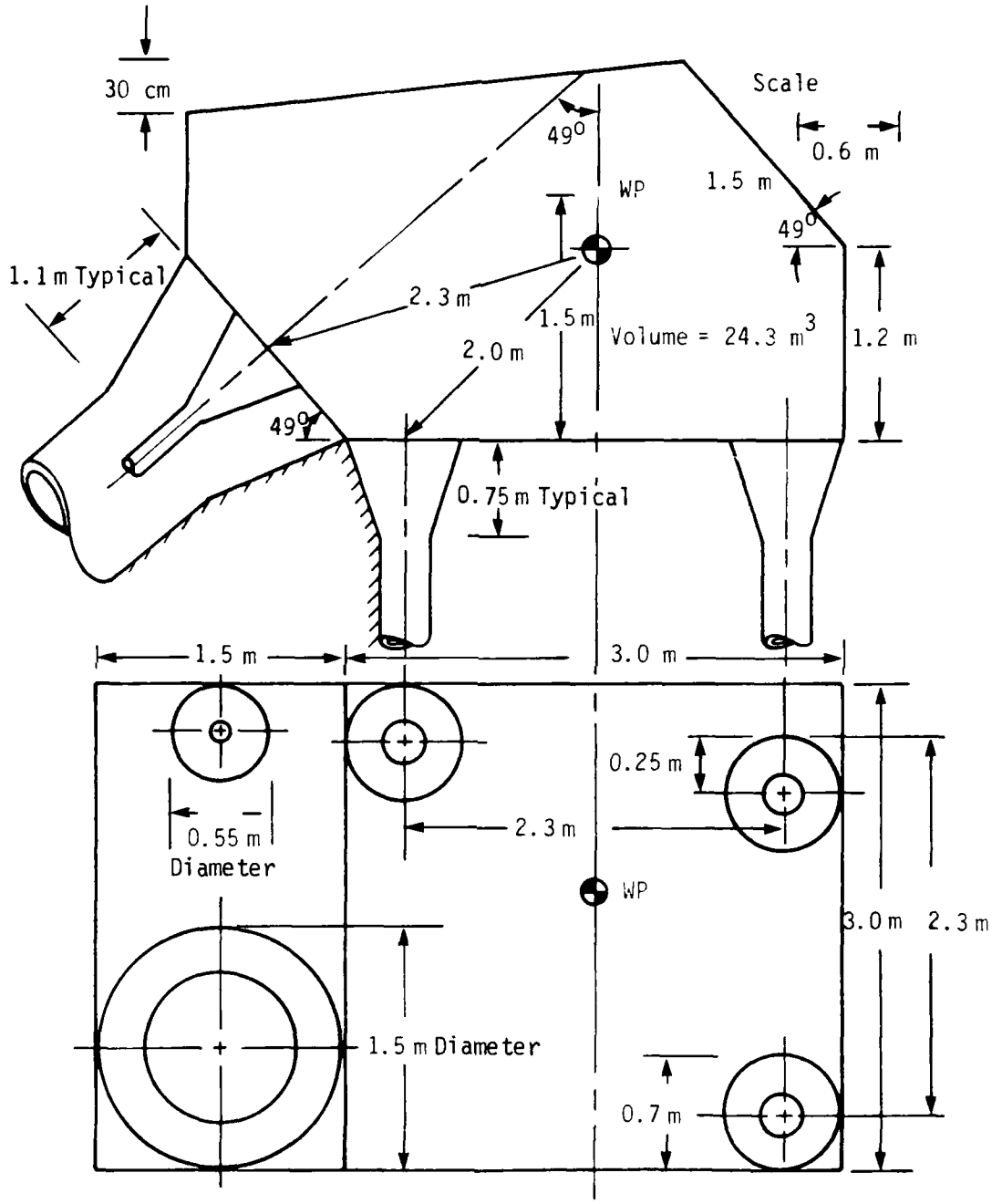

Figure 3-7. HYBLA GOLD zero room configuration, final design.

In the auxiliary drift, the experiment pipe in the upper right-hand corner was moved vertically downward approximately 0.25 m to accommodate, if required, water as an alternate ablator. The pipe that would contain water for the ablation study had to be level along its entire length to ensure that the water was of uniform level throughout the pipe length and did not collect at one end. Since the drift was constructed on a slope for drainage purposes, it was necessary to move the subject pipe down at the zero room wall end.

The dimensions of the flared openings for each pipe resulted from calculations performed by Los Alamos Scientific Laboratory (Reference 5). The purpose of the conical flares was to delay pipe closure, which could be caused by ground shock from the zero room. Loss of contact between the driver and driven gas prior to the formation of a well-defined shock in the pipe flow could influence the attenuation rate in each experiment pipe differently. The data analysis would become much more difficult as it would be necessary to separate results from two attenuation mechanisms. This was contrary to the original objective of a simple experiment that would be easily analyzed.

The HYBLA GOLD tunnel and experiment pipe layout is shown in Figure 3-8 (Reference 6). This drawing illustrates one of the early containment issues; namely, the close proximity of an old working point.

3.4 TEST CONDITIONS

3.4.1 Proposed Test Conditions

Table 3-1 shows the test conditions that were expected in the driver and driven gas (Reference 1). An experiment was planned to generate about a 20 electron volt (2×10^5 ^{o}K) shock which corresponds to about 50 kb, or roughly, 700,000 psi. These conditions would produce a

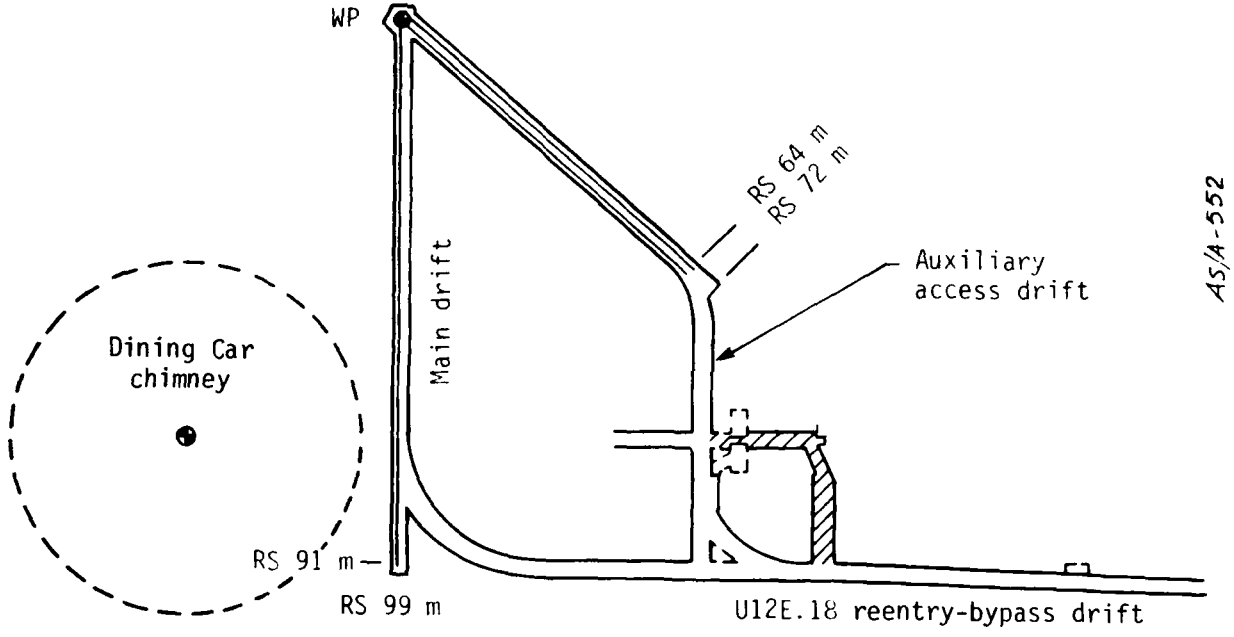

Figure 3-8. HYBLA GOLD tunnel and pipe layout.

TABLE 3-1. HYBLA GOLD PROPOSED TEST CONDITIONS

Driver Gas	Driven Gas
Reservoir material - 1000 psi air - Liquid air - Plastic foam - High explosive Reservoir conditions $\rho \sim 0.06$ gm/cc $P \sim 700$ kb (10^7 psi) $\theta \sim 40$ ev (4×10^5 ^oK)	Normal density air Initial shock conditions $\rho \sim 0.008$ gm/cc $P \sim 50$ kb $\theta \sim 20$ ev Final shock conditions $\rho \sim 0.08$ gm/cc $P \sim 1$ kb $\theta \sim 1$ ev

density behind the shock gas of about 0.008 g/cm^3, roughly eight times normal air density. To achieve the required conditions and to match the contact surface discontinuity would require a driver density of approximately 0.06 g/cm^3, and would also require a yield of 1 kt that provided a 700 kb driver pressure and about 40 ev in the driver gas. These conditions are also desirable since the temperature of the gas in the driver would be low enough that radiation transport in the driver gas would not be a significant energy transport mechanism.

Producing an initial density of 0.06 g/cm^3 in the driver gas was a considerable problem, and there were a number of different possibilities to solve it, the most obvious being high-pressure air. This density corresponds to roughly 1000 psi which produced some unique problems, the most significant of which was the requirement for a diaphragm between the driver and the driven section. It was believed that this diaphragm would introduce undue complexity in the test since it would be such a significant source of extraneous debris that the experiment could be dominated by high-velocity diaphragm debris propagating down the pipes. Thus, pressurized air was considered to be an undesirable option.

Some other alternatives under investigation were liquid air, plastic foam, and high-explosive detonation products. Liquid air has unique problems of its own, such as the air having to be flooded into the reservoir just prior to zero time when the device was detonated. The flooding would produce some mixing; however, there was concern about how well the liquid air and the residual air in the reservoir would mix. Substantial density discontinuities could exist during the first hundred or so microseconds, introducing spurious pressure pulses which might cause undesirable complexity.

The alternatives that seemed most desirable were plastic foam or high-explosive detonation products. Plastic foam could simply be a polystyrene foam, easily manufactured and well-controlled in this density range. Relatively easy to handle, it could be emplaced in the driver section well before zero time. Its drawback is that it does not reproduce the atomic constituents of air, most noticeably the oxygen, and therefore any molecular reactions (i.e., oxidation) that might occur in the driver gas would not be reproduced. Furthermore, the chemistry of carbon linking at low temperature is exceedingly complex.

It seemed that these chemistry problems were rather minor drawbacks. The temperatures of the driver gas range from several electron volts up to 40 ev in the reservoir initially. At these energy densities, the energetics of any molecular processes are inconsequential. There is always concern, however, about the possibility of some molecular reactions occurring in the ablation boundary layer where the energy densities are lower. It is possible that these molecular reactions could affect the ablation phenomena, or that the Prandtl number of the gas near the pipe wall could be much different which could affect the heat transfer. However, the plastic foam was considered to be undesirable for containment reasons related to the formation of a residual hydrocarbon gas.

Another alternative was the use of high-explosive detonation products as the driver gas. A number of pellets of high-explosives would be detonated just prior to, or at the time of the nuclear source detonation, which would produce the required density in the reservoir. The high-explosive has the desirable feature of containing a significant amount of oxygen in the explosive products so that it would more nearly duplicate the molecular processes as they would occur in pure air. The initial high energy density

of the driver gas would dissociate any molecules, so the exact nature of the compounds formed by the explosive products was inconsequential.

This alternative has the dual problem of mixing of the pellets of high-explosives and the safety of a ton or more of high-explosives in the reservoir. The test time for the experiment was expected to be about 2 msec; that is, the time for the shock to traverse the 100 m pipe, reflect off the end, and allow for a measurement of some portion of the reflected shock.

3.4.2 Final Test Conditions

Only minor changes were made to the originally proposed test conditions listed in Table 3-1 (Reference 1). The final test conditions are outlined in Table 3-2. The most significant change was the choice of reservoir material because of some elimination of the options as previously noted.

Several different plastic materials, with a wide range of chemical compositions, were investigated by Systems, Science and Software (Reference 7). From a hydrodynamic viewpoint, there is little difference between any of the materials. The gases resulting from all the plastic materials are mostly electrons (70 to 80 percent). Because all the gases are mostly electrons, no real differences exist for heat transfer characteristics.

All the materials and their associated gases which were investigated are within 10 to 20 percent in mass. Boundary layer growth is proportional to the one-fifth power of mass; therefore, no significant differences exist.

The choice of reservoir material was further reduced by eliminating materials that would form noncondensable gases. This requirement, as

TABLE 3-2. HYBLA GOLD FINAL TEST CONDITIONS

Driver Gas	Driven Gas
Reservoir material - Spun fiberglas (SiO_2)	Normal density air Initial shock conditions $\rho \sim 0.008$ gm/cc $P \sim 50$ kb $\theta \sim 20$ ev
Reservoir conditions $\rho \sim 0.05$ gm/cc $P \sim 1$ Mb (10^7 psi) $\theta \sim 40$ ev (4×10^5 ^oK)	Final shock conditions $\rho \sim 0.08$ gm/cc $P \sim 1$ kb $\theta \sim 1$ ev

previously noted, was based on the containment evaluation. Furthermore, the material chosen must be readily available, easy to handle, and possess a highly uniform density. It was not satisfactory to have the average density of the entire room to be approximately 0.05 gm/cm^3; the density of the material at any point in the zero room had to be approximately 0.05 gm/cm^3.

The above criteria led to a choice of Owens-Corning Fiberglas insulation. This material was readily available in large sheets which could be cut and stacked to fill the geometrical shape of the zero room, and was of uniform density. Because the material is chiefly SiO_2, the gas formed was readily acceptable from the standpoint of chemical reactions.

3.5 EXPERIMENTAL TEST PIPES

3.5.1 Proposed Test Pipes

As previously indicated in Section 2, different tasks were being attempted in the experiment; one to conduct the diameter scaling study, and the other to investigate the utility of various ablators and wall materials. In the scaling study, three pipes were planned, as indicated in Table 3-3, ranging in size from 15 cm to 1 m in diameter (Reference 1). The pipes were to be made out of a sand and/or concrete mixture. The scaling of any aggregate poses numerous questions. In the real case, the concrete may have a stone aggregate up to about 1 cm in diameter. Scaling that 1 cm down to the test dimensions showed similarity to normal sand grain dimensions, so it was decided that, for simplicity reasons, the sand would be equally as appropriate.

A normal sand roughness wall finish not including the ribs for the scaling study was desired. The ribs would introduce a complicated

TABLE 3-3. HYBLA GOLD PROPOSED TEST PIPES

Diameter (m)	Material	Wall Finish
Scaling study		
1.0	Sand concrete	Smooth
0.3	Sand concrete	Smooth
0.15	Sand concrete	Smooth
Ablator study		
0.3	Iron fiber concrete	Smooth
0.3	Sand concrete	Rough
0.3	Plastic ablator	Smooth

flowfield with multiple interacting shocks which could confuse both the instrumentation and understanding of some basic ablation physics mechanisms. The smooth wall results would be easier to interpret and would provide more definitive information on scaling.

The influence of the rough wall would be addressed by including a 0.3 m diameter rough wall pipe with scaled ridges also made out of sand and/or concrete. These ridges would be scaled in size taken from the MX baseline trench concept. Instrumentation was planned for this pipe to understand the influence of the rough wall. Also, a 0.3 m diameter iron, fiber-reinforced concrete pipe would be added.

Finally, there would be an investigation of whether other ablative materials, such as a small amount of water on the floor of the pipe, or some spray-on plastic which may be useful in attenuating the flow, would be feasible. Therefore, an additional 0.3 m diameter pipe which could be used to test the effectiveness of the ablator was included. All of these 0.3 m diameter pipes could be directly compared with the data from the 0.3 m diameter smooth wall data.

3.5.2 Final Test Pipe Configuration

The final test configuration selected (Section 3.3) determined the allocation of the test pipes for the experiment. The diameter scaling study was considered to be the most important issue; therefore, three of the five available test pipes were selected. The alternate ablator study was reduced to only two pipes and the 30 cm diameter smooth wall pipe.

After much discussion, the leading candidates for the ablator study were prioritized as:

1. Normal sand roughness pipe with water in the bottom
2. Normal sand roughness pipe with ribs

3. Normal sand roughness pipe with a liner material insert that would ablate

At the time of the initial planning, there was a possibility that the ribbed pipe might not be available due to construction problems. If the ribbed pipe could not be constructed, then the two alternate ablator study pipes would be priorities 1 and 3. Discussions with representatives of the Air Force MX Systems Program Office convinced us that the fiber reinforced pipe should be disregarded as a candidate for the ablator study (Reference 8).

3.5.2.1 Diameter Scaling Study

Several construction problems were encountered due to the requirement that the test pipes have a normal sand roughness wall. These problems could not be overcome, and as a result, the test pipes were constructed of a standard concrete mix design (Reference 9). A nominal mix is listed in Table 3-4. The results of a chemical analysis of the El Toro Type II cement used can be found in Table 3-5. A sieve analysis of the fine and course aggregate was prepared, with the results shown in Tables 3-6 and 3-7. Table 3-6 indicates the sieve analysis for the washed sand and the course aggregate used in the 0.91 m diameter pipe. Table 3-7 indicates the sieve analysis for the course aggregate used in the 15 cm and 30 cm diameter pipes.

The nominal dimensions for the test pipe sections (Reference 9) are depicted in Figure 3-9 (0.91 m diameter) and Figure 3-10 (15 cm and 30 cm diameter).

Although these pipes would be more difficult to analyze, funding and schedule constraints did not allow further investigation into the construction of a normal sand roughness test pipe. However, since the

TABLE 3-4. TEST PIPE CONCRETE NOMINAL MIX DESIGN, KG

Mix Design	15 cm to 30 cm Pipe	0.91 m Pipe
Cement	245	280
Sand	635	770
Aggregate	545	950
Water/Concrete ratio	Varies	Varies
Average density (gm/cm^3)	2.4	2.5

TABLE 3-5. CHEMICAL ANALYSIS -- EL TORO TYPE II CEMENT

Chemical Analysis	Percent
SiO_2	21.1
Al_2O_3	4.9
Fe_2O_2	4.5
CaO	63.9
MgO	1.5
SO_3	2.1
Insoluble residue	0.2
Ign loss	1.3
Combined alkaline	0.50

TABLE 3-6. SIEVE ANALYSIS OF AGGREGATE -- 0.91 m DIAMETER PIPE

Washed Sand	
Sieve Size	Percent Passing
3/8 in.	100.0
No. 4	98.0
No. 8	80.0
No. 16	69.0
No. 30	49.0
No. 50	17.0
No. 100	4.0
No. 200	1.8
Course Aggregate (3/4 in. to No. 4 Gravel)	
Sieve Size	Percent Passing
1 in.	100
3/4 in.	97
1/2 in.	52
3/8 in.	28
No. 4	4

TABLE 3-7. SIEVE ANALYSIS -- 15 cm AND 30 cm DIAMETER PIPES

Course Aggregate (3/8 in. to No. 8 Gravel)	
Sieve Size	Percent Passing
1/2 in.	100
3/8 in.	98
No. 4	23
No. 8	6
No. 16	3

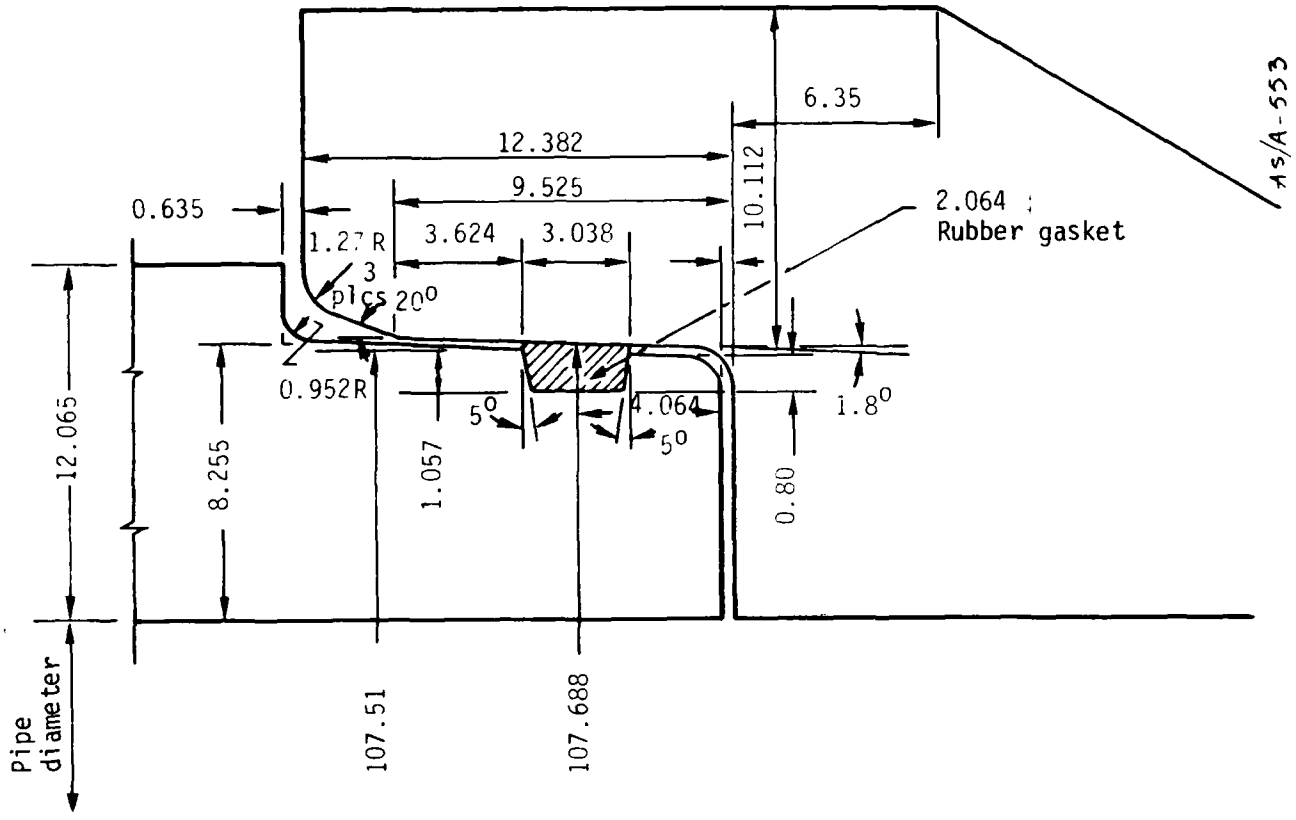

Figure 3-9. Dimensions (cm) of 0.91 m diameter pipe wall section.

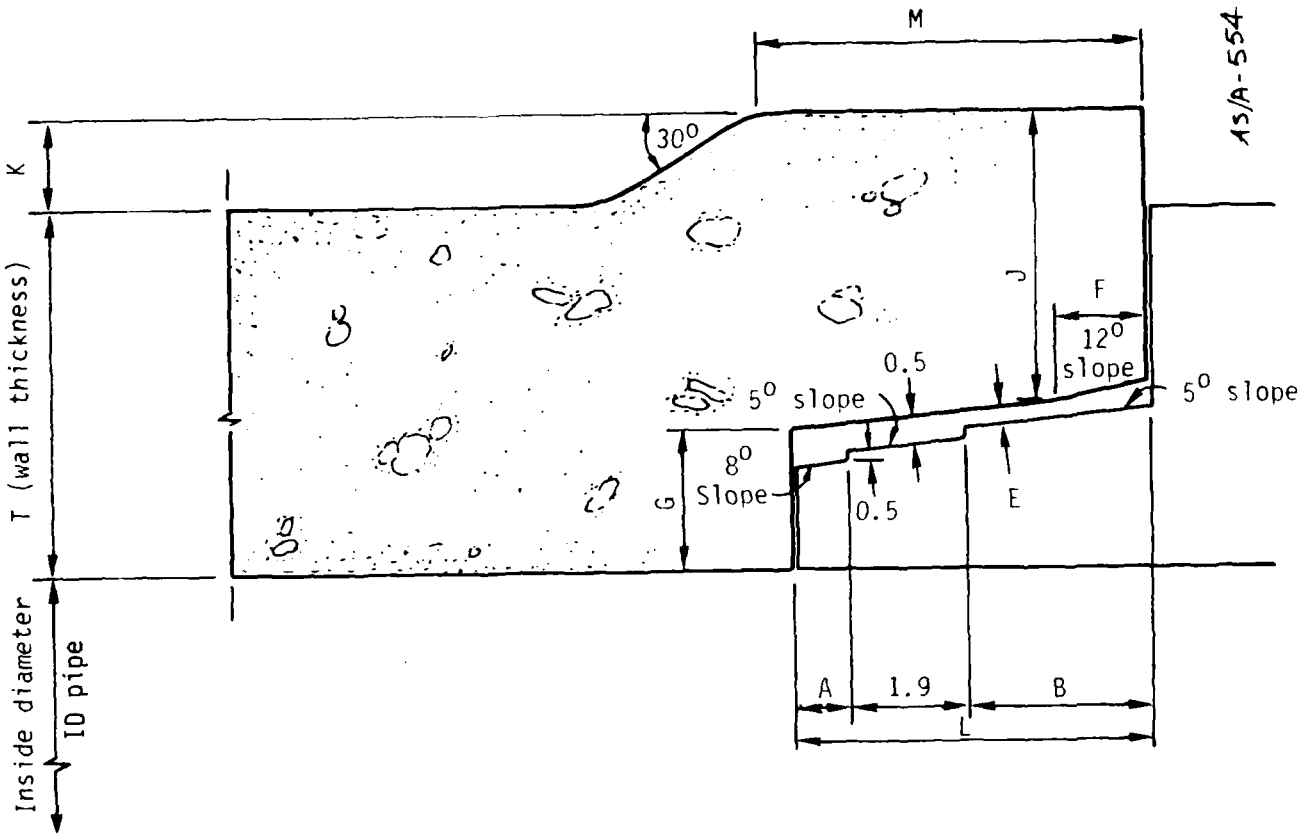

Schedule of Dimensions											
ID pipe	T	L	A	B	E	F	G	J	K	M	Max. length
30	5.1	5.7	0.8	3.0	0.2	1.3	2.5	3.6	1.6	7.0	183
15	2.5	4.6	0.8	1.9	0.2	1.3	2.5	3.5	4.1	7.0	122

Figure 3-10. Dimensions (cm) of 0.15 m and 0.30 m diameter pipe wall section.

real trench would be constructed of concrete (to include aggregate) the test results were considered valuable enough to continue.

3.5.2.2 Alternate Ablator Test Pipes

Construction problems with the rib pipe were solved; therefore, it was selected as an alternate ablator. The concrete mix for the rib pipe was identical to the mix used for pipe construction in the diameter scaling study. The only change was the size of the course aggregate. A sieve analysis of the aggregate is shown in Table 3-8 (Reference 9). The average density of the rib pipe was slightly lower than the pipes in the diameter scaling study. The difference (~5.0 percent) was not considered to be significant.

The nominal dimensions of a rib pipe section are depicted in Figure 3-11 (Reference 9). It should be noted that the inner diameter of the rib pipe is actually 33 cm, not 30 cm as in the smooth test pipe in the scaling study. Also, the pipe walls, for construction reasons, are not the same width as the previous 0.3 m diameter pipe. These differences were not considered to be significant to the test results.

The second ablator test pipe was a 0.3 m diameter pipe containing water. This test pipe was constructed in an identical manner to the 0.3 m diameter pipe in the scaling study. A water level of 7.5 cm in the bottom of the pipe was selected.

3.5.2.3 Test Pipe Configuration

The final arrangement (configuration) of the test pipes is shown in Figure 3-12. As previously mentioned, it was desirable to maintain similar driving conditions for each of the five pipes. Since it was not possible to guarantee similar conditions for the three test pipes in the auxiliary drift, it was necessary to slightly alter the original test pipe

TABLE 3-8. SIEVE ANALYSIS -- RIB PIPE

Course Aggregate (1/4 in. Chips)	
Sieve Size	Percent Passing
1/2 in.	100
3/8 in.	100
No. 4	79
No. 8	12
No. 16	4

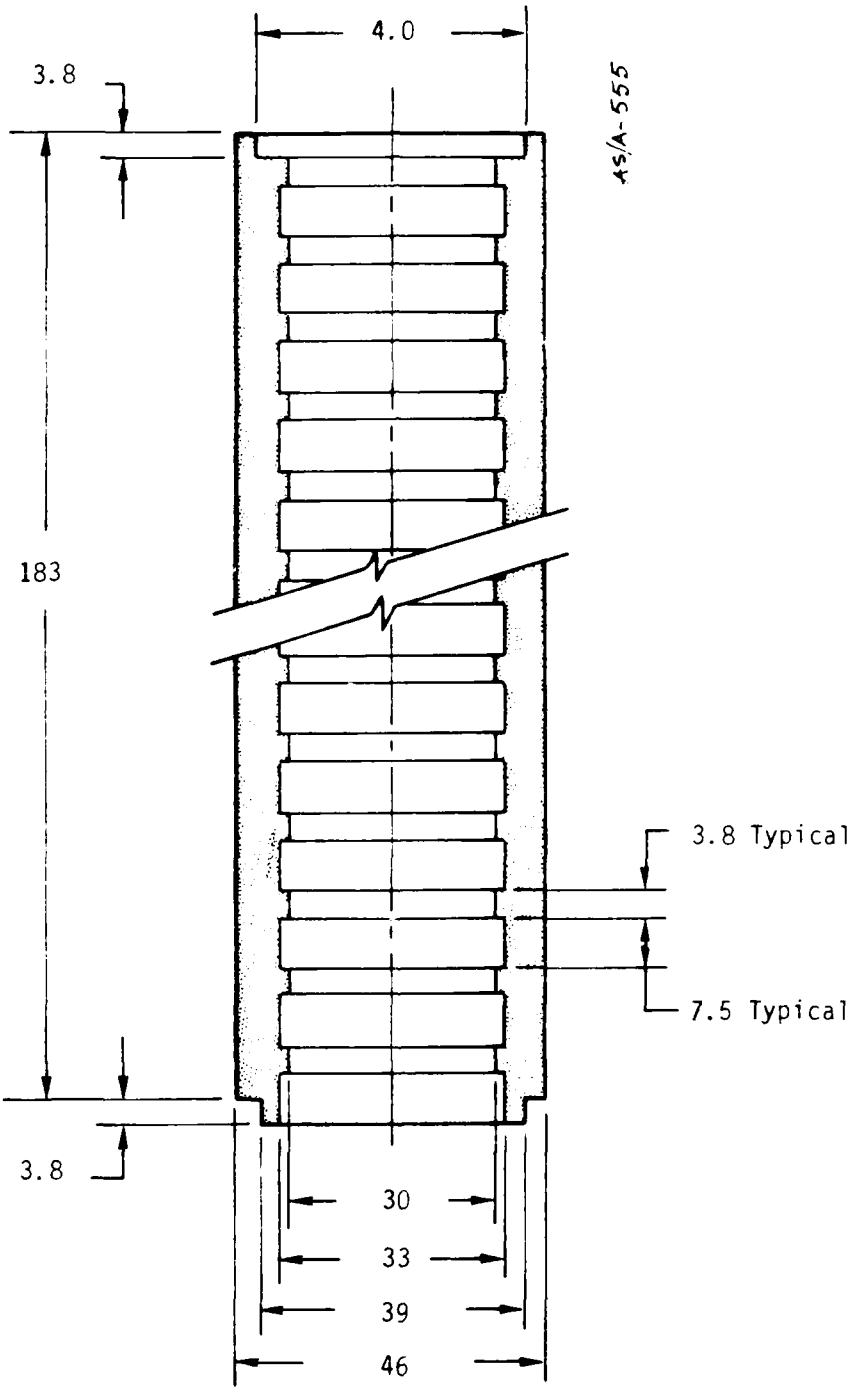

Figure 3-11. Dimensions (cm) of 0.30 m diameter rib wall test pipe section.

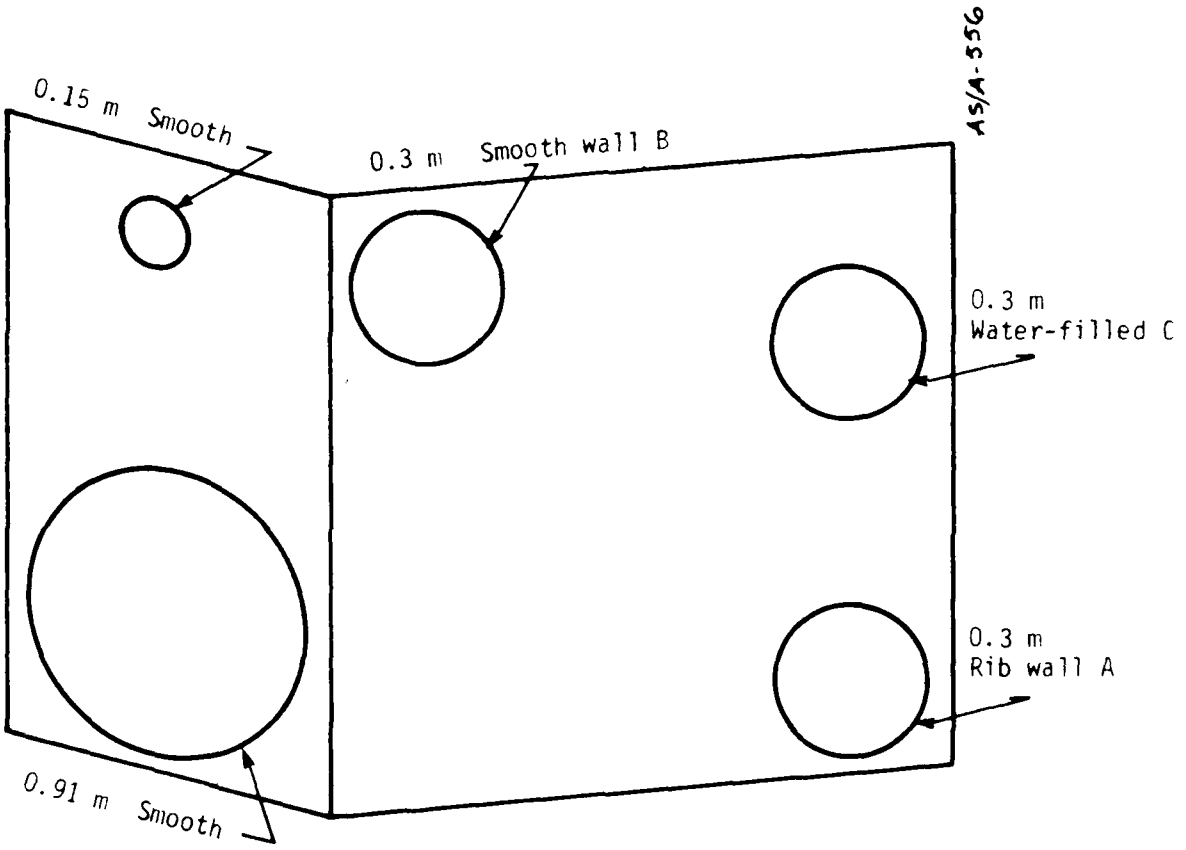

Figure 3-12. Final test pipe configuration.

configuration in the first few meters of length. The two alternate ablator test pipes were installed in two parts. The first 15 m consisted of pipe sections identical to the smooth wall pipe, i.e., the rib pipe and water filled sections began approximately 15 m from the test pipe opening. A dam for the water-filled pipe was constructed of 0.6-cm plexiglas, 10 cm in height to contain the water at the 15-m location.

The water level in the test pipe was measured by Science Applications, Inc. (Reference 28) using a series of thermistors positioned on a lucite rod that protruded into the pipe. The thermistor was operated in a self heat mode such that its resistance was a function of the current through it and the media it was in contact with. Since the conductivity of water is about five times greater than air, we expected about a factor of 10 resistance change between air and water contact. A monitor panel containing LED indicators for each thermistor was installed. When the thermistor was operating in its low resistance mode (no water) the LED was lighted, and when the thermistor was in contact with water the light was on.

These gages were disconnected prior to the shot to ensure that they would not couple radiation generated noise into other instrumentation systems. As a result, no water level was monitored for the last week prior to the shot. At the time of disconnection, the water level was at 7.5 cm in the water filled pipe (the desired preshot level).

Instrumentation (pressure time and TOA) in the smooth wall sections of the 30 cm diameter test pipes would be used to confirm the similarity of the driving conditions for the alternate ablator study.

3.6 HYBLA GOLD SCHEDULE

The schedule for the HYBLA GOLD experiment is shown in Table 3-9 (Reference 1). The readiness date was 1 November 1977.

Data returns started immediately after the experiment execution and continued through December 1977. Recalculations of the in-trench environment have begun based on these early revisions and are briefly presented as part of the HYBLA GOLD data analysis discussion.

TABLE 3-9. HYBLA GOLD SCHEDULE

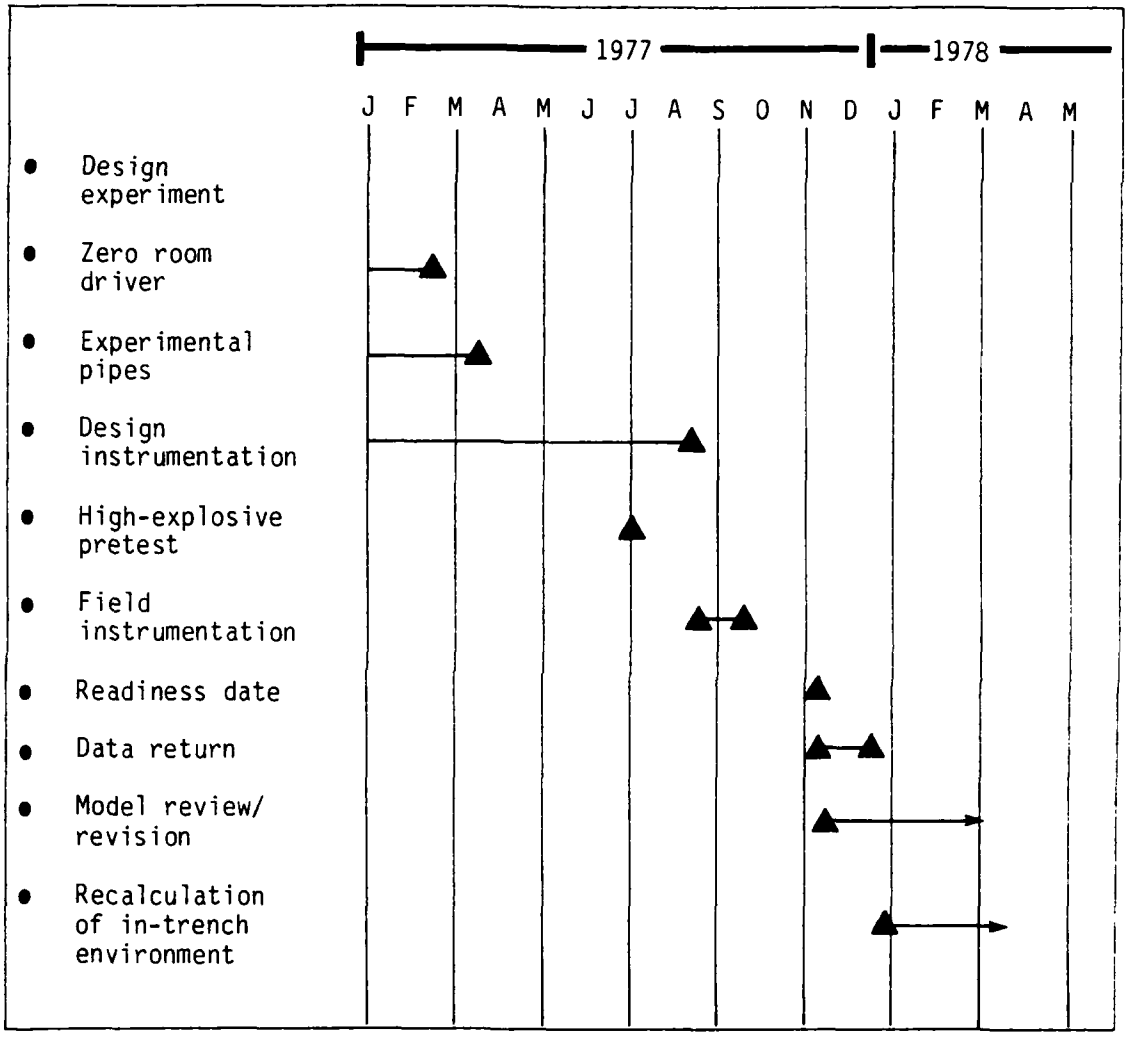

SECTION 4

INSTRUMENTATION FOR HYBLA GOLD EXPERIMENT

This section discusses the instrumentation for the HYBLA GOLD experiment. This instrumentation constitutes a rather extensive suite of measurements necessary to sufficiently understand the ablation and pipe expansion phenomena such that a relatively unique empirical model could be developed. This model could then be used to predict, with more confidence, the in-trench environment for the real case.

Table 4-1 shows the general type of measurements needed, as well as some indication of the state of development of the instrumentation, and an estimate of confidence in the instrumentation (Reference 1). It should be realized that high confidence means high confidence in a nuclear environment; with the complexity of a nuclear test, nothing is truly high confidence.

4.1 PROPOSED INSTRUMENTATION

The first set of measurements were shock time-of-arrival (TOA), both in or near each test pipe and in the stemming region between the pipes. This provided information about the arrival of the main shock front in the pipe and indicated whether there was any hydrodynamic interaction between one pipe and another. There are several state-of-the-art techniques available to measure TOA which include slifers, time domain reflectometry (TDR) and light pipes (fiber optics). These measurements

TABLE 4-1. HYBLA GOLD PROPOSED INSTRUMENTATION

Measurement	Location	Development Status*
Shock time-of-arrival (TOA)	In pipe	SOA-1
	In stemming	SOA-1
Wall static pressure vs time	In pipe	SOA-2
	In stemming	SOA-2
Areal density vs time	Across pipe chord	D-3
Shock front profile	Across pipe diameter	D-2
Wall ablation vs time	At wall	SOA-2
Pipe wall expansion vs time	At wall	D-2
Heat transfer to pipe wall vs time	At wall	SOA-2
Debris	At end wall	D-2
	At discrete locations	

*SOA: Generally state-of-the-art instrumentation
D: Instrumentation under development
1: High confidence
2: Moderately high confidence
3: Intermediate confidence

are relatively easy to obtain and are of rather limited value by themselves. In fact, if TOA were the only measurements which could have been made on HYBLA GOLD, the experiment would not have been justified.

To try to increase understanding, an extensive set of wall static pressure measurements were fielded in which it was expected to measure static pressure as a function of time at a number of locations along each pipe. In addition, the same measurements were made at the end wall to determine the total or stagnation pressure versus time. Some pressure measurements in the region around the driver section were also made which would be used to confirm the calculations of the driver itself. The proposed static pressure-time history measurement systems were Manganin resistance gages, Ytterbium flatpac gages, quartz crystal/Ytterbium bar gages, and fluid coupled transducers.

The possibility of making aerial density measurements versus time was investigated using x-ray transmission measurements using high-energy pulsed x-ray tubes. These data would provide an estimate of the material density in the tube at several times, assuming that it was possible to make an independent measurement of the change in pipe diameter versus time. Aerial density measurements would be made not only across the diameter, but also across various chords of the pipe in an attempt to determine the mixing of the ablated wall material into the flow pipe. There were obvious problems associated with the neutron and gamma background and, perhaps more importantly, the survivability of the x-ray tube and the x-ray detector for times long enough to allow measurements after the initial shock front has passed the detector location. This measurement was extremely desirable because it is the only technique known for determining the distance from the pipe wall the ablated material

actually moves. The models assume that any material ablated from the pipe wall is uniformily and instantaneously mixed across the diameter. It may be, however, that the flow is sufficiently intense that material removed from the wall stays in a rather small annular ring near the wall. In this case, ablated wall material would have a much different effect, especially in a 4 m tube, than the models would predict.

There has been concern regarding the possibility of a shock front precursor; that is, the shock propagating in the heated layer near the pipe wall which might extend to greater ranges than the normal shock front. This phenomenon has been observed in nearly every nuclear test and occurs due to the preheating of the region near the wall by the radiation emitted by the shock. The concern here is not so much that it is a dominant energy mechanism, but rather that it has an influence on the pressure-time history which might be confused with an effect caused by ablation. To determine the existence and extent of the precursor, an array of very light time-of-arrival gages was placed at several radial locations inside the pipe. These would not introduce significant additional debris but allowed a mapping of the shock front profile.

It was highly desirable to measure wall ablation as a function of time to obtain a clearer understanding of how much material was removed from the wall either by ablation or spall (popcorning). It was proposed to make these measurements with a series of pin gages embedded in the pipe wall at different depths. The pins were hardened to withstand the initial shock transient and would simply change from either normally opened or closed positions when the wall materials were removed. Both opened and closed pins should be used in an attempt to understand how the material is being removed. A normally closed pin would tend to open as the material

was spalling off the wall and being injected into the flow while still not bathed in the plasma, whereas a normally opened pin would simply stay open in these set of circumstances. Alternatively, if the high enthalpy gas were simply eroding the wall material away and exposing the pin, then a normally closed pin would stay closed due to the high conductivity of the gas; however, a normally opened pin would close. An extensive number of pins arrayed both azimuthally and along the length of the tube was fielded to investigate the ablation mechanism.

The change in resistance of pin gages as a function of time was used to measure the temperature rise at various locations in the wall. By knowing the temperature and the position of the pin, it was possible to infer some information about the energy transfer into the wall.

As previously indicated, the pipe wall expansion produces a significant attenuation mechanism even in this fully stemmed configuration. To distinguish wall expansion from ablation, the motion of the pipe wall as a function of time was measured at a number of locations. The technique for making such measurements was a radar waveguide that would reflect off a metal conductive surface at the edge of the pipe wall. That is, the waveguide was radially directed inward toward the pipe and terminated at the reflecting surface at the edge of the pipe wall. As the pipe wall expanded, this reflector moved relative to the radar source. By using the radar waveguide in a Michaelson interferometer setup, the reflected wave from the moving surface would alternately, both constructively and destructively, add to the incident wave. By noting the timing of the cancellation nodes (fringes), the position of the moving surface was determinable as a function of time. A grout-matching

dielectric (e.g., Teflon) was used inside the waveguide so that the pipe could expand into a relatively homogeneous media.

Another proposed technique for measuring wall motion was the mutual inductance gage. This technique is still being developed and has not been proven yet.

Finally, there was concern about debris motion inside the pipe. This may be a source of somewhat hostile environment for any plug, and therefore, an idea of the magnitude of the momentum and the velocity of such debris was useful. These measurements were made at the end wall of the pipe and provided information on the first arrival of debris at discrete locations in the end wall. Information about the times-of-arrival of the debris at these discrete locations was expected as well as the size and the momentum of the debris.

4.2 INSTRUMENTATION FIELDED

The major criteria for choosing the instrumentation selected for the HYBLA GOLD ablation experiment were primarily cost constraints and development status. It should be remembered that less than 6 months of time were available for instrumentation development and construction. Therefore, the majority of the measurement techniques selected were state-of-the-art as developed previously by the DNA test instrumentation development (TID) program; the specific application to the HYBLA GOLD experiment was the only development permitted.

The details of the instrumentation with regard to actual measurement location layout is not discussed in this report. Rather, a general description of the measurement techniques and the relative division of the measurements between the various experiment pipes is described. Details of each individual measurement may be found in

separate reports from the responsible agency (References 25, 27, 28, 29, 30, and 31).

Many of the issues and concerns addressed here could not be remedied prior to HYBLA GOLD fielding. There are certain limitations on the ability of HE testing to simulate the hostile environment which will be present on the nuclear test which is, of course, one of the reasons for doing the nuclear test. In some cases it was necessary to rely on calculations to aid in decisions regarding gage construction and installation. In other instances, not enough testing was accomplished because of time and resource limitations. Furthermore, we recognized that only a nuclear experiment would answer the questions regarding gage survivability and performance. The following paragraphs will identify each major gage system, and the major issues and concerns associated with that system.

The areal density measurement could not be developed within the test schedule constraints; therefore, it was necessary to drop this much desired measurement.

4.2.1 Shock TOA

Although all gages generally provide TOA data, two continuous measurement techniques were fielded. Time domain reflectometry (TDR) measurements were fielded by Los Alamos Scientific Laboratory to provide information about the arrival of the shock front in each pipe as well as the ground shock in the stemming (Reference 10). The ground shock in the stemming material could result from either the cylindrical expansion of the test pipes or the nearly spherical shock produced by the device detonation itself. This latter ground shock was expected to travel much slower than the shock front in the test pipes.

This simple technique (TDR) utilized a known pulse being transmitted through a small (~10 g/cm, cable, reflected off the electrically shorted end of the cable, and subsequently measured transit time of the reflected pulse. The electrical short in the cable is created by the shock front passing over and crushing the cable. By measuring the total transit time of the input pulse and the reflected pulse and using a predetermined electrical wave speed in the cable, one can determine the location of the shock front as a function time. Since the cables are located a few feet from the source region, their sensitivity to gamma radiation must be minimal. Unfortunately, the most gamma resistant dielectrics (Teflon, polyethelene, etc.) are the most difficult to crush. The trade-off studies were conducted by LASL, and the RG174 cable was selected.

In addition to the gamma sensitivity, a major problem which could arise is the significance of a thermally driven precursor that could be enhanced by the outer plastic insulation of the cable. The blow-off of the outer insulator may cause a premature crushing of the cable, possibly producing an erroneous TOA signal. To minimize the development of a precursor, the outer insulator was stripped from cables installed inside the test pipes.

Sandia Laboratories fielded conventional slifer cables which were located approximately 10 cm from the outside of each pipe wall along the entire length (Reference 11). Slifer cables were also installed between the pipes in the stemming material. No particular problems or concerns were anticipated since these are standard TOA measurements which have been routinely made on several nuclear events.

4.2.2 Wall Ablation Gages

4.2.2.1 SSS Pin Ablation Gage

The rate of ablation of the pipe wall by the plasma was measured by Systems, Science and Software (SSS) using a gage similar to one that was developed and tested on the ORION program (Reference 12). The gage consisted of two ribbon conductors, the ends of which are covered with a known thickness of material mounted flush with the inner surface of the pipe wall (Figure 4-1). When the covering material is ablated away, the ends of the conductors are exposed to the plasma and thereby electrically shorted by the high conductivity of the plasma. Ablation measurements of this type were made at several depths at various locations to determine the rate of wall removal.

One of the major issues surrounding this measurement technique was the concern over the EMP effects on the gage circuitry. This problem was solved by using a balanced circuit. Some concern was expressed regarding the possibility of the induced conductivity in the surrounding grout medium due to nuclear radiation, and thermal heating from the plasma could shunt the electrode resistors (Reference 13). Calculations were performed showing that this was not a serious problem.

4.2.2.2 SRI Pin Ablation Gage

As an alternative approach, Stanford Research Institute (SRI) measured the ablation of the pipe walls using a normally shorted twinax pin system that was embedded in the pipe wall (Figure 4-2). The foil shorting cap covering the twinax pin, would ablate (along with the pipe wall) when the wall material above it had been removed. This subsequently caused a change in the shorting resistance. This technique could also measure popcorning wall material whereby chunks of material are removed

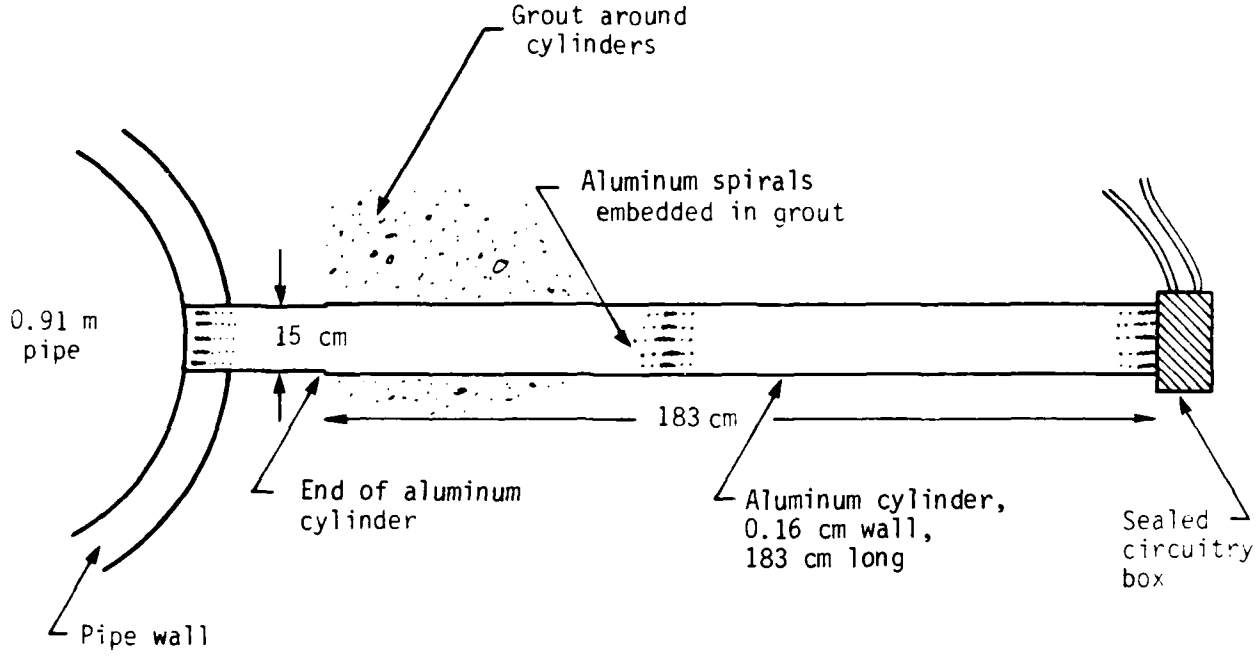

Figure 4-1. S^3 ablation pin gage, section view.

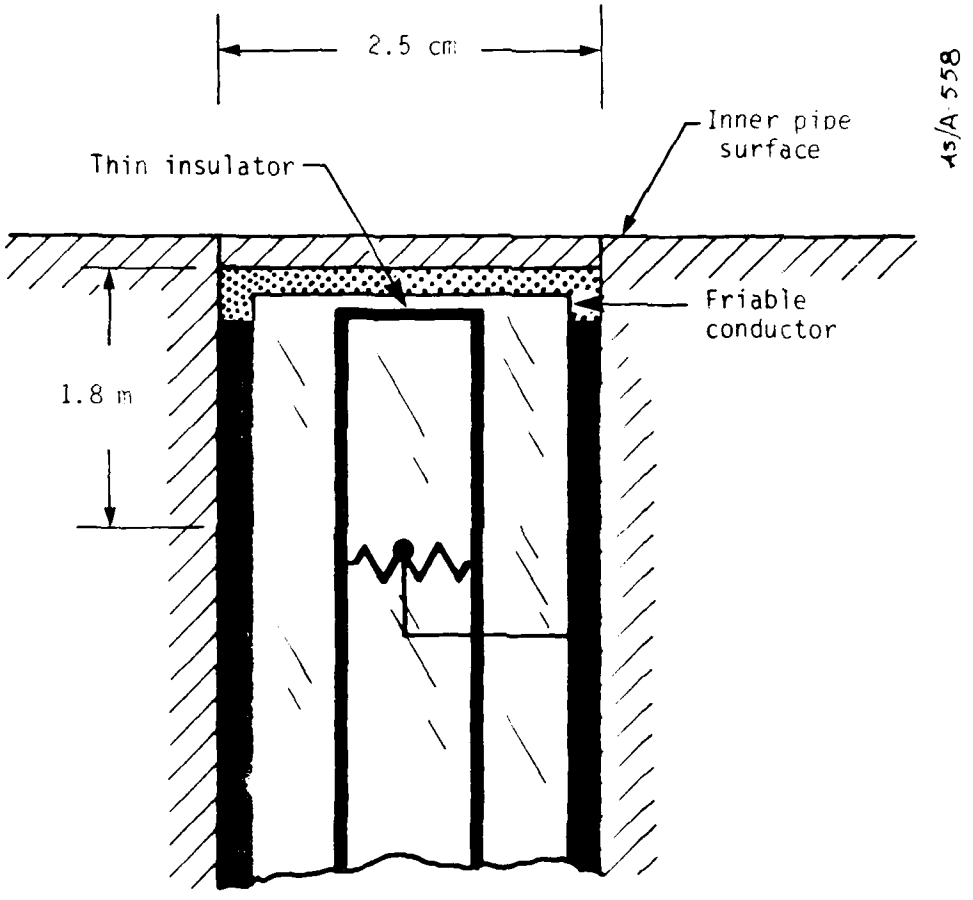

Figure 4-2. SRI ablation pin gage.

rather than continuous thermal ablation, since the chunks may also remove the shorting cap.

This measurement technique was quite simple and had no major technical problems. The circuitry was balanced to minimize any EMP pickup. In addition, the pins were externally shielded (Reference 14).

In the region of severe pipe expansion for both the SSS and SRI pin systems, the survivability of the gage was a major concern. Several HE tests were conducted at SRI to examine this problem for the SRI gage (Reference 15). The results of these tests indicated gage survival for a pipe wall expansion of approximately 20 percent of the initial radius. Gage failure in these tests was believed to be caused by the separation of the gage end cap as the wall expansion increased.

4.2.3 Pipe Wall Pressure

4.2.3.1 SRI Flatpac Gage

Outside pipe wall pressure was measured by SRI using flatpac steel gages previously developed for LOS pipe pressure measurements (Reference 14). The detector grid was mounted between two thin steel plates as shown in Figure 4-3. The sensing element was Ytterbium or Mangagin, depending on the pressure level to be measured. Ytterbium has a dynamic response upper limit of ~25 kb, but when compared with Manganin, it has increased sensitivity at the lower pressures. Manganin has been calibrated up to 1.5 Mb.

The results of several HE tests conducted at SRI were very positive (Reference 15). The steel flatpac gages survived for several hundred microseconds in the region of substantial wall expansion. Aluminum flatpac gages were also tested, but for reasons which are unclear, their survivability was poor.

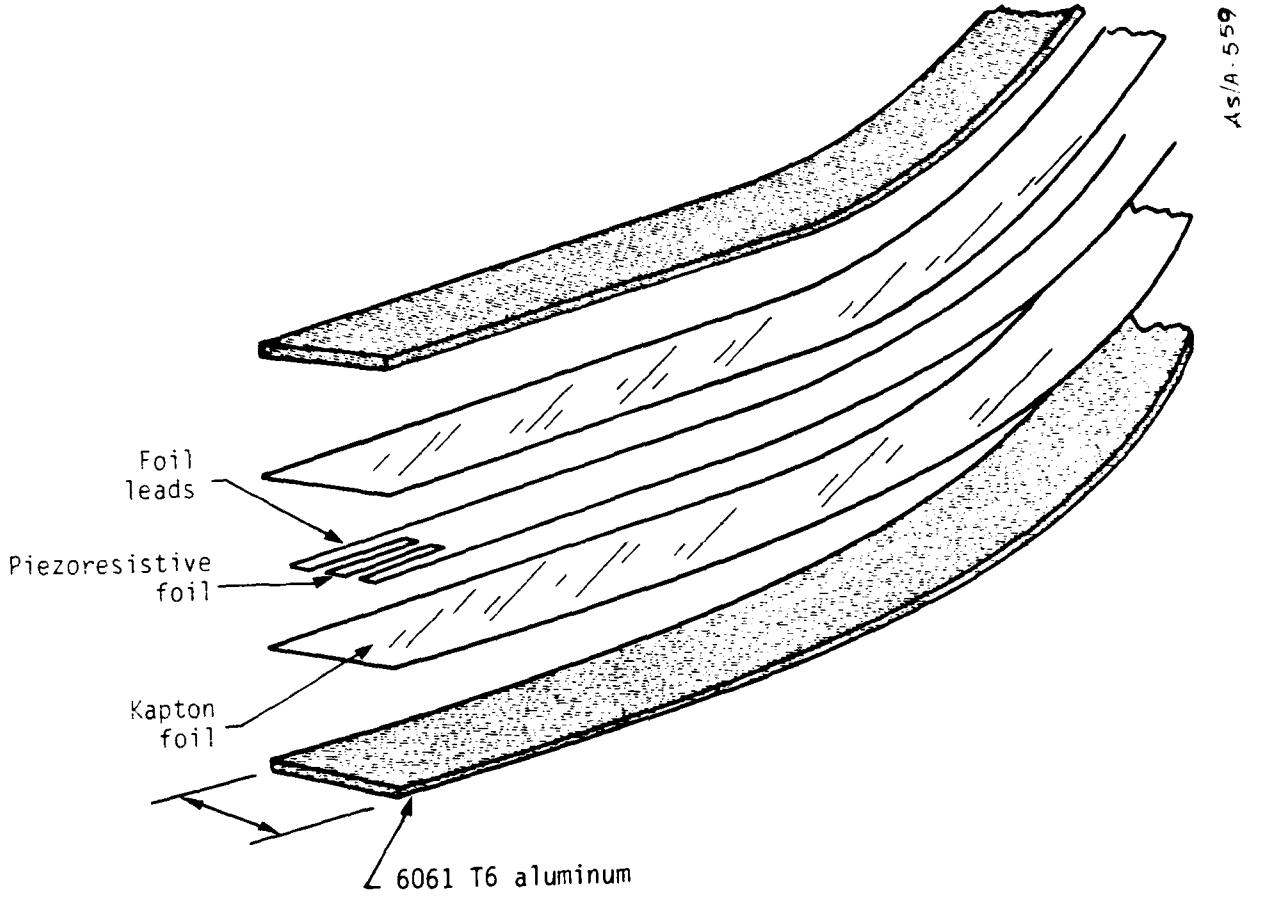

Figure 4-3. SRI aluminum flatpac gage.

Initially, it was planned to use aluminum for the metal cladding of the gage since it would minimize the impedance mismatch between the surrounding grout and the gage, thus reducing the ringing and differential motion which could cause gage failure. The unsuccessful tests using aluminum flatpac gages led to the selection of steel over other possible materials (Reference 16). Simple calculations suggested that the differential motion is small for the thin 0.3 cm steel plates. However, as the pre-HYBLA GOLD HE test at Sandia Laboratories indicated, there was considerable ringing in the steel during the early pressure-time history. This ringing time is short compared to the measurement times-of-interest for the HYBLA GOLD conditions.

It should be noted here that a major problem in the analysis of this gage system is related to its position relative to the plasma flow in the pipe. Namely, the pressure-time history records must be corrected by calculations since the measured pressure is at the outside of the pipe wall; the concern was the pressure of the flow inside the test pipe. It was necessary to perform equation-of-state experiments at SRI to determine the characteristics of the pipe wall concrete and surrounding grout to make these important corrections.

4.2.3.2 SSS Bar Gage

The pressure on the inside walls of the pipe was measured by SSS using bar gages similar to those that had been previously used on several events, including DIAMOND DUST, DIAMOND MINE, and PRE-MINE DUST (Reference 12). The basic design (Figure 4-4) of the bar gages was not altered between these early tests and the present experiment, although, as discussed below, the front end of the bar was modified to minimize the effect of the large wall expansion. In this technique, the sensing

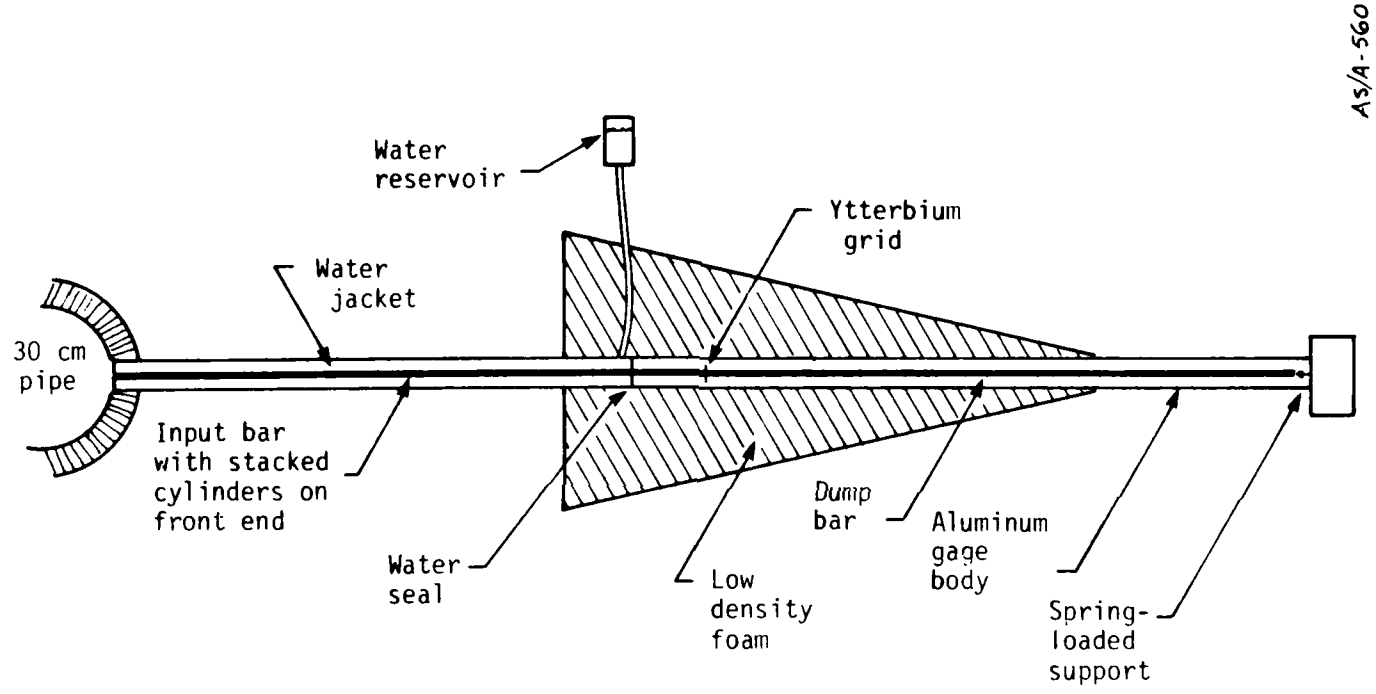

Figure 4-4. S^3 bar gage schematic, section view.

element is well removed from the pipe wall so that it is protected from the hostile environment.

Early uses of the bar gage were the measurements of cavity pressure at the cavity wall. Some of the bar gages on the PRE-MINE DUST events were up to 43 m long, with the sensing element 15 m from the cavity wall. The metal rods and piezoelectric sensing crystal were contained inside heavy steel housings for added protection.

In the HYBLA GOLD experiment, the measurement of high pressures near the front of the pipe utilized tungsten-carbide as the input rod and titanium as the dump rod. Tests have shown that this type of bar gage can measure pressures up to 30 kb (the yield strength of the titanium rod is exceeded above 30 kb). Lower pressures, further down the pipe, were measured with steel bar gages which have an upper limit of 20 kb. Ytterbium was the sensing element for all the bar gages. In all cases, the high density and low particle velocity of the metal rods, compared with the surrounding grout, would cause them to protrude into the pipe flow as the pipe expanded. A technique to minimize this effect is outlined in subsequent paragraphs.

There were two major issues associated with the bar gage. To obtain pressure-time data on the waveform, the gage must remain intact for at least 500 μsec. The rapid pipe extension and subsequent radial shock can tend to cause severe strain at certain critical locations along the bar (e.g., the junction at the detector element and the cable connection at the dump rod). A foam collar was designed by SSS as a means of protecting the sensing element and the dump rod.

The second major issue is related to the front of the input rod which was exposed to the high velocity plasma flow. As the pipe wall

expands, the input rod will protrude into the flow. To minimize the distrubance to the flow and the spurious signal that would be generated by the partial stagnation of the flow against the input rod, the front of the rod was made of several chips, 1.9 cm long, that were designed to separate from the bar when exposed to the flow. The mechanism for this removal seems simple enough in theory, but no experimental evidence existed indicating that the chips would be removed cleanly without causing distortion of the measured waveform. Other than a nuclear experiment, no technique was devised preshot to simulate both the pressure-time history (with the associated wall expansion) and the high axial velocity of the flow. Thus, HYBLA GOLD was to be a proof test of the segmented bar concept.

4.2.3.3 Pressure Transducers

Diaphragm pressure transducers were installed in the pipe walls by Kaman Science Corporation (KSC) to measure the static pressure-time history of the shock front (Reference 17). Similar transducers had been fielded on one previous nuclear event and several HE test events to measure shock pressure in a blast environment. The gage is limited to a peak pressure of 10 kb due to the failure in shear of the diaphragm at this level. The transducer was recess-mounted in the gage housing and was not flush with the inner surface of the pipe wall. Figure 4-5 shows a schematic of the gage assembly.

Although this type of transducer had been fielded on conventional HE tests and successfully proven at a pressure greater than 4 kb, it was not designed for the pipe expansion environment that the gage must necessarily survive in the HYBLA GOLD test. The mounting fixture of the gage was critical, since it must move with the pipe wall during

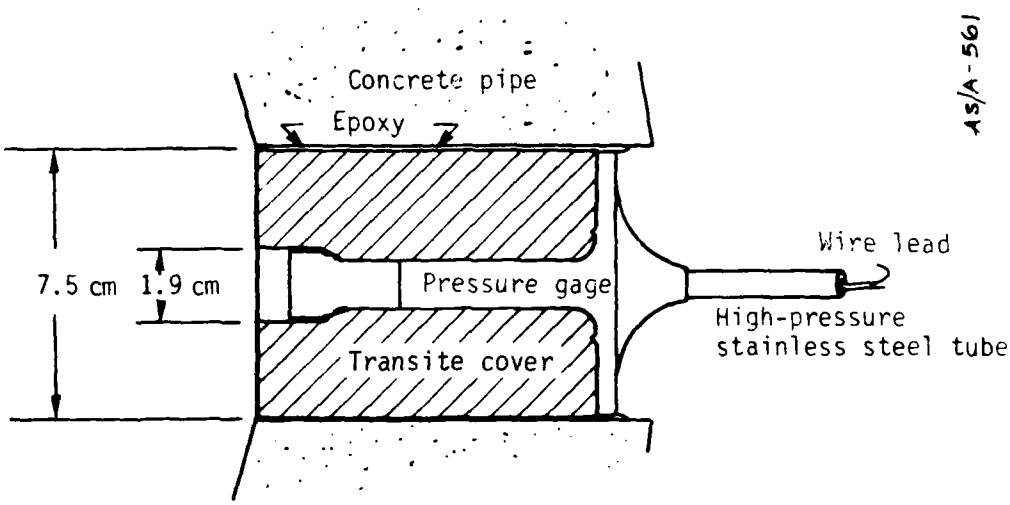

Figure 4-5. KSC pressure transducer schematic.

expansion. The pressure mount was designed such that the average density of the mount matched the concrete pipe wall. However, the gross mismatch between the pipe wall material and the steel rod which held the transducer element could cause the gage assembly to move slower than the surrounding material, and hence be directly exposed to the plasma flow. This exposure could result in destruction of the gage assembly.

Another critical issue was cable survival. The signal cable exited the gage canister within 30 cm of the pipe wall. The transition from the rigid steel gage assembly to the signal cable is very important because a mismatch at this location would result in cable failure caused by shear. This effect was minimized by the design of a signal cable in the shape of a helix, thereby reducing the possibility of relative motion between the gage assembly and the signal cable.

4.2.3.4 Fluid Coupled Plate (FCP) Gage

Pipe flow pressure measurements in the 1 to 5 kb range were obtained by Sandia Laboratories, Albuquerque (SLA) using their standard FCP technique (Reference 11). This pressure transducer has been used on several tests and is a standard SLA pressure measurement technique.

Since these gages have a relatively low dynamic response limit inherent in the gage design, they could only be used near the ends of the test pipes. The small, 5 cm port diameter gage has an upper limit of 2 kb and the large, 15 cm port diameter gage has an upper limit of 5 kb.

Large differential motions between the expanding pipe wall and the gage assembly would cause problems similar to those already outlined in the discussions of the SRI flatpac gage and the KSC pressure transducers. In addition, these gages are also located on the outside of the test pipe wall and must be corrected to obtain pipe flow pressure histories.

4.2.3.5 Ytterbium and Manganin Pressure Gage

Sandia Laboratories also fielded Ytterbium and Manganin piezoresistive pressure gages along the outside wall of the pipes. These pressure gages consisted of 50 ohm wire grids cast in epoxy and potted in grout. The Ytterbium gage was designed to measure pressure-time history in the 10 to 20 kb region. The Manganin gages have an upper response limit of a few hundred kilobars. There are no particular problems associated with this type of gage, and the sensing grids were located far enough away from the source region such that radiative or shock heating problems were negligible.

4.2.4 Pipe Wall Expansion

4.2.4.1 Radar Waveguide

TRW fielded a microwave waveguide system on HYBLA GOLD to measure the radial displacement of the pipe wall during pipe expansion (Reference 18). An electromagnetic waveguide contains the incident propagating wave from the oscillator and a reflected wave from the moving target. The target is a thin metal plate attached to the wall of the test pipe. The interaction of these two waves is a standing wave with the waveguide wavelength. The velocity of the moving target, which is assumed to be equal to the particle velocity of the expanded wall material, is determined by the known waveguide wavelength and the time interval between voltage nodes observed at the detector.

The principle advantage of the waveguide system is that the sensor can sustain major structural damage but still remain electrically continuous. Furthermore, dielectric constant changes can be tolerated because of the proper design of the waveguide core dimensions, dielectric materials, and excitation frequency.

The waveguide sensor design is shown in Figure 4-6. The waveguide design included two systems; the dielectric-dielectric waveguide, and the metal waveguide with dielectric filler. The dielectric-dielectric waveguide has been successfully fielded on high-explosive tests in which polystyrene was used for the outer sheath and then filled with a powder which has a much higher dielectric constant. The advantage of this system is that nearly all the energy propagated down the guide is confined to the core. The metal waveguide was simply a metal rectangular core filled with Teflon as the dielectric material. Teflon was chosen because its hugoniot is the best approximation of the surrounding grout. The metal waveguide had not been tested prior to HYBLA GOLD. The advantages of the metal waveguide are its simplicity, low cost, and small cross-sectional area.

One outstanding issue not addressed in HE tests is the effect of the distortion of the waveguide during the severe pipe wall expansion. Numerical calculations to determine the change in waveguide wavelength associated with the dimensional changes that could occur were made at TRW. Based on these calculations, proper orientation and size of the rectangular waveguide was determined to minimize any effects (Reference 19). Another potential issue is the possibility of rupturing the end cap on the metal waveguide which could cause spurious reflections and/or loss of power. Laboratory tests were completed by TRW to determine the effects of waveguide distortion; however, the necessary experiments to investigate the effect of tearing the outer metal sheath were not conducted.

All tests conducted prior to HYBLA GOLD used waveguides less than 0.6 m long. The waveguides on HYBLA GOLD were approximately 1.8 m long. It was very important that attenuation measurements be made prior to HYBLA GOLD execution to ensure that the expected signal levels are adequate. These

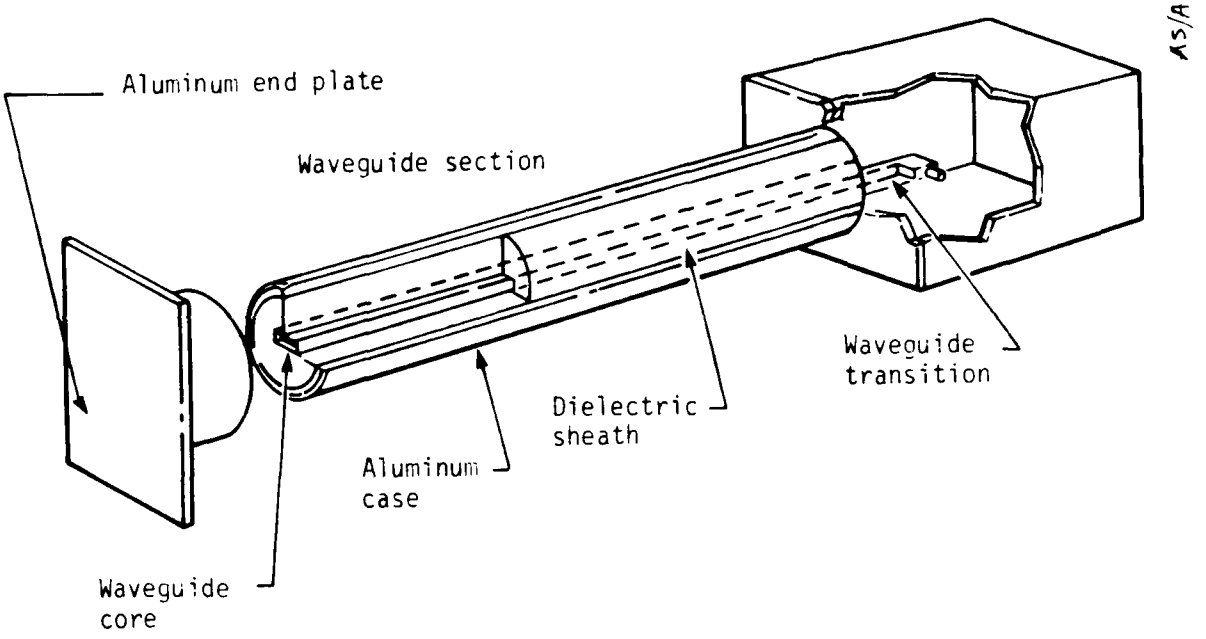

Figure 4-6. TRW waveguide experiment packaging.

measurements were not fully completed because of time constraints. It should be noted that the signal attenuation increases exponentially with waveguide wavelength.

4.2.4.2 Electromagnetic Pipe Expansion Gage

Another measurement technique to determine pipe wall expansion was developed by SSS for HYBLA GOLD. This system was not a state-of-the-art technique and was regarded as an instrumentation development experiment. A schematic of the gage operation is illustrated in Figure 4-7 (Reference 12). An oscillator drives a current through a coaxial cable which is terminated by a loop of wire concentric with the pipe wall. A thin metal conductor (aluminum, in this case) several feet long covers the outer surface of the pipe wall. During wall expansion, the inductance of the wire loop is altered by the expanding metal conductor due to the induced eddy currents. As the inductance changes, the impedance at the input to the coaxial cable is changed, thus producing a voltage-versus-time output. Based on preshot laboratory calibrations and calculations, the voltage signal can be converted into a pipe wall displacement dimension resulting in a wall displacement-versus-time measurement.

Although the theory involved in this system is relatively simple, a major issue associated with analyzing the data is how the electrical conductivity of the grout surrounding the medal conducting cylinder and the wire loop will effect the measurement. Calculations indicated that large signal attentuations could occur if the conductivity was too high ($\sim 400\,\Omega\,cm^{-1}$). In addition, the conductivity of the grout could change during the test time due to radiative heating and/or a high-pressure shock passing through the grout. Any changes in conductivity that might occur during the test time would not be measured.

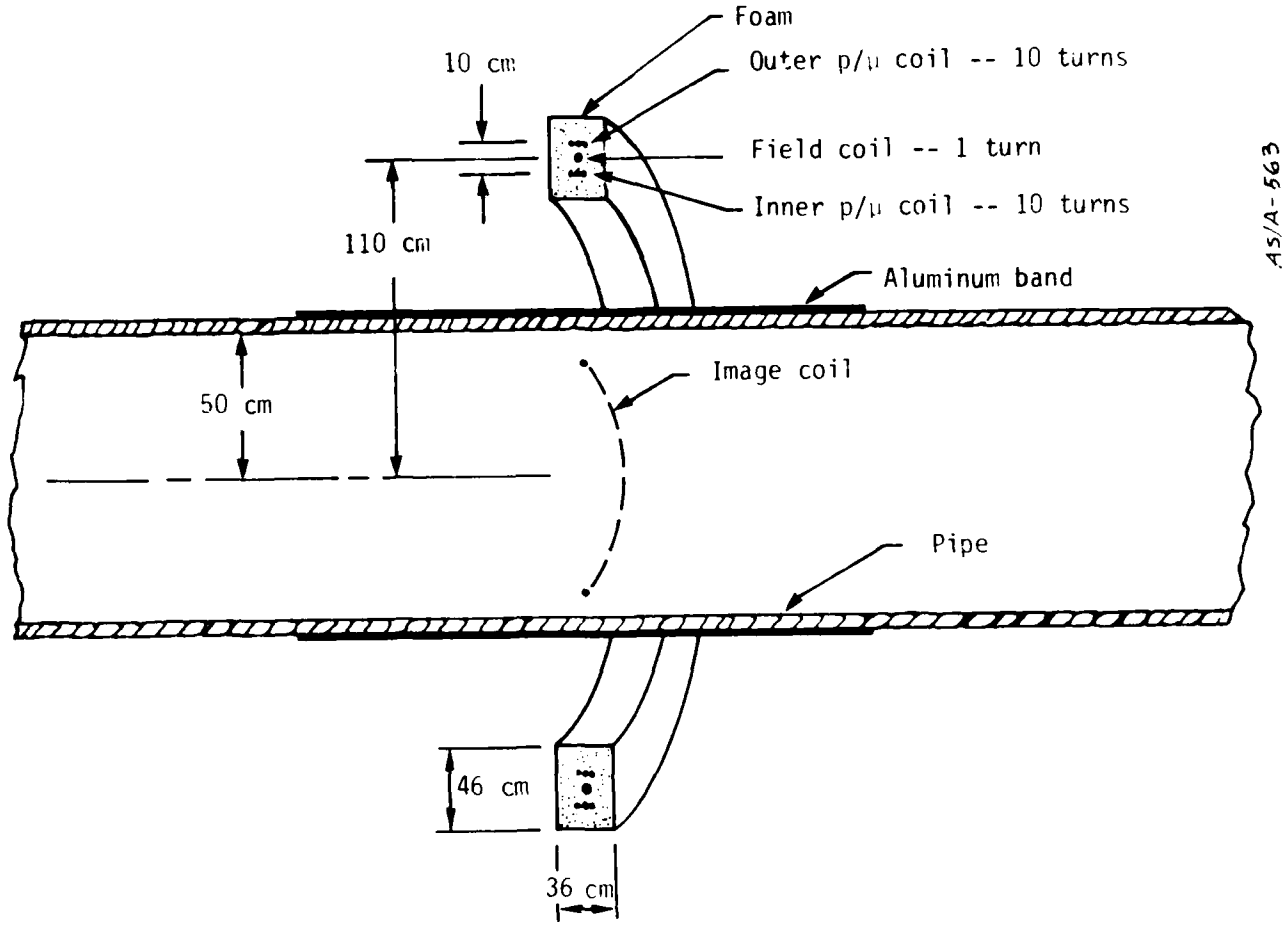

Figure 4-7. S^3 pipe wall expansion gage.

The in-situ calibration of the gage was not accomplished prior to test execution because of schedule constraints. The only in-situ measurement performed was the self-inductance of the current loop prior to and subsequent to the grout emplacement. The lack of this information could contribute to a large uncertainty in the reduced wall displacement data.

4.2.5 End Plug Debris

High-velocity, solid debris which could arrive at the downstream end of the pipes was to be measured by SSS using a stacked plate arrangement similar to that used on the HYBLA FAIR test. The detector consists of a stacked array of aluminum plates, nonuniform in width. An array of flat ribbon conductors embedded in an insulating material was placed between the aluminum plates. A schematic of this arrangement is shown in Figure 4-8.

When a high-velocity solid particle strikes the front of the array, a crater is produced which will short any conductor that is either sufficiently crushed or broken. Hypervelocity impact theory allows us to determine the approximate size of the incoming particle based on the size of the crater produced. The detectors configured for the HYBLA FAIR event could only indicate the first particle that arrived since all the conductors were interconnected. The HYBLA GOLD design was revised to permit the measurement of more than one impact, provided that subsequent impacts did not occur in the same area (Reference 20).

Survivability is the major issue associated with this measurement technique. The paths of the ribbon conductors as they exit the stacked array is the most critical element of the gage design since these thin ribbons will fail in shear quite easily. Differential motions between the

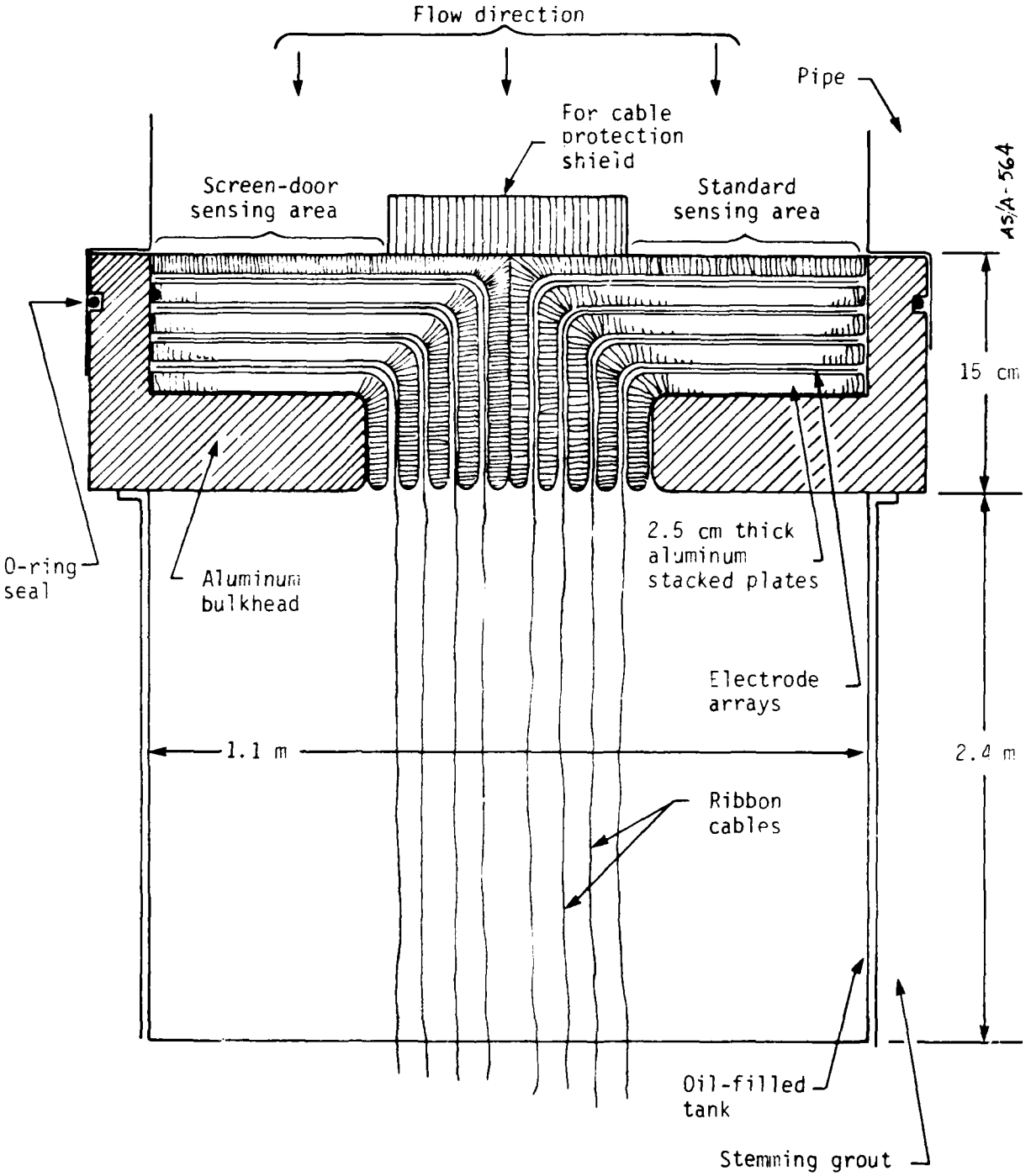

Figure 4-8. S^3 stacked plate debris gage, section view.

plates could cause failure in shear at any of the several locations where the ribbons are bent prior to exiting. Differential motions between the entire end plug and the surrounding medium could cause failure at the exit point. In addition, the ribbon conductors are concentrated in a 5 cm wide strip as they exit the array, thus allowing a single impact in this area to short a majority of the conductors and produce erroneous signals. These issues were not resolved prior to test execution.

4.2.6 Ground Shock Measurements

Measurements of the pressure history in the source and close-in pipe region were made by SRI and SLA using Manganin gages similar to those developed for the HUSKY PUP event. These gages consisted of low-resistance (0.05 to 1.0Ω) Manganin foils embedded in cylinders of grout. The foil was bonded between thin sheets of fuzed quartz to insulate the Manganin from the surrounding medium. These gages are capable of pressure measurements in the 1 Mb range.

The major issues associated with these stress gages are the combined heating effects of the Manganin from radiation and hydrodynamic shock, and the survival of the gage element and cable leads after shock arrival. The foils must be located at a sufficient distance from the source to prevent melting, yet close enough to allow for meaningful measurements of the close-coupled source to the surrounding medium. Calculations were performed to estimate the radiation environment and the close-in hydrodynamic shock; the results were used to select the stress gage locations near the zero room. One of the SRI gages was positioned very close to the predicted melting point in an attempt to determine its performance under extreme heating conditions. The remaining gages were located in a predicted benign preheat environment.

4.2.7 Instrumentation Location

The total number and individual allocation of measurements related to the ablation test pipes for the HYBLA GOLD event are shown in Table 4-2.

4.3 PRE-HYBLA GOLD HIGH-EXPLOSIVE SIMULATION EXPERIMENT

The pre-HYBLA GOLD HE simulation experiment conducted at Sandia Laboratories was designed to simulate peak pressures typical of those predicted for a region of the HYBLA GOLD nuclear event (Reference 21). However, the axial velocity, impulse, and particle displacements predicted could not be achieved in an HE experiment. Hence, the HE experiment represents only a limited test of the HYBLA GOLD instrumentation.

4.3.1 HE Experiment Configuration

A 140 kg charge of comp C4 high explosive (HE) was placed coaxially inside a 0.91 m diameter concrete pipe as shown in Figure 4-9. The pipe was placed vertically below the ground surface and surrounded by grout. Water filled the space between the charge and the pipe wall to increase the impulse and duration of the propagated shock. The number and types of gages installed, and their locations are given in Table 4-3 (Reference 21). The installed gages are shown in Figure 4-10.

4.3.2 HE Experiment Calculation

A calculation of the HE experiment was carried out by Mr. R. Bass of Sandia Laboratories using CSQ, a two-dimensional hydrodynamic code (Reference 22). Individual gage location profiles were not included. The calculated pressure profile at a point 60 cm above the charge base predicted a peak pressure in the first wall zone of 14 kb, arriving at about 140 μsec after HE initiation (Figure 4-11). The pressure profile is constant over approximately a 60 cm vertical band (0.3 to 0.9 m above the charge base). A peak particle velocity of 0.25 mm/μsec was also predicted

TABLE 4-2. HYBLA GOLD GAGE LOCATION

Agency	Gage Type	Measurement	Zero Room	0.91 m Smooth Pipe	0.3 m Rib Pipe	0.3 m Smooth Pipe	0.3 m H2O Pipe	0.15 m Smooth Pipe	Total No.
LASL	TDR	TOA	2	5	2	3	2	1	15
SSS	Bar-WC/Ti	P vs t		4	2	2	2	2	12
	Bar-steel	P vs t		9	1	1	1	1	13
	Ablation pin	Wall ablation		12	3	3	3	4	25
	Expansion	Wall motion		3	1	-	-	-	4
	Debris	Particle		2	-	1	1	-	4
	Precursor	Shock front TOA		1	1	1	1	-	4
SRI	Mn, grout	Stress vs t	6	-	-	-	-	-	6
	Flatpac, Yb	P vs t		5	2	3	2	3	15
	Flatpac, Mn	P vs t		9	4	5	4	3	25
	Ablation pin	Wall ablation		5	2	2	2	-	11
KSC	Press. transducer	P vs t		4	4	4	3	3	18
TRW	Waveguide	Wall motion		5	1	3	2	1	12
SLA	Mn, grout	Stress vs t	3	-	-	-	-	-	3
	Mn, pipe flow	P vs t		1	1	1	1	1	5
	Yt, pipe flow	P vs t		5	2	2	2	2	13
	FCP, 6-in. dia	P vs t		3	-	-	-	-	3
	FCP, 2-in. dia	P vs t		-	2	2	2	-	6
	Slifer	TOA		2	2	2	2	1	9
Total			11	75	30	35	30	22	203

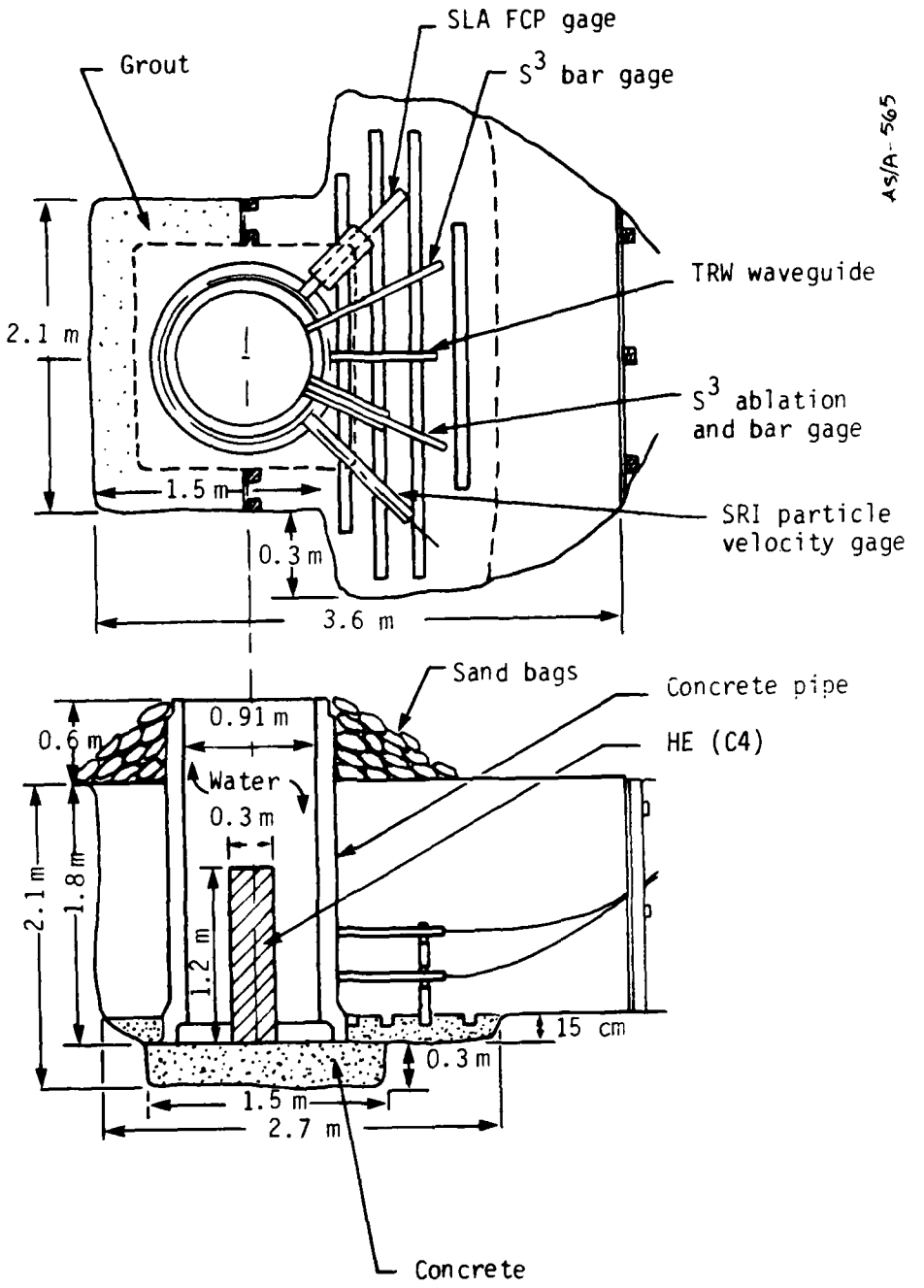

Figure 4-9. Pre-HYBLA GOLD HE experiment, test bed configuration.

TABLE 4-3. INSTRUMENTATION INSTALLED ON PRE-HYBLA GOLD EVENT

No.	Designation	Type	Arc Dist. from Pipe CL, mm	Dist. from Bottom of Pipe, mm
1	KSC-D-1	Diaphragm	-152	1524
2	KSC-D-2	Diaphragm	+152	1511
3	KSC-D-3	Diaphragm	+203	1486
4	SRI/SLA-Man	Manganin	+120	550
5	SRI-PV	Particle velocity	-495	457
6	SRI-Man-1	Manganin	-500	1000
7	SRI-Yb-1	Ytterbium	+120	800
8	SRI-ABX	Ablation	+260	768
9	SSS-BG-1	Bar gage	-254	762
10	SSS-BG-2	Bar gage	+254	457
11	SSS-ABX	Ablation	-254	457
12	TRW-1	Waveguide	0	603
13	TRW-2	Waveguide	0	857
14	SLA-Yb-1	Ytterbium, FCP	+445	470
15	SLA-Yb-2	Ytterbium, FCP	+445	470
16	SLA-Yb-3	Ytterbium	+406	648
17	SLA-Yb-4	Ytterbium	0	444
18	SLA-Yb-5	Ytterbium	+711	635
19	SLA-PV	Particle velocity	+559	686

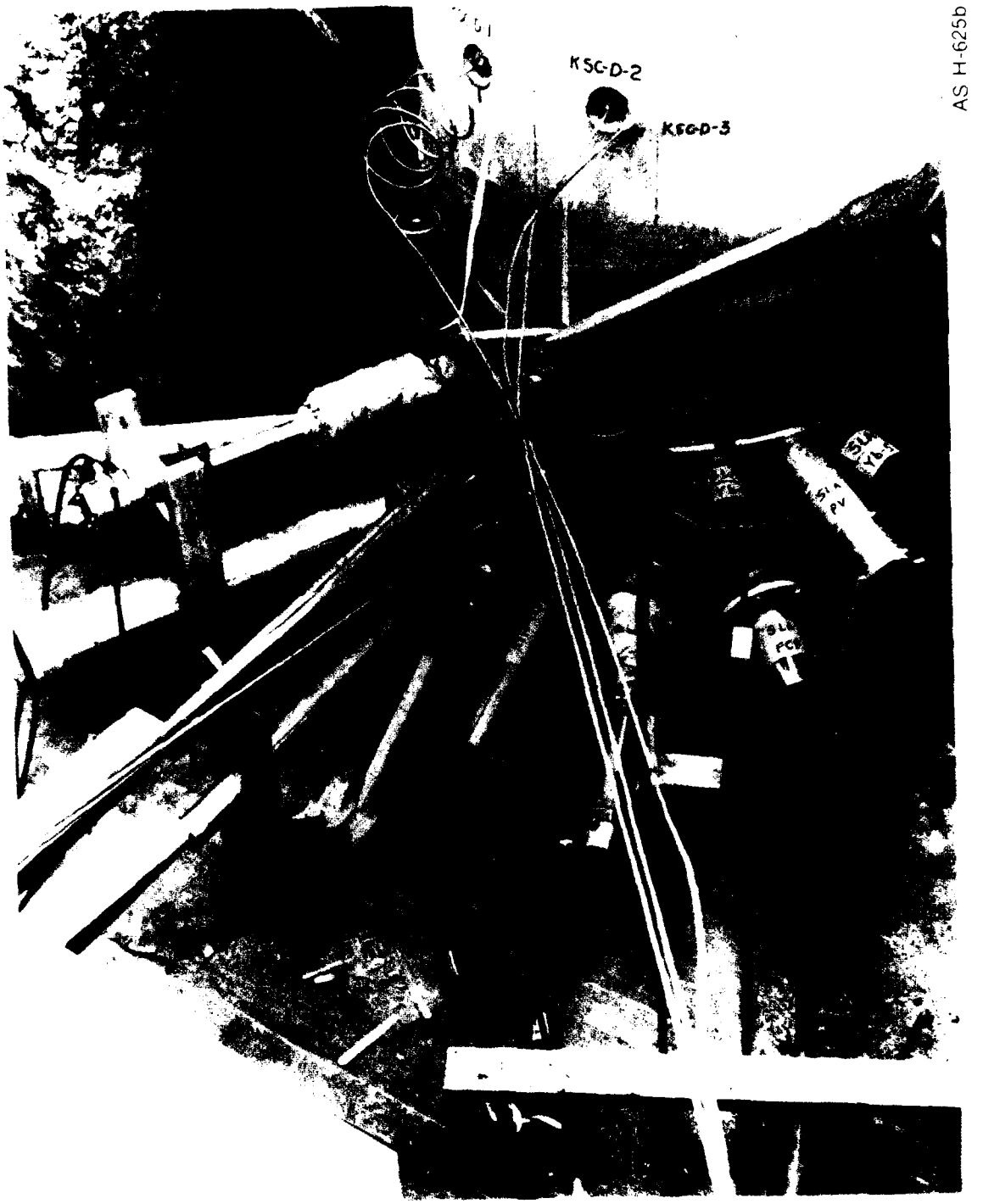

Figure 4-10. Pre-HYBLA GOLD HE experiment, instrumentation layout.

at this location. All of the instrumentation, except the KSC diaphragm pressure gages, were located in this 60 cm vertical band.

The KSC diaphragm pressure gages were located 150 cm above the charge base where a peak pressure of 4.8 kb was predicted, arriving at about 240 μsec after HE initiation. At this location, the shock intersects the pipe wall at a 40 degree angle from the vertical.

4.3.3 HE Experiment Results

A summary of the experiment and test results is shown in Table 4-4 (Reference 23). The results are further depicted in Figure 4-12 (TOA data), and Figure 4-13 (stress versus distance). The TOA data indicate a shock velocity of about 2.2 mm/μsec in the grout. The stress levels fall on a curve that can be approximated by the equation:

$$\sigma(kb) = 3.8R(m)^{-2.5}$$

as compared to the predicted curve:

$$\sigma(kb) = 3.8R(m)^{-1.6}$$

The test achieved the desired goal of exercising the various gage systems and the quantitative results are in essential internal agreement.

A brief summary of the individual experiment results follow.

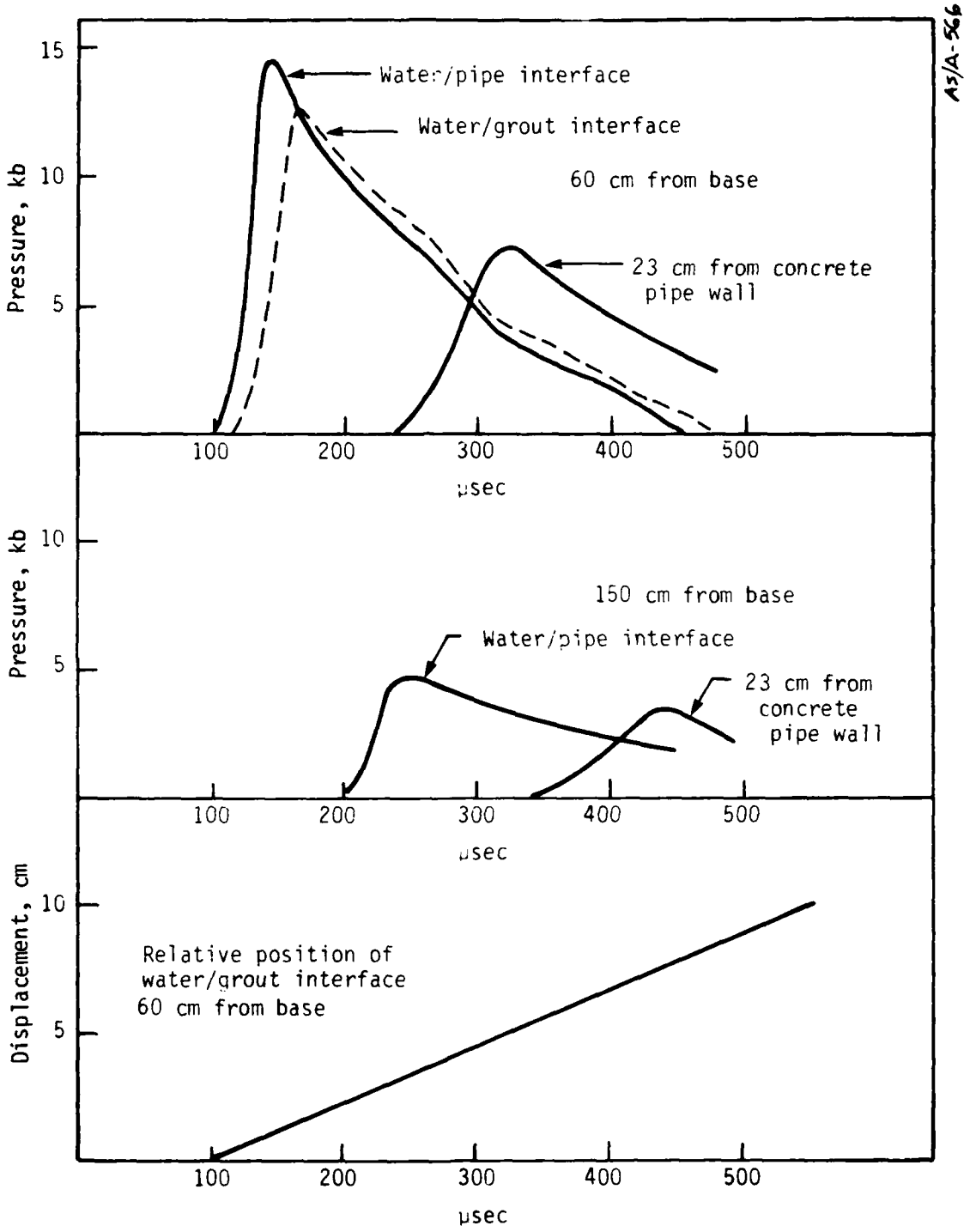

Figure 4-11. Pre-HYBLA GOLD HE experiment calculation.

TABLE 4-4. PRE-HYBLA GOLD HE TEST RESULTS

Agency	Experiment	Peak Predicted,* kb	Peak Measured, kb	Record Duration, μsec	Remarks
SRI	Ytterbium pressure gage	~7.0	13	800	Mounted between 100 mil Fe plates. Good record with small amount of "ringing" during rise. Gage did not break.
SLA	Ytterbium pressure gage	8.5	16.5	230	Good pressure record until gage broke.
SLA	Ytterbium pressure gage	8.5	17.5	160	Good pressure record for 160 μsec. No indication of gage breaking.
SLA	Ytterbium pressure gage	7.0	10	130	Structure of waveform at peak and at later times not understood. No evidence of gage breaking. Unusual behavior possibly due to motion of waveguide ~5 cm from this gage.
SRI	Manganin pressure gage	8.5	No data	0	Mounted between 200 mil Al plates. Failed at HE zero time apparently due to electrical malfunction.
SLA	Fluid-coupled plate gage	5.5	11.0	0	Off-scale due to higher-than-predicted pressures. Bellows and cable failure occurred after shock arrival.
SLA	Manganin gage	8.5	No data	0	Failed on shock arrival.
SLA	Particle velocity gage	0.025 cm/μsec	0.035 cm/μsec	77	Recorded until shock arrival at cable broke current to gage.
SRI	Particle velocity gage	0.025 cm/μsec	Off-scale	0	Gage driven to band edge on shock arrival due to excessive motion.
S^3	Bar pressure gage	12.5	24	~35	Anamolous second shock structure at 30 μsec.
S^3	Bar pressure gage	12.5	21	~55	Anamolous second shock structure at 30 μsec.

*Calculation by R. Bass, Sandia Laboratories

TABLE 4-4. (CONTINUED)

Agency	Experiment	Peak Predicted,* kb	Peak Measured, kb	Record Duration, μsec	Remarks
KSC	Diaphragm pressure gage	5.0	No data	0	Apparent failure of diaphragm and cable due to higher-than-excessive pressure.
KSC	Diaphragm pressure gage	5.0	No data	0	Apparent failure of diaphragm and cable due to higher-than-excessive pressure.
KSC	Cable noise	5.0	No data	0	Resistor only element meant to be baseline channel. Resistance changed during test and data not valid.
SRI	Ablation gage	N/A	N/A	300	Purpose of test was to measure gage survival time until expansion broke cables.
S^3	Ablation gage	N/A	N/A	100	Purpose of test was to measure gage survival time until expansion broke cables.
TRW	Waveguide wall motion gage	Teflon-filled metal waveguide records appear to yield shock and particle motion data.			
TRW	Waveguide wall motion gage	No data from dielectric-dielectric waveguide.			
SLA	Cavity pressure steel tubing		15		Test results showed tubing did not fail on shock arrival.

*Calculations by R. Bass, Sandia Laboratories

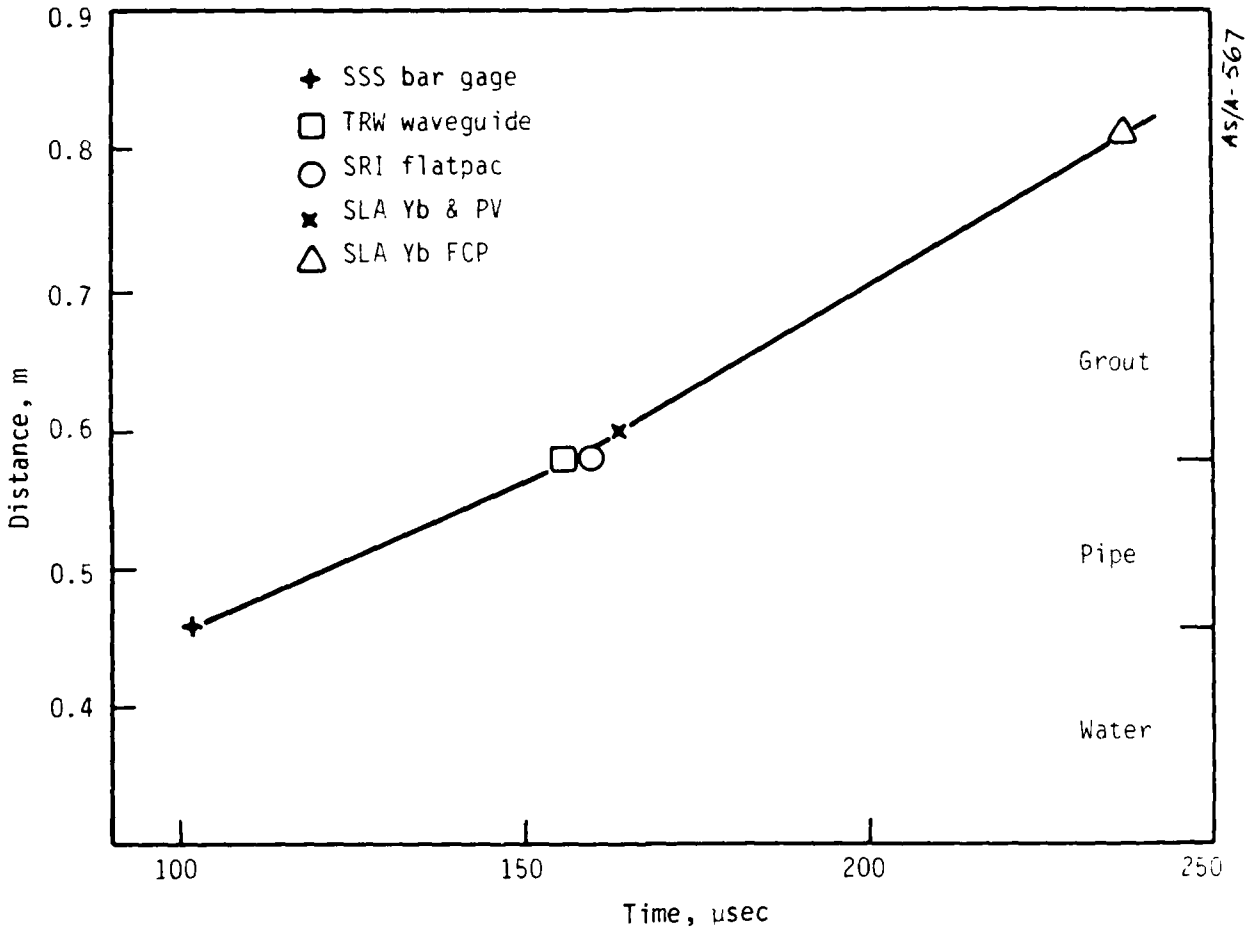

Figure 4-12. Pre-HYBLA GOLD HE experiment TOA data.

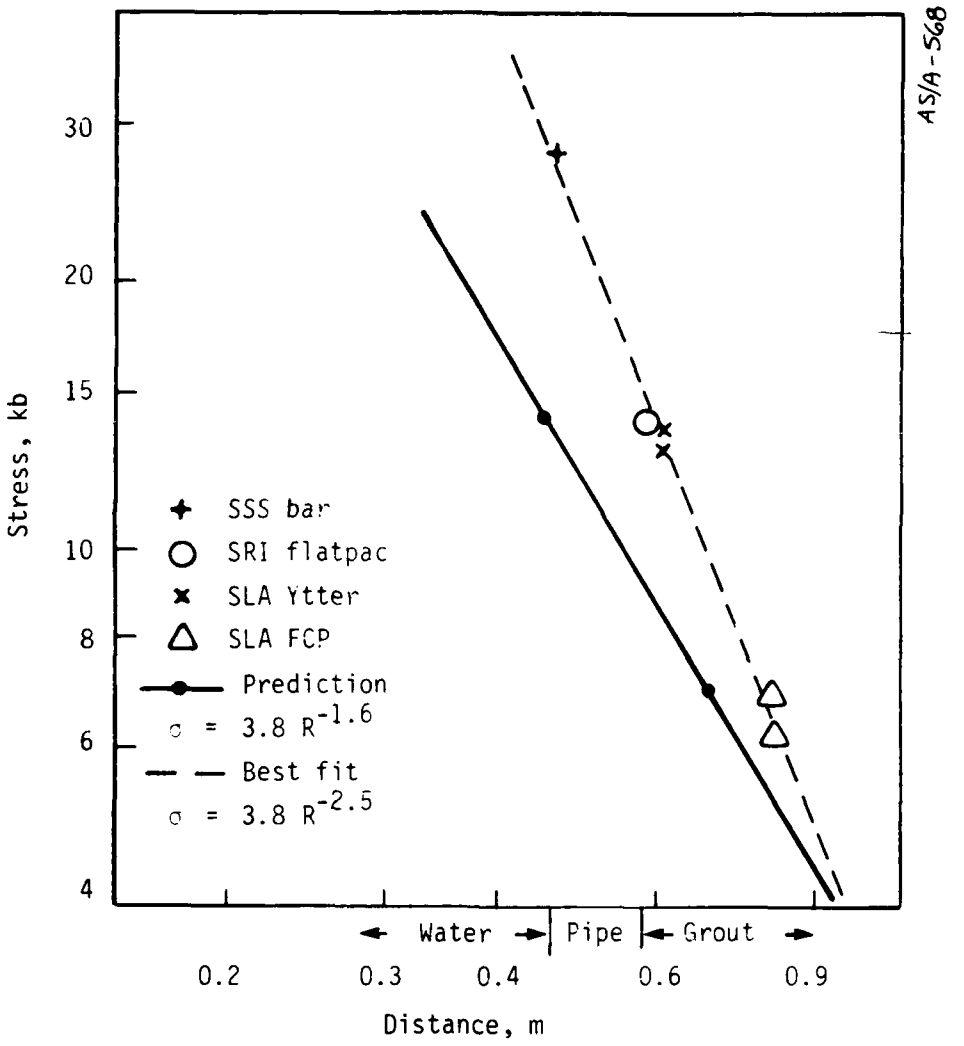

Figure 4-13. Pre-HYBLA GOLD HE experiment stress vs distance data.

4.3.3.1 Stanford Research Institute

SRI fielded a flatpac gage consisting of a Ytterbium element sandwiched between two steel plates. The data record has a peak value of 14 kb and a duration of about 300 μsec. The gage survived for 1.3 msec, at which time the ground shock reached the cable connections. No data record were obtained from the aluminum flatpac with the Manganin element. The recorder was driven to band-edge at power supply turnon. However, postshot analysis of the gage revealed that the gage was still in good condition, and it appeared that it was disconnected electrically prior to the shot.

SRI fielded a wall ablation gage which was used to measure pipe wall ablation on HYBLA GOLD. Although no ablation occurred on the HE test, the gages were installed to demonstrate survivability following shock arrival in the expanding environment. While the pipe expansion was less than that anticipated for HYBLA GOLD, the gage did perform satisfactorily in that it remained intact until the ground shock arrived at the cable leads at the end of the gage assembly.

4.3.3.2 Systems, Science and Software

SSS fielded two bar gages in the pre-HYBLA GOLD HE experiment located at the water and pipe interface. Records for both gages were similar and the recorded data was consistent with other observations at greater ranges. Both gages failed prematurely at approximately 30 μsec after shock arrival. Subsequently, a number of gage failure hypotheses were tested in the HE shots conducted at SSS. An improved lead support and the elimination of flexural wave propagation into the Ytterbium sensor element led to the design utilized on HYBLA GOLD.

AD-A095 170 ACUREX CORP/AEROTHERM MOUNTAIN VIEW CA AEROSPACE SY--ETC F/G 18/3
SUMMARY REPORT, HYBLA GOLD EVENT.(U)
NOV 79 J R STOCKTON DNA001-79-C-0404
UNCLASSIFIED ACUREX-FR-79-15-/AS(6988) DNA-5107F NL

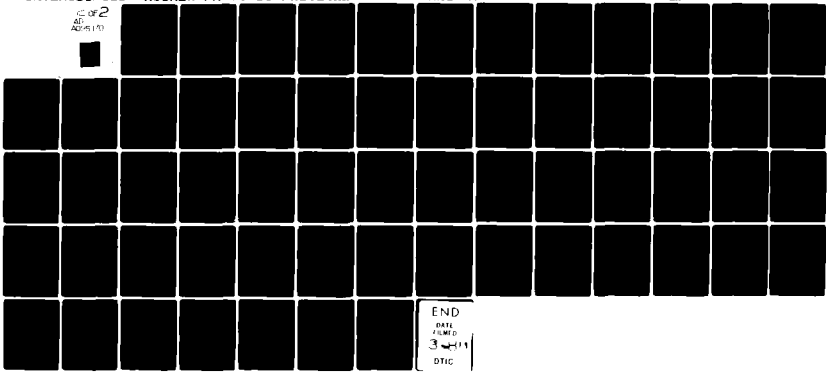

4.3.3.1 Stanford Research Institute

SRI fielded a flatpac gage consisting of a Ytterbium element sandwiched between two steel plates. The data record has a peak value of 14 kb and a duration of about 300 μsec. The gage survived for 1.3 msec, at which time the ground shock reached the cable connections. No data record were obtained from the aluminum flatpac with the Manganin element. The recorder was driven to band-edge at power supply turnon. However, postshot analysis of the gage revealed that the gage was still in good condition, and it appeared that it was disconnected electrically prior to the shot.

SRI fielded a wall ablation gage which was used to measure pipe wall ablation on HYBLA GOLD. Although no ablation occurred on the HE test, the gages were installed to demonstrate survivability following shock arrival in the expanding environment. While the pipe expansion was less than that anticipated for HYBLA GOLD, the gage did perform satisfactorily in that it remained intact until the ground shock arrived at the cable leads at the end of the gage assembly.

4.3.3.2 Systems, Science and Software

SSS fielded two bar gages in the pre-HYBLA GOLD HE experiment located at the water and pipe interface. Records for both gages were similar and the recorded data was consistent with other observations at greater ranges. Both gages failed prematurely at approximately 30 μsec after shock arrival. Subsequently, a number of gage failure hypotheses were tested in the HE shots conducted at SSS. An improved lead support and the elimination of flexural wave propagation into the Ytterbium sensor element led to the design utilized on HYBLA GOLD.

The results of the SSS wall ablation gage were similar to those indicated for the SRI ablation gage. The gage survived until the ground shock arrival at the cable connection.

4.3.3.3 Sandia Laboratories

SLA fielded three Ytterbium piezoresistive pressure gages on the HE experiment, two of which were located on the outside of the pipe wall and a third gage 0.2 m off the pipe. The two Ytterbium gages on the wall indicated peak pressures of 17 kb with pulse widths of 200 μsec. The gage 0.2 m off the pipe measured a peak pressure of 10 kb with a TOA of 230 μsec, which was nominal. The duration of all the records was consistent with ground shock TOA at the cable connectors.

One FCP containing two Ytterbium sensors was also located 0.2 m off the pipe. The records left the baseline at 240 μsec but were off-scale (10 kb) a few μsec later. This indicated that the gage response limit was exceeded, consistent with a postshot analysis which indicated evidence of strain in the Ytterbium sensors.

An end-on oriented Manganin piezoresistive gage was fielded on the pipe wall. The gage went to negative band-edge at the time of shock arrival, presumably due to a broken cable connection.

An inductively coupled particle velocity gage was fielded on the pipe wall to obtain an independent measurement of the particle velocity associated with the test configuration. A clean offset beginning at 160 μsec (shock TOA) and persisting for 77 μsec was observed, indicating a maximum particle velocity of 0.35 mm/μsec.

4.3.3.4 TRW Systems

TRW fielded two waveguides on the pre-HYBLA GOLD HE experiment; a metal rectangular guide filled with Teflon, and a dielectric-dielectric

type waveguide in which the inner core material had a large dielectric constant as compared to that of the outer sheath of polystyrene. The metal waveguide yielded both particle and shock velocity, while no data was observed on the dielectric-dielectric waveguide. The observed particle velocity from the metal waveguide was approximately a factor of three less than predicted from calculations. A thick (1.3 cm) aluminum end plate and container around the waveguide may have retarded the free-field motion of the Teflon core.

In subsequent HE experiments conducted at SSS, identical waveguides were tested and, in addition, a third dielectric-dielectric waveguide consisting of a K10 powder core enclosed in a Teflon sheath was tested. Only the metal waveguide provided data. Both shock and particle velocity were observed to be reasonably close to predicted values at 30 μsec after shock arrival. The data record at shock arrival could not be accurately resolved.

As a result of these HE tests, the waveguides fielded on HYBLA GOLD had a thin (3 mm) aluminum end plate. In addition, the majority of the waveguides (75 percent) were of the metal waveguide type.

4.3.3.5 KAMAN Sciences Corporation

KSC fielded two diaphragm pressure gages on the pipe wall at a predicted level of 5 kb. Both gages failed as a result of exposure to excessive pressures (~10 kb) which ruptured the diaphragms. Although this test was an extreme overtest of the gages, much useful information was obtained related to the failure modes of the sensor, probe, and cable assemblies. This information was applied to design modifications for HYBLA GOLD which were tested on subsequent HE shots at SSS.

4.4 HYBLA GOLD GROUNDING AND SHIELDING PLAN

The underground nuclear test program has raised many questions regarding the proper grounding and shielding techniques which should be used to obtain valid data. Many experimenters have adopted techniques based on non-nuclear environments and simple trial and error solutions that have worked on previous tests. As a result, there has never been a unified approach to the grounding and shielding problem. On HYBLA GOLD, the decision was made during the planning phase to design and implement a unified scheme required for all experimenters. A detailed discussion of the plan adopted and the rationale behind the scheme is included in Reference 24.

4.4.1 Background

On prior underground tests, significant noise has been present within the instrumentation and recording system. The dominant noise is direct irradiation of the sensors and signal cables that cause Compton replacement currents to flow on signal cable shields and center conductors. In addition to the prompt gamma-induced signal, the device-emitted neutrons generate similar signals, and captured-neutrons produce long term n-γ reactions. Other noise sources include ground current, changes in the local earth magnetic field, and signal cables exposed to atmospheric disturbances and coupling from 60 Hz power sources. The HYBLA GOLD grounding and shielding plan was directed at reducing this noise through: (1) providing return paths for radiation-induced currents that were independent of the instrumentation system, (2) minimizing noise currents reaching the signal cable shields, (3) providing methods to bleed noise signals to ground that reached the signal cable [illegible] and [illegible]ing the overall effect of the

remaining noise by spreading it over all channels. Each of these methods is discussed in the following subsections.

4.4.2 Return Current Paths

Steel cable trays in each drift provided the primary return paths for these currents. The zero room walls facing the main and auxiliary drifts were covered with a wire mesh and joined to the respective cable trays to provide a low-inductance distributive connection between these two large conductors.

4.4.3 Minimizing Noise Reaching Signal Cable Shields

All gages were required to be hardened and enclosed in Faraday cages. Solid shield cables were solid bonded both to the gage shield and the cable tray. Braided shield cables were bonded to the cable tray and enclosed in solid conduit which, in turn, was bonded to the gage shield and cable tray. Some cables are inherently noisy due to their proximity to the working point (arming and firing cables and zero room wall gages) while others carry strong signals (device reaction history experiment and driver cables). These cables required special treatment. The arming and firing cables, zero room wall gage cables, and the reaction history experiment cables were placed in a separate tray in the auxiliary drift. These trays were fully grouted to enhance the bleeding of noise signals from the cable shields and to ensure that this noise source was physically separated from the other signal cables. In the main drift, the driver cables for the pipe expansion experiment were run in separate conduits to the gages. All of these special cables rejoined the signal cable bundles at the ends of the cable trays.

A very limited number of cables, not amenable to this type of treatment because of the nature of the experiment, were positioned as far

away as possible from all other gages and signal cables to minimize their effect on the main signal cable bundle. Slifers and other exposed cables were EM shielded at the working point end.

4.4.4 Providing Bleed-Off Shield Noise

Lead shot and conductive resin areas at the portal end of each cable tray were installed to ensure good contact between all signal cable shields and their cable tray. The remaining volume of the trays was filled with grout to make the tray as lossy as possible. The cable trays were not tied to ground at individual point locations because the conductivity of the grout was considered to be high enough to provide an essentially continuous ground along the entire length. Wire mesh curtains, similar to those installed at the zero room wall, were placed perpendicular to the tray axes (the portal end of each tray) to ensure positive grounding of the trays to the tunnel boundaries.

All signal cable runs from both drifts were routed through lead shot and conductive resin pits prior to entering and after exiting the instrumentation alcoves. These pits were designed to facilitate the earth-grounding of the cable shields. In the original grounding scheme, each cable shield would have been grounded at the instrumentation alcove, but this requirement was deleted due to the high cost of modifying the existing cable plant. Cables that did not originate in the drifts (e.g., free-field ground shock measurements) passed through one or both of the grounding pits depending on their point of origin.

All cables were grounded to the unistruts at the overburden plug. Cable shields were bonded to the feedthroughs on the instrumentation recording vans. Efforts were made to make these vans as electromagnetic interference (EMI) tight as possible, including removal of all unnecessary

wiring penetrations, conductive covering of all holes, and placing emphasis on RF power filter and door gasket integrity.

4.4.5 Minimizing Common Node Residual Noise

The lead shot and conductive resin grounding pits served to spread the remaining noise over all channels to try and reduce the effect on any one channel.

4.4.6 Conclusions

The high quality of the data obtained on HYBLA GOLD would indicate that the grounding and shielding plan was successful. Cable plant ringing and other noise sources usually observed on underground nuclear tests were not observed. Although a detailed assessment of each element of the plan has not yet been completed, the overall success of the plan has demonstrated many of the basic assumptions that were used in developing a unified grounding and shielding plan. Future underground tests should include many of these same general grounding techniques specifically adapted to their particular requirements.

SECTION 5

HYBLA GOLD DATA ANALYSIS

The preceding section outlined the instrumentation fielded on the HYBLA GOLD event. This section will present the data obtained and the subsequent analysis. It is not the intent to present a detailed analysis of each gage record; rather, the intent is to present the data as a whole, then identify any existing inconsistencies. Each individual experimentor has prepared a Project Officers' Report (POR) for HYBLA GOLD. These reports contain detailed descriptions for the development, fielding, and results of all instrumentation.

Overall, 206 gages were fielded in support of HYBLA GOLD, 196 of which were operating properly. Valid data records were obtained from 103 channels. Data return would have been higher if the signal-to-noise ratios of the records had not fallen well below predictions. Signal levels were significantly lower than predicted; consequently, the magnitude of many signals was lost in the noise level. Several sources of difficulty and uncertainty are discussed in the individual PORs and are not discussed in this report.

5.1 SOURCE RELATED MEASUREMENTS

SRI International fielded Manganin ground shock gages within the zero room wall to provide data relevant to the source coupling. The records obtained were the first Manganin gage pressure-time history

records that have ever been obtained in the close-in nuclear test environment. Peak pressures exceeding 500 kb were recorded. In addition, SLA fielded similar Manganin gages which were located at or near the outside surface of the zero room wall. Figure 5-1 illustrates the TOA and peak pressure data from these Manganin stress gages. The best record was obtained at the 100 cm location (Figure 5-2). Shock wave arrival is at 150 μsec after nuclear zero. The final rise in the record is believed to be caused by gage stretching (Reference 25).

5.2 PIPE FLOW DATA -- 0.91 m PIPE

The 0.91 m diameter test pipe was the most heavily instrumented of all the test pipes. As previously mentioned, the data obtained from this test pipe would be used to increase our understanding of the relevant ablation physics. The data return (percentage of working gages) for the 0.91 m pipe was higher than any other test pipe, primarily because the signal-to-noise ratio was the largest value observed. However, the uncertainty associated with pressure levels below 5 kb is quite large for certain gage systems. The following paragraphs summarize the test data obtained and compare these data to preshot predictions.

5.2.1 Time-of-Arrival Data

Although all gages provide shock TOA, a specific measurement technique was employed to provide a continuous measurement of shock arrival instead of more widespread individual gage locations.

The LASL developed the TDR system to measure the shock front position as a function of time. The principles of the TDR operation, as well as the design, fielding, and data analysis are included in the Project Officers' Report. The location of the five TDR experiments in the

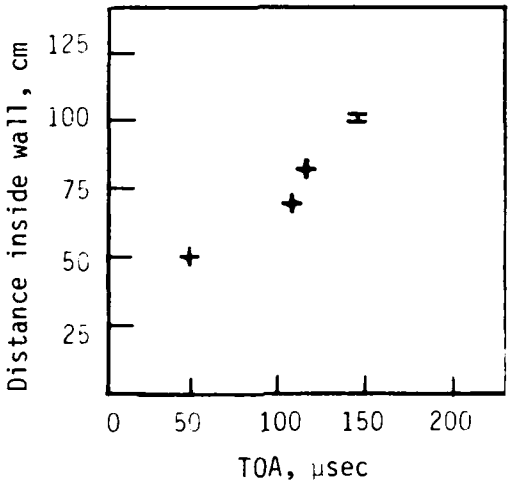

AS/A-569

(a)

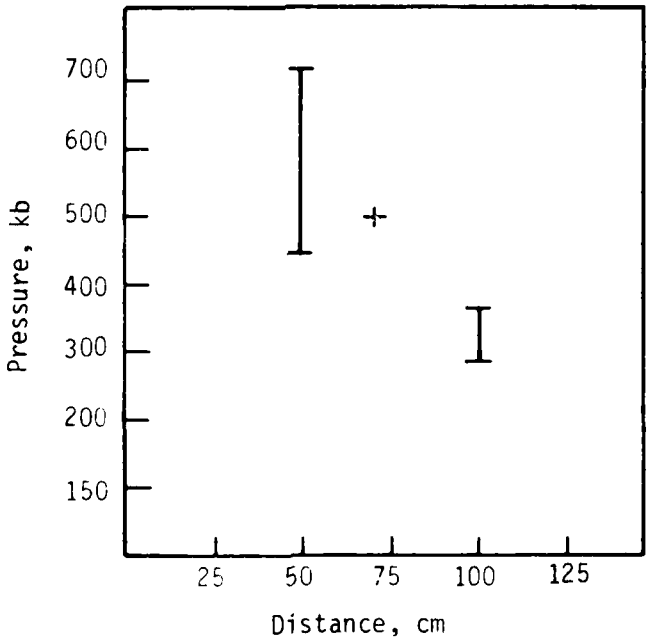

(b)

Figure 5-1. Close-in Manganin gage results.

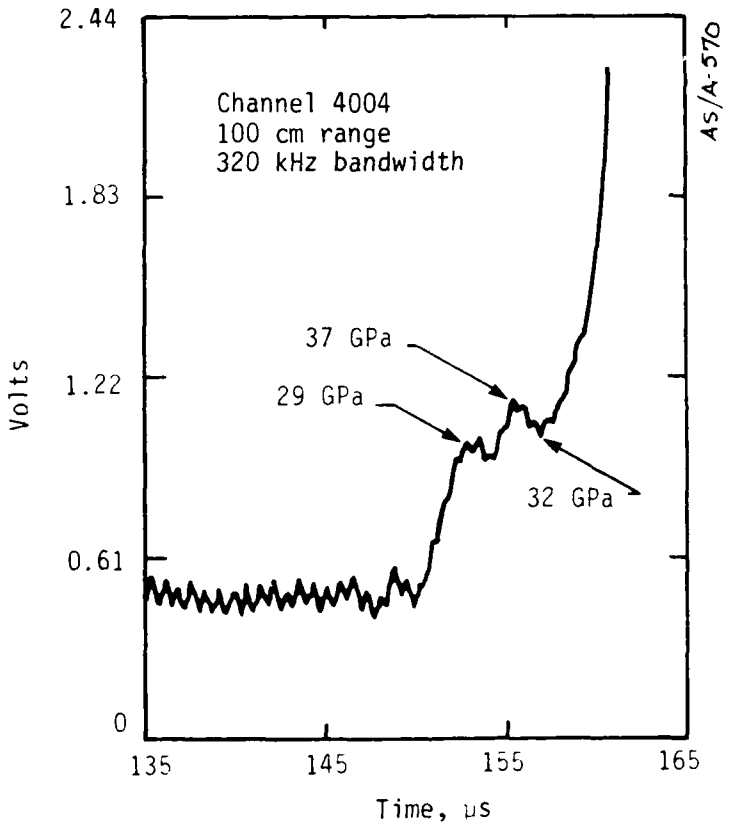

Figure 5-2. Close-in SRI Manganin gage record.

0.91 m test pipe is shown in Figure 5-3 (Reference 26). This array of cables and its associated supports did not introduce significant additional debris, but did provide a mapping of the shock front profile. One concern was the possibility of a shock front precursor; that is, the shock propagating in the heated layer near the pipe wall which could extend to greater ranges than the normal shock front. This phenomena has been observed in nearly every nuclear test. Figure 5-4 depicts the TOA data from the TDR array and shows that there was no indication of a strong thermal precursor present in the test pipe. At the end of the test pipe, SSS fielded plasma TOA sensors to detect the presence of a precursor on the pipe wall. This gage probably failed preshot, so confirmation of the LASL TDR data regarding a precursor is not available.

Individual gages also provided discrete TOA data (Figure 5-5). These gage locations were all located on the inner surface of the test pipe wall. Although there are several different experimental systems (stress, ablation, etc.) shown in Figure 5-5, the data is very consistent (References 25, 27, and 28). The line constructed is the best least squares fit to the LASL TDR data (Figure 5-4).

In addition to the in-pipe gage data, several experiments were located outside the test pipe wall in the surrounding grout. These data also provide us information concerning the shock front in the pipe and the expansion in the pipe walls. As outlined in Section 5.1.3, pipe wall pressure on the outside of the pipe was measured by SRI and Sandia Laboratories, Albuquerque (SLA). Slifer cables fielded by SLA and the LASL TDR system were located in the surrounding grout parallel to and between the test pipes, extending the entire pipe length. Figure 5-6

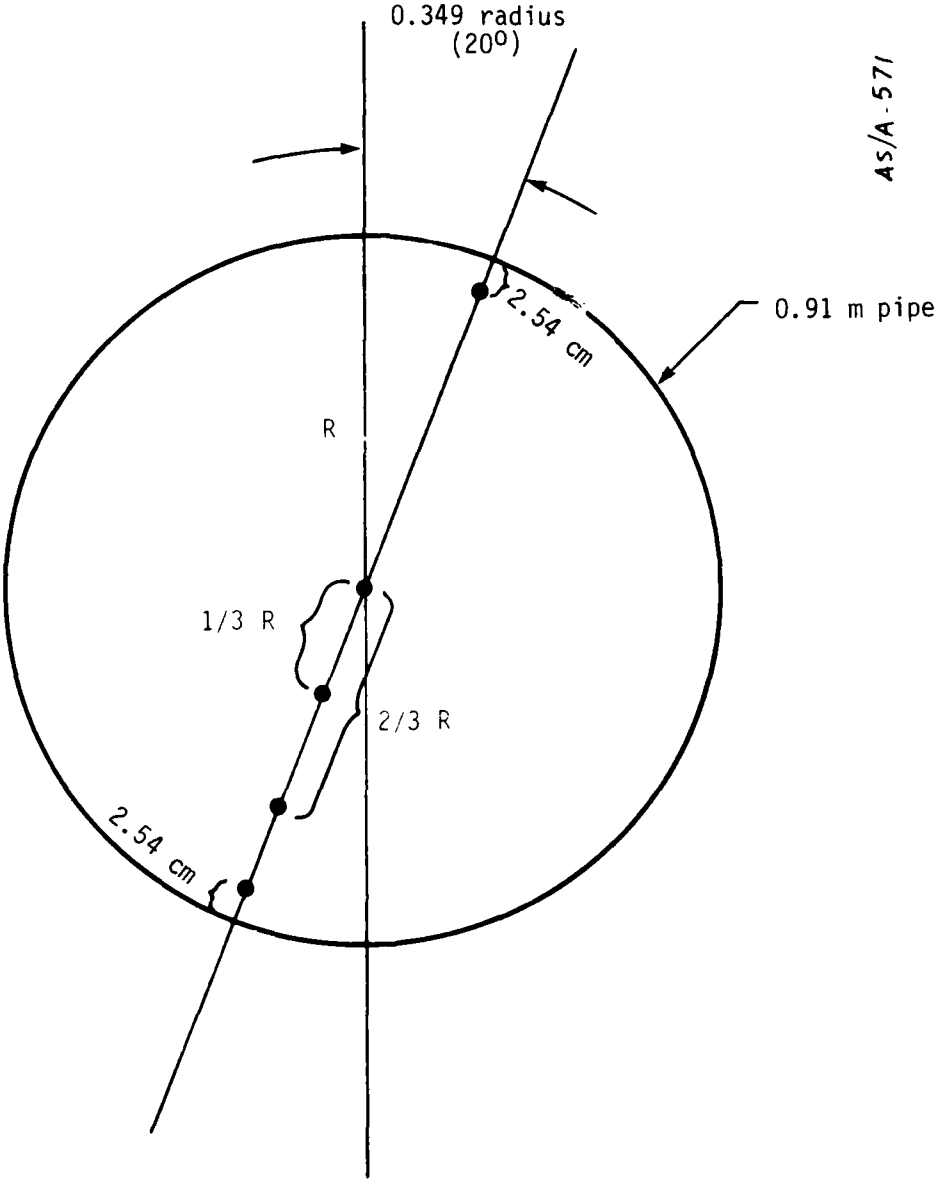

Figure 5-3. Location of LASL TDR experiment, 0.91 m pipe.

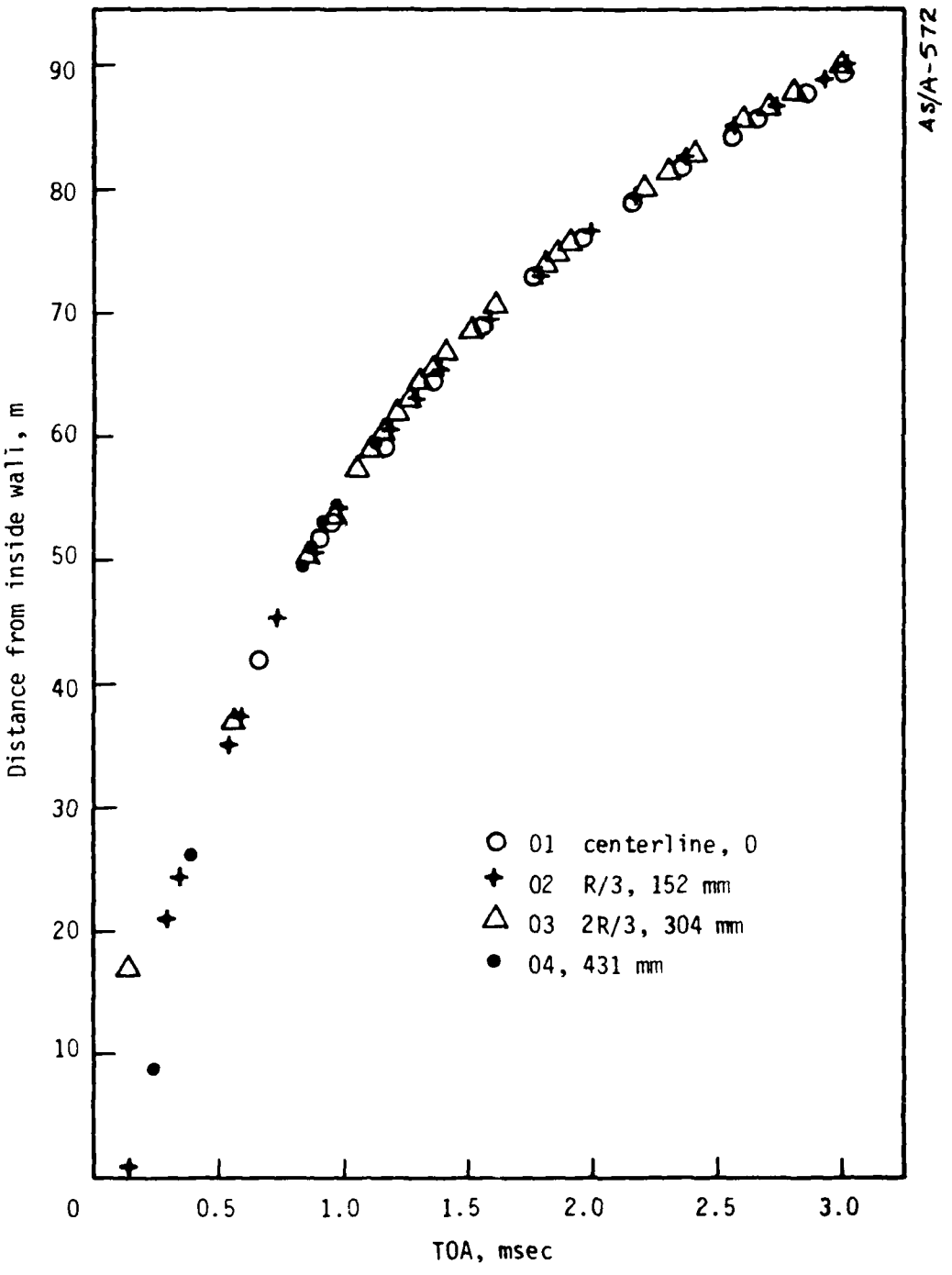

Figure 5-4. LASL TDR TOA data, 0.91 m pipe.

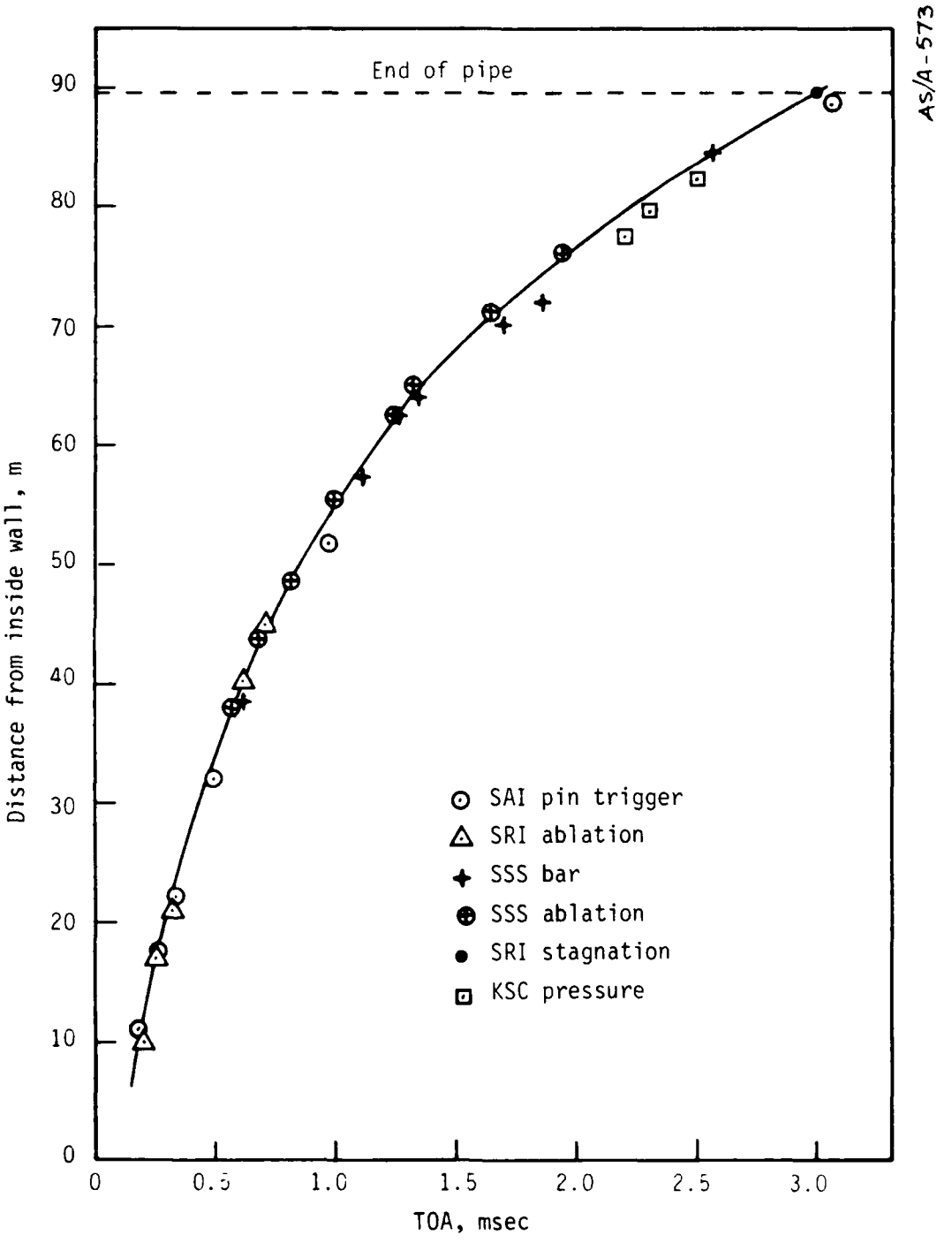

Figure 5-5. Pipe flow gage TOA data, 0.91 m pipe.

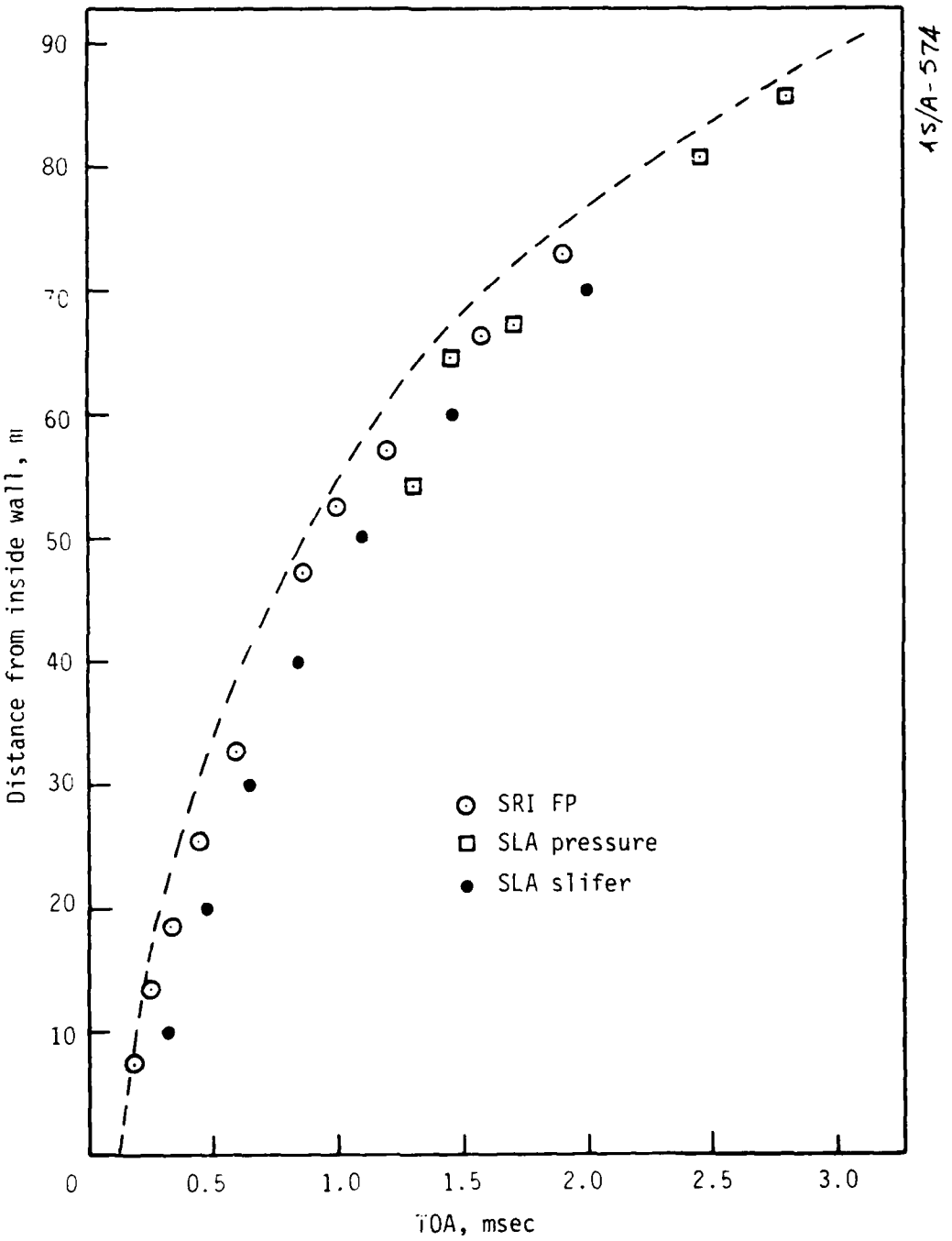

Figure 5-6. TOA data from gage locations outside pipe wall, 0.91 m pipe.

illustrates the TOA data from the aforementioned gages (References 25 and 29). The following lists the gages and their locations.

- SRI flatpac stress gages are on the outer surface of the pipe wall
- SLA Yb and pressure transducers are located 2.7 to 3.8 cm from the outer pipe wall
- SLA slifer cable are approximately 10.2 cm from the outer pipe wall

The least-squares fit to the TDR data is plotted as the dashed line to indicate the consistent relationship between the pipe flow data and the outside wall data.

Comparisons of Figures 5-4 through 5-6 are favorable and quite consistent. However, the TOA data are insufficient to understand the pipe flow and ablation effects, and the pressure-time data must be examined.

5.2.2 Pressure Attenuation

The pressure gage data obtained in HYBLA GOLD was of two varieties; pipe wall-grout interface pressure, and plasma pressure behind the shock front. The SRI flatpac gage data and the SLA Ytterbium and fluid coupled plate gages were located at the pipe wall-grout interface as indicated in the previous section. The SSS bar gages and the KSC pressure transducers were mounted flush with the inner wall of the test pipe. The pressure data obtained for each of the two groups are presented separately.

The plasma shock pressure can be calculated from the shock velocity, which is determined from the TOA data presented in Section 5.2.1. Assuming that the strong shock relationships in air are valid for

the air shock in the pipe, the shock pressure can be calculated from the relationship

$$P = \frac{2}{\gamma+1}\rho U^2$$

where P is the pressure at the shock front, ρ is the density, U is the shock velocity, and γ is the adiabatic exponent. Since many of the strong shock relations depend on the conditions of the ambient air in the pipe, the uncertainty in the density, ρ, is very important.

At an elevation of 1800 m, atmospheric pressure is about 8×10^4 Pa and the density of dry air is 1.0 kg/m^3. However, the ambient conditions in the test pipes were such that the relative humidity was closer to 100 percent and the temperature may have been as high as 80°C (based on temperature measurements in the high-strength grout at shot time). At 40°C and 100 percent relative humidity, the density of air at a pressure of 8×10^4 Pa is approximately 0.76 kg/m^3. At 80°C and 100 percent relative humidity, the density of the air is about 0.61 kg/m^3.

Using the TOA data from Figure 5-4, and the strong shock relationship, the calculated shock pressure is shown in Figure 5-7. The adiabatic exponent, γ, has been assumed to be equal to 1.3. The three curves represent the different assumptions regarding the ambient air conditions as

- dry air with ρ = 1.0 kg/m^3
- 40°C and 100 percent relative humidity with ρ = 0.76 kg/m^3
- 80°C and 100 percent relative humidity with ρ = 0.61 kg/m^3

The TOA data available at ranges less than 20 m is sparse with large uncertainties. Therefore, the calculated shock pressure shown in

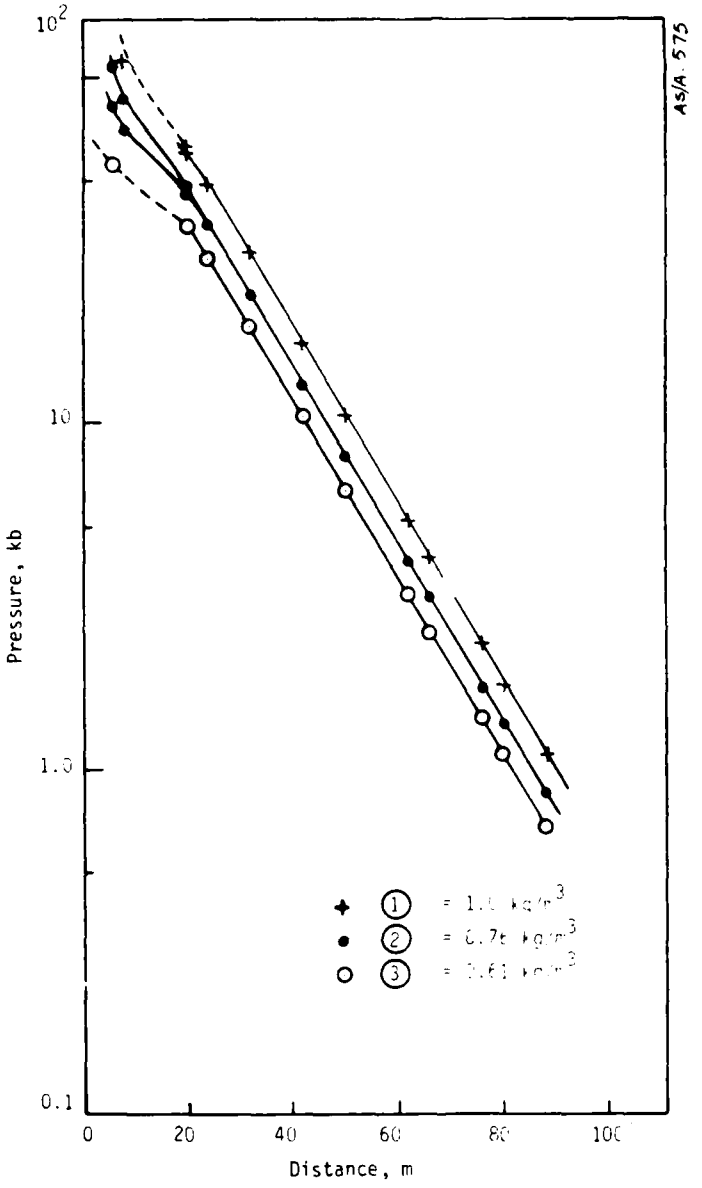

Figure 5-7. Pipe flow Hugoniot pressure derived from TDR data, 0.91 m pipe.

Figure 5-7 is also uncertain. Errors in the TOA data on the order of 10 μsec can have a large effect on the calculated shock velocity in this region. Shock velocities may be as high as 15 cm/μsec at a distance of 5 m from the pipe opening.

The peak pressure data and the associated experimental error for the SSS bar gages and the KSC pressure transducers are shown in Figure 5-8 (References 27 and 30,. The dashed line represents the curve (2) from Figure 5-7. It should be emphasized that we are comparing the peak pressure gage data with the calculated shock pressure values at a given location. The SSS peak pressure measurements are consistent with the shock velocity data. Near the end of the 0.91 m test pipe, these measurements are approximately a factor of two times greater than the KSC measurements. There is currently no explanation for the apparent discrepancy between the SSS bar gage records and the KSC pressure transducer records. The reader should refer to the KSC Project Officers' Report (Reference 30) for a description of the uncertainties in these pressure measurements.

The peak pressure data at the pipe wall-grout interface for the 0.91 m pipe are presented in Figure 5-9 (References 25 and 29). Because the concrete is an electrically lossy material, and because the grout has a lower shock impedance than the concrete, the pressure pulse recorded by these gages can differ significantly from the pressure pulse inside the pipe (plasma shock pressure). At distances greater than 40 m, the peak pressure attenuation at the pipe wall-grout interface, as measured by the SRI flatpac gages, is less than the calculated shock pressure attenuation. In contrast, the SLA pressure measurements tend to be approximately one-third the calculated shock presssure at all ranges.

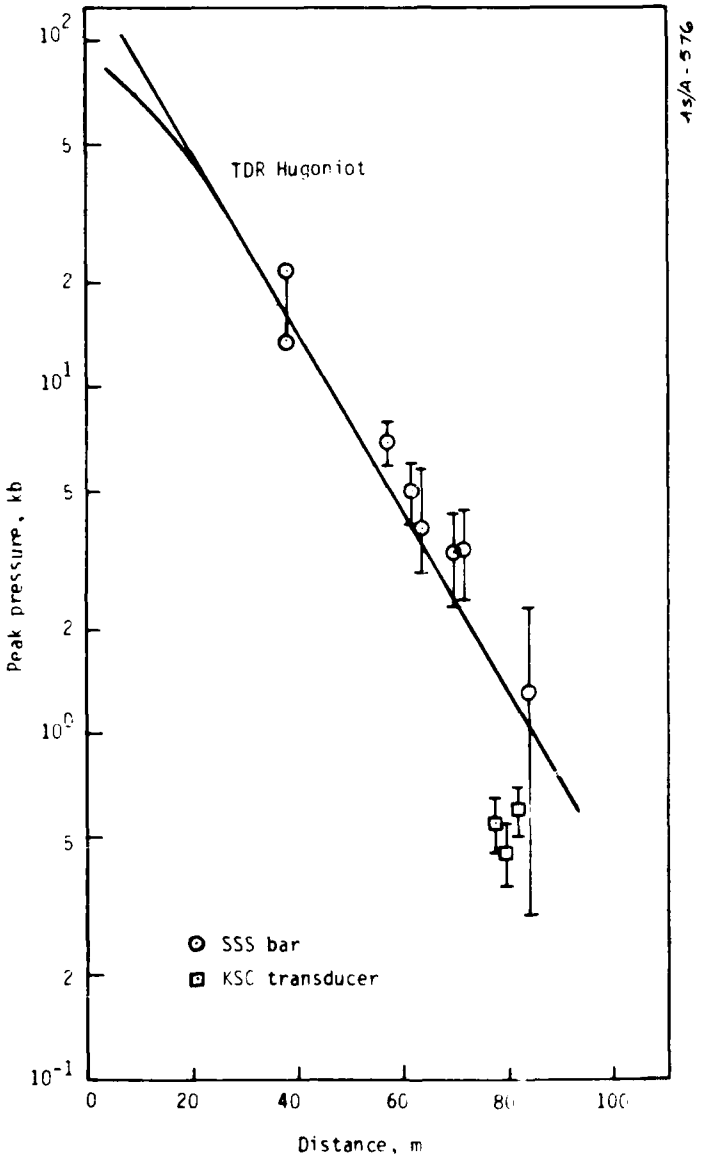

Figure 5-8. Pipe flow pressure data compared to calculated Hugoniot, 0.91 m pipe.

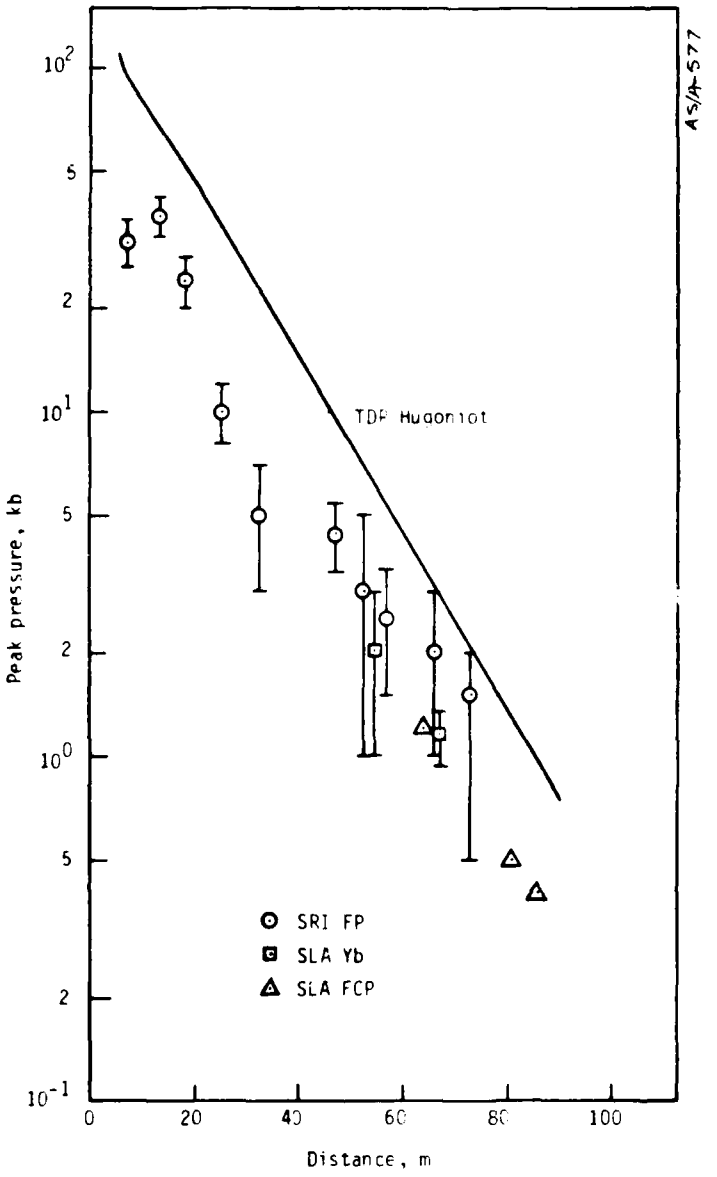

Figure 5-9. Pipe wall grout interface pressure data compared to calculated Hugoniot, 0.91 m pipe.

SRI performed a series of flyer plate experiments (Reference 25) to determine mechanical loading and release behavior in water-saturated grout (stemming material surrounding the pipes). The materials were fully saturated for these experiments, primarily because we have no way to determine the actual water content at the time of the test. The flyer plate experiments show that both materials are hysteretic (with concrete being more so), and that the saturated concrete impedance is greater than that of the grout. This impedance mismatch was also found to be stress-sensitive; greater at lower stresses (0.5 GPa) than at higher stresses (3.2 GPa). This phenomenon might aid in explaining the different attenuation rates in the plasma shock pressure and the wall-grout interface pressure measurements of SRI.

Figure 5-10 (References 25 and 27) illustrates the discrepancy between the measured waveform of the bar gages and the flatpac gages. Although they are not located at the same rarge, the waveforms are typical for each set of gages. In particular, there is a slow rise to a peak, and then nondecaying characteristics of the flatpac record. Corrections to the observed flatpac data have been made by SRI to determine the pressure profile in the pipe (Reference 25). Although these adjustments are believed to be qualitatively correct, they are, nevertheless, estimates. More quantitative and detailed estimates of the plasma pressure profile could be made via iterative calculations using the predetermined shock properties of the concrete and grout.

Stagnation pressure at the aluminum end plug was measured by SRI and SLA using Ytterbium pressure gages emplaced in the end plug. The data

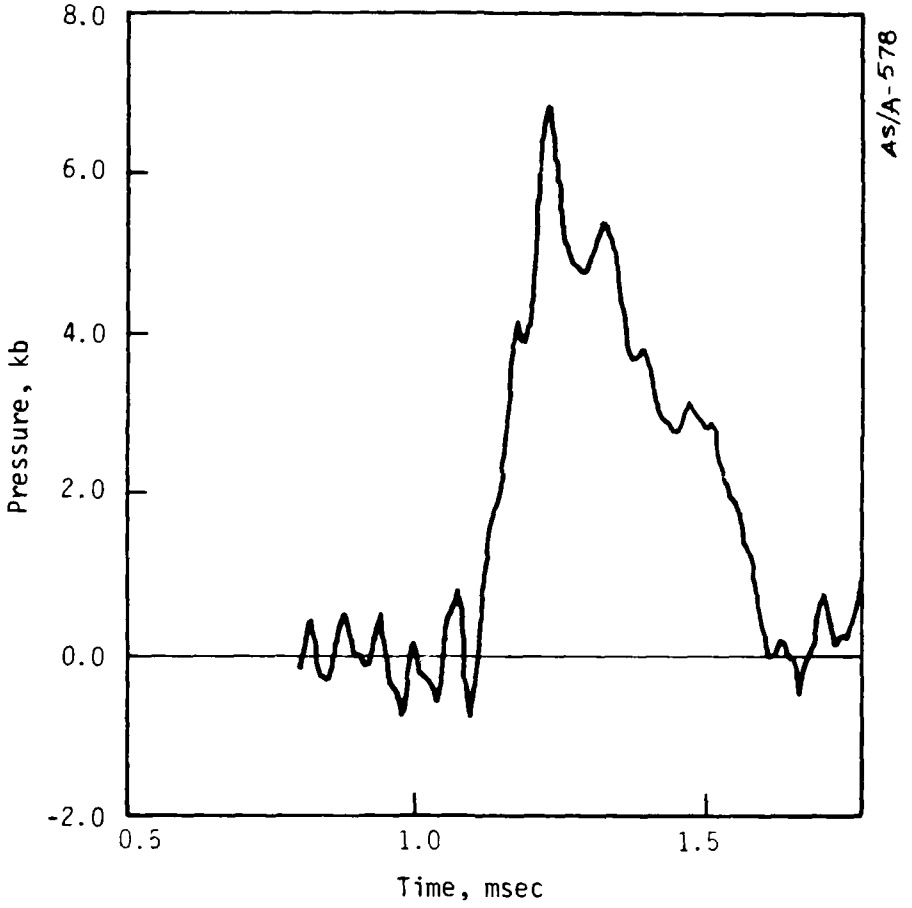

Figure 5-10(a). S^3 bar gage profile at 57.3 m range.

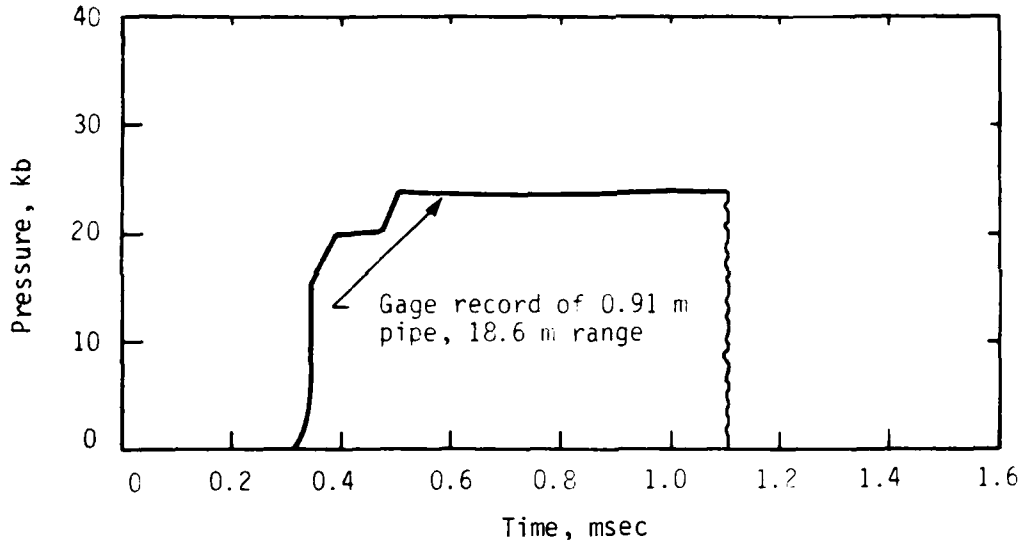

Figure 5-10(b). SRI flatpac profile at 18.6 m range.

obtained from these gages is summarized in Table 5-1 (References 25 and 27). Assuming the relationship

$$\frac{P^1}{P} \approx \frac{3\gamma-1}{\gamma-1}$$

where P is the incident pressure and P^1 represents the reflected pressure is valid, the ratio of pressures is ~9.7, for $\gamma = 1.3$. The calculated Hugoniot pressure at the end of the pipe is between 0.8 kb and 1.0 kb (Figure 5-7), which would yield a reflected pressure between 7.5 kb and 10 kb. The SRI measurement is certainly indicative of this value.

5.2.3 Rate of Ablation

The objective of the ablation gage systems fielded by S^3 and SRI was to measure the depth of ablation as a function of time. This information is important because the prediction of the pressure attenuation for the plasma flow is strongly dependent on the rate of ablation and the total mass ablated. The ablation gages were designed to provide information on the ablation rate, not the total mass ablated. The analysis and interpretation of the ablation gage records was a difficult task requiring certain assumptions regarding the plasma conditions and the gage signals themselves. Details of the analysis and interpretation of the results may be found in the Project Officers' Reports (References 25 and 27).

The S^3 ablation gage system consisted of electrodes buried at depths of 1 mm, 2 mm, and 10 mm in the test pipe wall at a given location. When the electrode was exposed by ablation to the highly conductive plasma, conduction through the plasma to a reference electrode led to a unique signal. The SRI ablation gage consisted of three

TABLE 5-1. STAGNATION PRESSURE MEASUREMENTS, 0.91 m PIPE

Gage	Location†	TOA, msec	Peak Pressure, kb
SRI 4014	1.5 mm	3.00	9 ± 3
SRI 4015	100 mm	3.02	5 + 5 - 2
SLA 3015	1.5 mm	3.05 ± 0.05	3 ± 1

†These distances are measured from the front surface of the end plug.

resistance elements embedded in the pipe wall to depths of 1 mm, 2 mm, and 3 mm. The ablation signal is produced when the circuit of the resistance element is broken by ablation or fracture. It should be noted that the element could fracture prior to ablation.

A summary of the ablation gage results is presented in Table 5-2 (References 25 and 27). The uncertainties associated with the data are such that we can only infer a maximum ablation rate at the gage locations. It can be readily seen, however, that the ablation was significantly higher than the value of 200-400 g/cm^2-sec used in the preshot prediction calculations.

5.2.4 Pipe Expansion

Only one gage gave meaningful pipe expansion data on the HYBLA GOLD experiment. The S^3 electromagnetic gage located at the 59.4 m range of the 0.91 m pipe provided information to determine the change in radius (ΔR) versus time (Figure 5-11). This curve is for the expansion of an aluminum band wrapped around the outside of the pipe and not the movement of the inner radius of the pipe wall. Figure 5-11 (Reference 27) shows that after an initial acceleration, the pipe expanded at a nearly constant velocity of approximately 330 m/sec. These data are a strong indication that the plasma pressure in the pipe remained at a high level for a long period of time. This tends to support the bar-gage records that show slow decaying pressure pulses.

No data were obtained by the waveguide gage system fielded by TRW (Reference 31).

5.2.5 Comparison with Preshot Predictions

In general, the preshot predictions of S^3 indicated high plasma shock pressures (tens of kilobars) lasting for several hundred microseconds,

TABLE 5-2. SUMMARY OF ABLATION GAGE RESULTS, 0.91 m PIPE

Range, m	Plasma Arrival, μs	Max. Ablation Rate, g/cm^2-sec	Est. Plasma Conductivity, mho/m
10.0	180 ± 20†	~9000 ± 3000	$>10^4$
12.7	≤ 239*	~8000 ± 2500	
17.1	260 ± 20†	>8000	$>10^4$
21.1	320 ± 20†	~5000	$\sim10^3$ (< 500 μs) $>10^4$ (>500 μs)
21.7	≤ 317*	~1800 ± 400	
28.5	≤ 512*	~3000 ± 800	
33.0	≤ 520*	~300 ± 20	
37.9	567 ± 10	1700 ± 240	
40.3	620 ± 20†	~900 ± 400	$\sim10^3$
43.8	684 ± 10	365 ± 56	
44.9	710 ± 30†	~1300	$\sim10^3$
48.7	817 ± 10	1460 ± 180	
55.5	996 ± 10	390 ± 40	
62.5	1246 ± 10	200 ± 10	
64.9	1325 ± 10	220 ± 20	
71.2	1645 ± 10	155 ± 5	
76.0	1942 ± 10	145 ± 5	

*Quoted as upper limit because of possible preshot lead breakage within the gage body

†TOAs estimated using TOA data from other gages

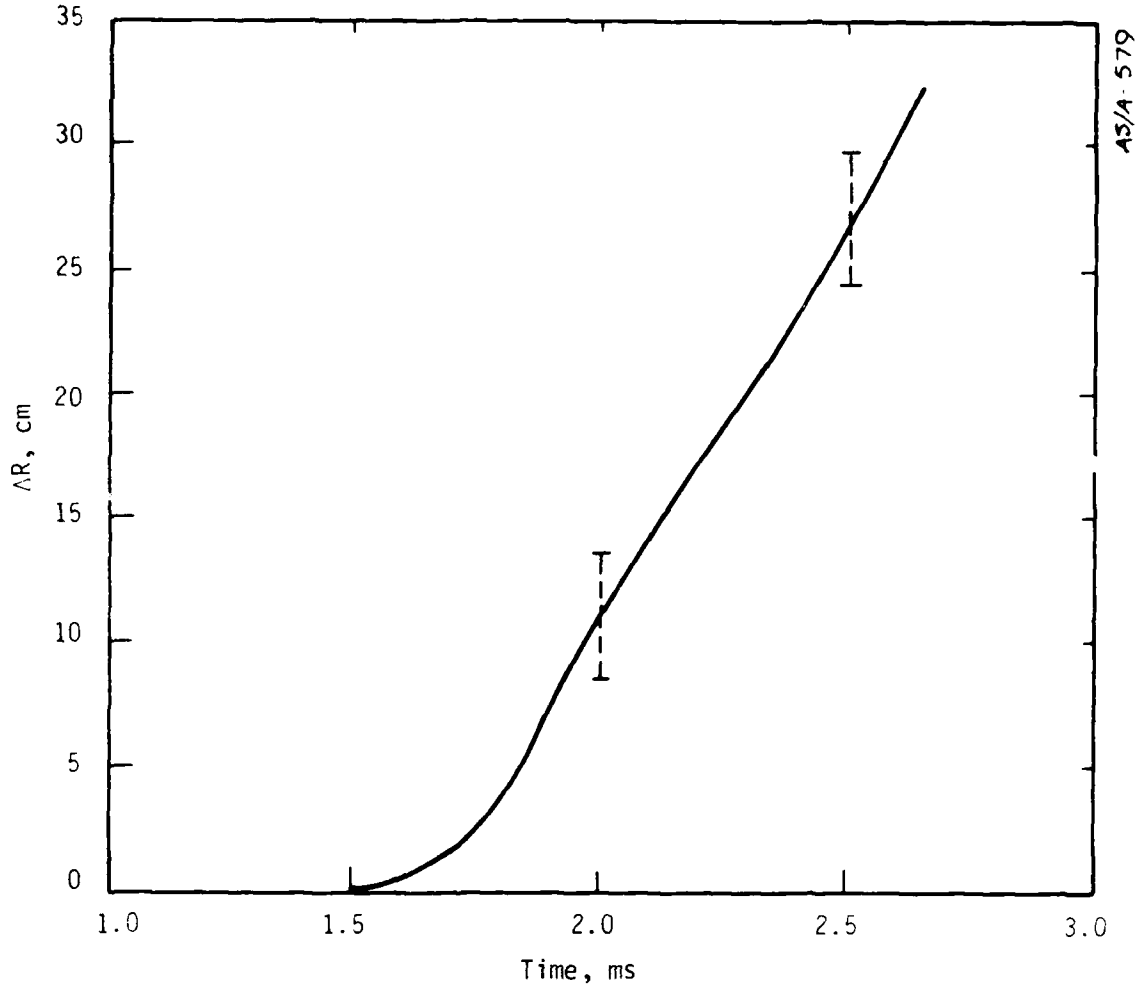

Figure 5-11. Pipe expansion vs time at 59.4 m range, 0.91 m pipe.

a small amount of ablation ($\sim$1 mm), and pipe expansion equivalent to its original diameter during the test time. As the previous sections have shown, the shock pressure attenuated quite rapidly and the indicated ablation was much greater than 1 mm. The following graphs will look at these comparisons in detail.

The shock TOA data from Figure 5-4 and the S^3 preshot prediction are compared in Figure 5-12. This comparison shows reasonable agreement between the prediction and the data. However, further examination shows that this relatively favorable comparison is indeed a false indication.

The Hugoniot pressure derived from the TOA data (Figure 5-7) and the predicted shock pressure, as a function of distance, are shown in Figure 5-13. This comparison clearly illustrates a much more rapid attenuation of pressure than was predicted. Additional confirmation of this fact is illustrated in Figure 5-14 in which the bar gage peak-pressure data is compared with the predicted shock pressure. The discrepancy in the rate of attenuation can be readily seen. It should be noted that these figures are not criticisms of the preshot predictions; the primary motivation for conducting HYBLA GOLD was the recognized uncertainties that existed in understanding, not in capabilities.

Two additional comparisons can be made between the experimental data and the preshot predictions -- pipe expansion and ablation. The predicted pipe expansion at a range of 60 m in the 0.91 m pipe is shown in Figure 5-15, as compared to the data from Figure 5-11. The prediction indicates that the pipe expands uniformily at approximately 270 m/sec, which is somewhat slower than the data would suggest. This difference

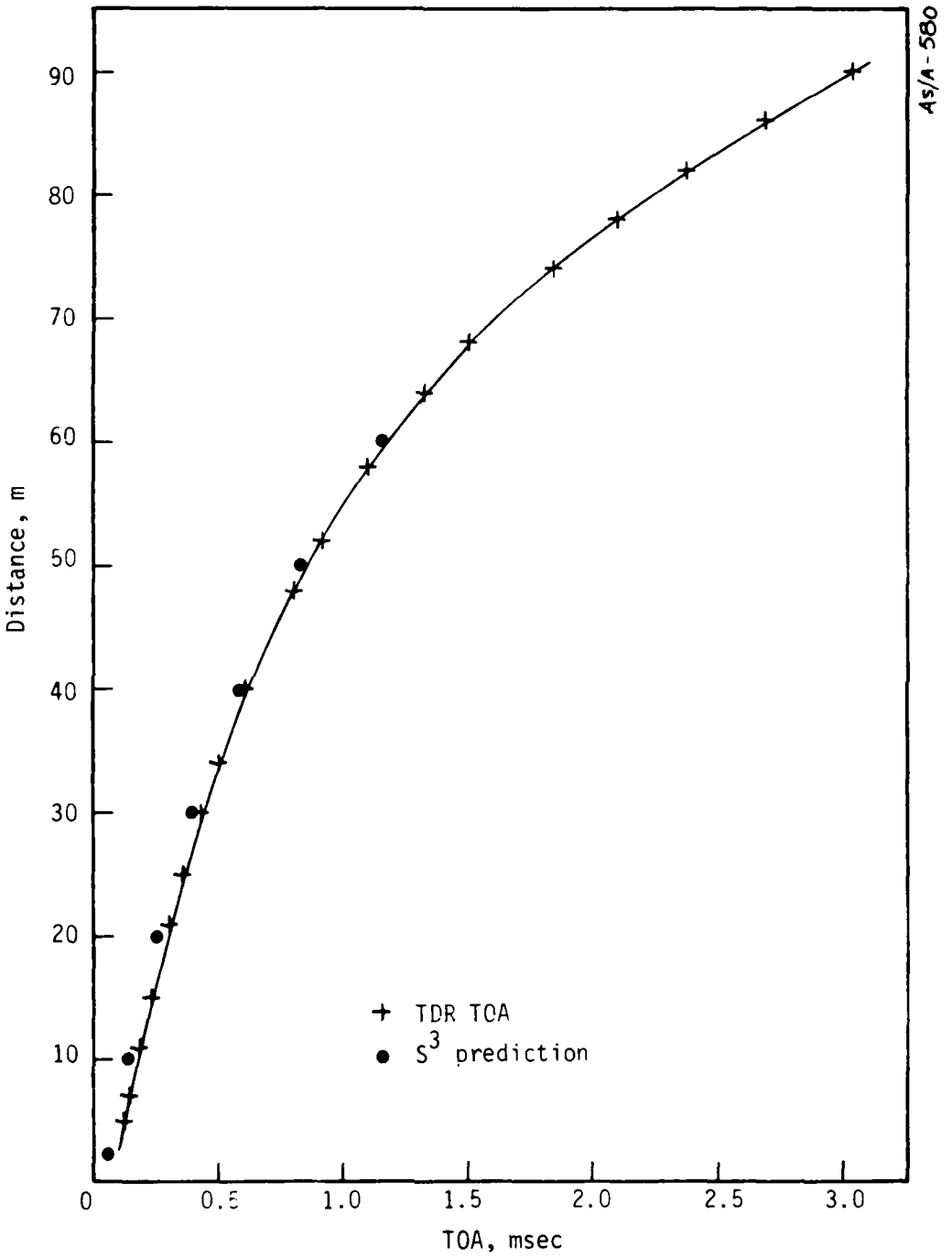

Figure 5-12. TOA data vs preshot prediction, 0.91 m pipe.

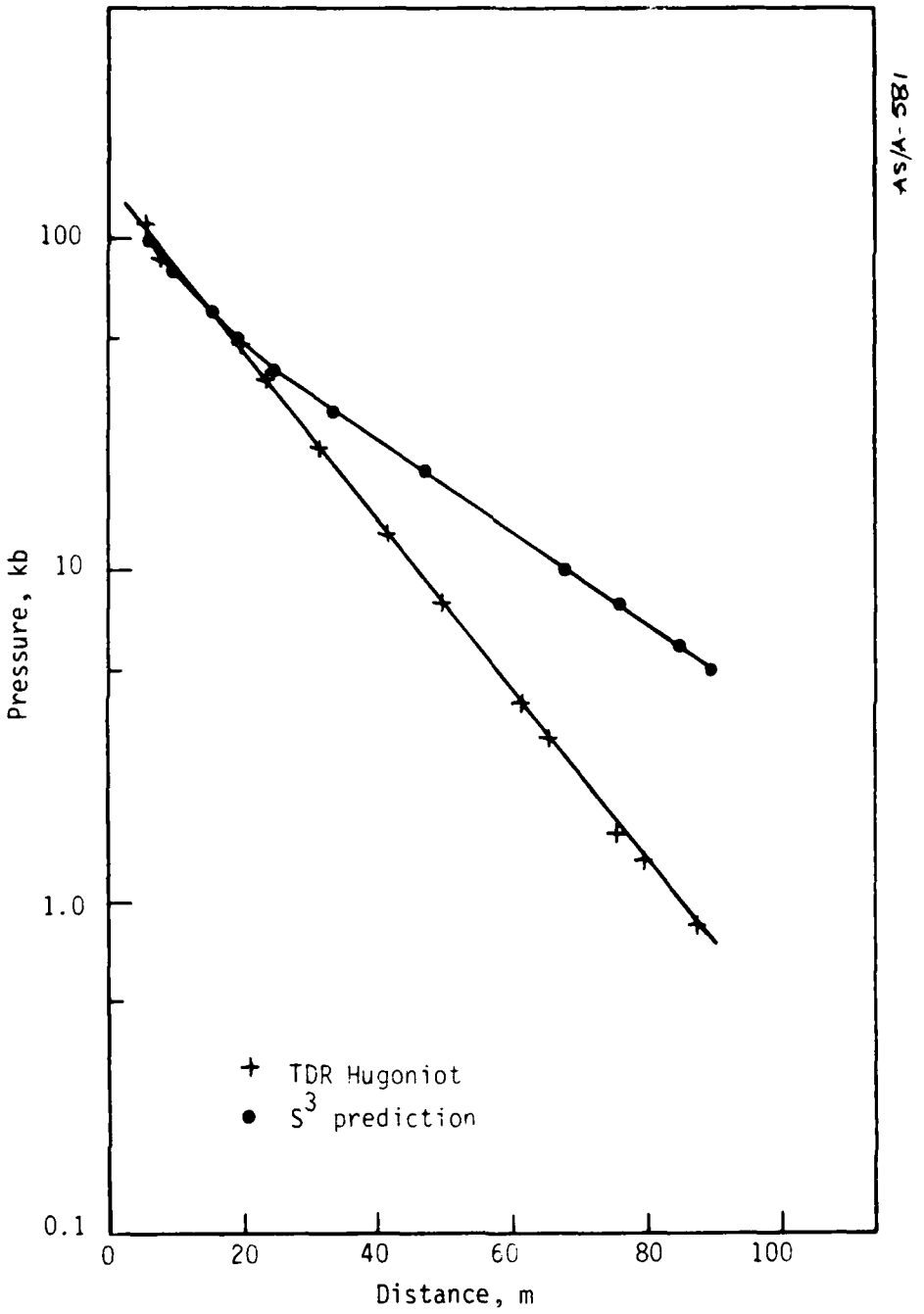

Figure 5-13. Hugoniot pressure derived from LASL TDR data vs preshot shock pressure prediction, 0.91 m pipe.

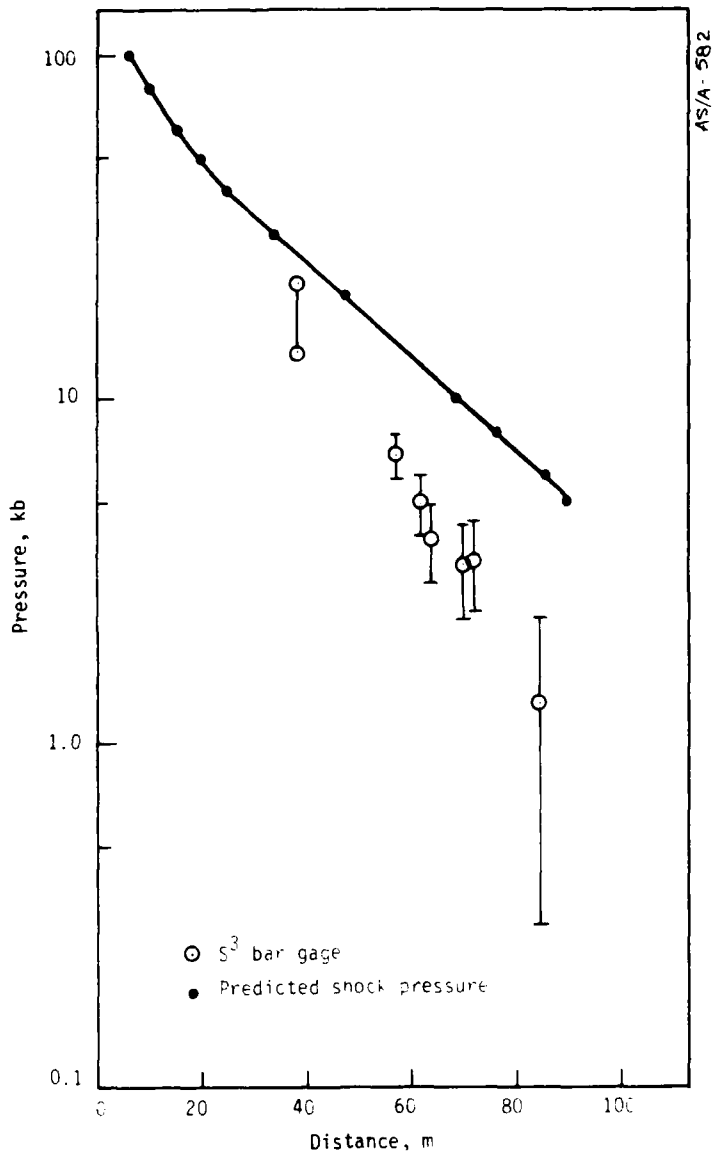

Figure 5-14. S^3 bar gage peak pressure data vs preshot shock pressure prediction, 0.91 m pipe.

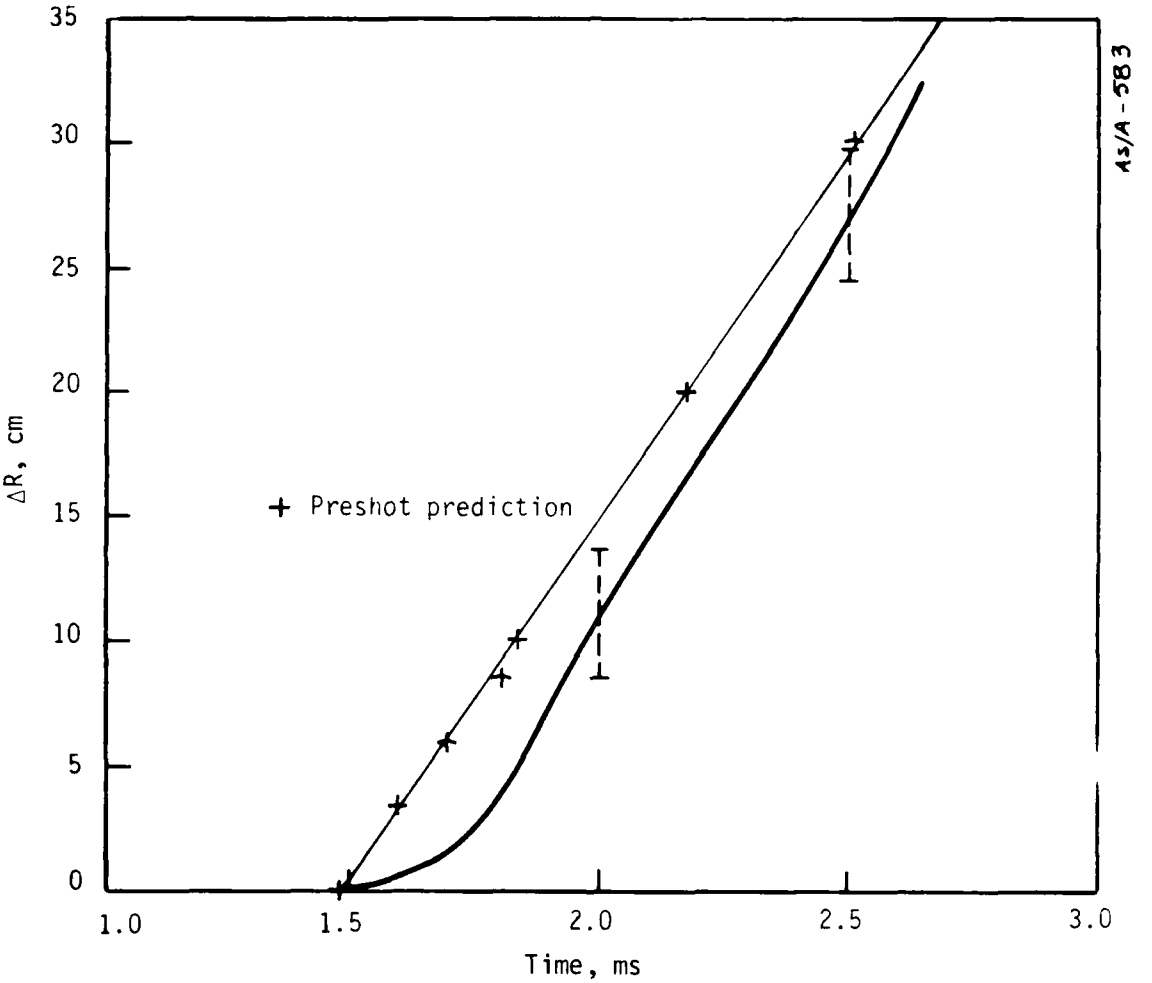

Figure 5-15. Pipe expansion data (59.4 m range) vs preshot prediction, 0.91 m pipe.

does not seem to be large enough to account for the discrepancy in pipe pressure attenuation.

The comparison of the ablation data and the predicted ablation rate is not as simple as the pipe expansion comparison. Figure 5-16 is an attempt to illustrate the apparent discrepancy between the data and the prediction. The S^3 and SRI data are plotted to indicate the time required to ablate a given depth of material at a given distance along the pipe. For example, at the 10 m range the SRI gages show the shock arriving at 180 μsec followed by the ablation of 1 mm of material at 220 μsec, 2 mm of material at 235 μsec, and 3 mm of material at 250 μsec. The S^3 gages located at the 33 m range indicates shock arrival at 520 μsec, and the ablation of at least 1 mm of material at 1360 μsec. It should be noted that the S^3 gages may be indicating as high as 10 mm of ablation at certain locations, but the only conclusion that can be drawn from the records is that at least 1 mm was ablated. Likewise, the SRI gages which indicate 3 mm of ablation before 1 or 2 mm of ablation may be the result of cracks in the pipe wall or large chunks of material being ablated at a given location. Neither of these uncertainties can be reduced or eliminated from the present data available. The curves in Figure 5-16 indicate the time necessary to ablate a given depth of material at any location along the pipe. Note that the prediction assumes a smooth continuous ablation rate as a function of time. The observation which can be drawn from this graph, with a certain degree of certainty, is that a much larger amount of material was ablated from the walls, for whatever reason, than was predicted. This could account for the more rapid attenuation of pressure as observed in the experiment.

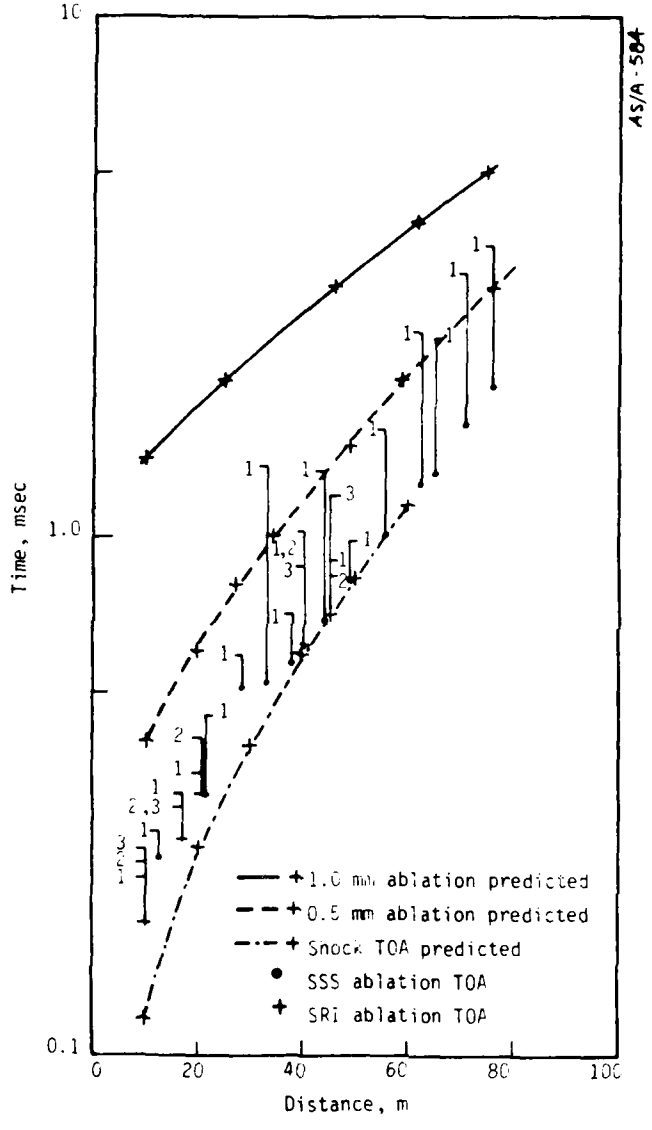

Figure 5-16. Predicted ablation depth vs time compared to data, 0.91 m pipe.

The preceding comparisons of the prediction and the measured data have all been based on absolute quantities such as peak pressure at a given location. The pressure-time history record is equally important in the analysis to improve understanding of the pipe flow characteristics. A comparison of the pressure-time records and the associated predictions is shown in Figure 5-17. The predictions are not for the exact gage locations, but rather for the 40 m and 60 m locations, respectively. The discrepancies between the waveforms are quite obvious, and it is not necessary to examine the details of the differences. Although there are uncertainties associated with the bar gage records, it is believed that the qualitative nature of the pressure-time records is substantially incorrect. The reader should refer to the S^3 Project Officers' Report for details regarding the bar gage uncertainties (Reference 27).

In summary, it is possible to conclude that the pressure attenuation in the 0.91 m pipe was much larger than originally predicted, due in part to the higher rate of ablation. Postshot analysis concentrated on different ablation models to provide a better prediction of the HYBLA GOLD experiment.

5.3 PIPE FLOW DATA -- 0.3 m PIPES

Unfortunately, data return from the 0.3 m pipes was not as high as the 0.91 m pipe. The more rapid attenuation of pressure in the flow resulted in pressure levels that were too low to detect at ranges >20 m. Therefore, the majority of the data available are TOA, not pressure-time or ablation-time histories. The TOA data does provide some insight into the flow characteristics of the three 0.3 m pipes.

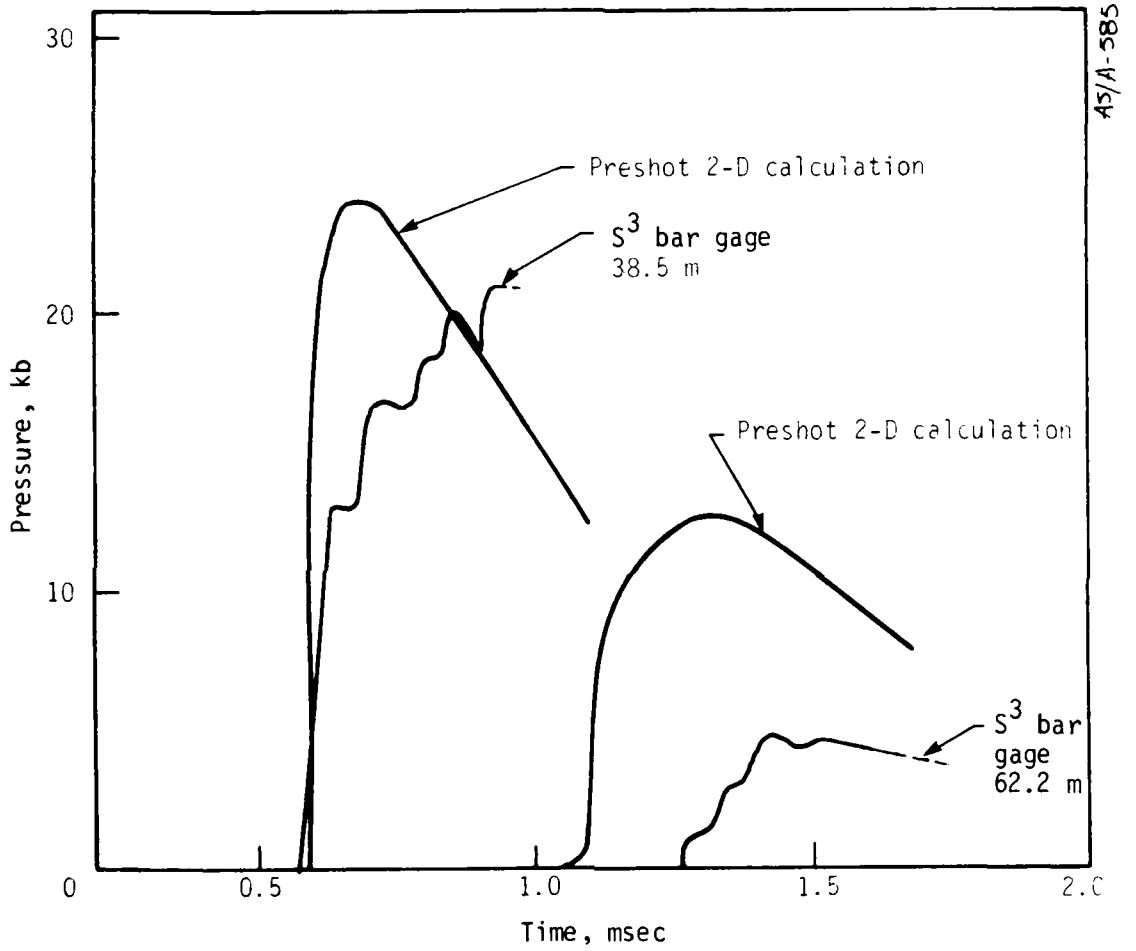

Figure 5-17. Measured pressure profiles compared to present predictions.

As previously discussed in Section 4.3.3, the three 0.3 m test pipes were identical smooth wall pipes for the first 15 m of length. Data return in this region was very sparse, including TOA data. The similarity in the initial conditions of the 0.3 m pipes is discussed in the following subsections. A more complete analysis and interpretation of the TOA data in the 0.3 m pipes was completed by the LASL personnel where significant amount of postshot testing and data analysis has been completed. This summary report does not include these details.

5.3.1 Smooth Wall 0.3 m Pipe B

The LASL TDR system is the basis for the TOA curve shown in Figure 5-18. Additional gage data has also been plotted, and agrees with the TDR data trace. The calculated shock pressure, derived from the TOA data in Figure 5-18, is depicted in Figure 5-19. Although no shocks were clearly evident at the bar gages, upper limits can be established for the shock pressure. These upper bounds have been plotted on Figure 5-19, and agree with the calculated shock pressure. Also, the SRI wall pressure measurements are approximately a factor of two less than the shock pressure, which is consistent with the results of the 0.91 m pipe data.

5.3.2 Ribbed Wall 0.3 m Pipe A

The TDR data for the 0.3 m ribbed wall pipe are shown in Figure 5-20 with the corresponding gage data. The calculated shock pressure based on this TOA data can be seen in Figure 5-21. The peak pressure data available has been plotted for the 0.3 m ribbed wall pipe. The conclusions are the same as stated for the 0.3 m smooth wall pipe. In addition to the flatpac

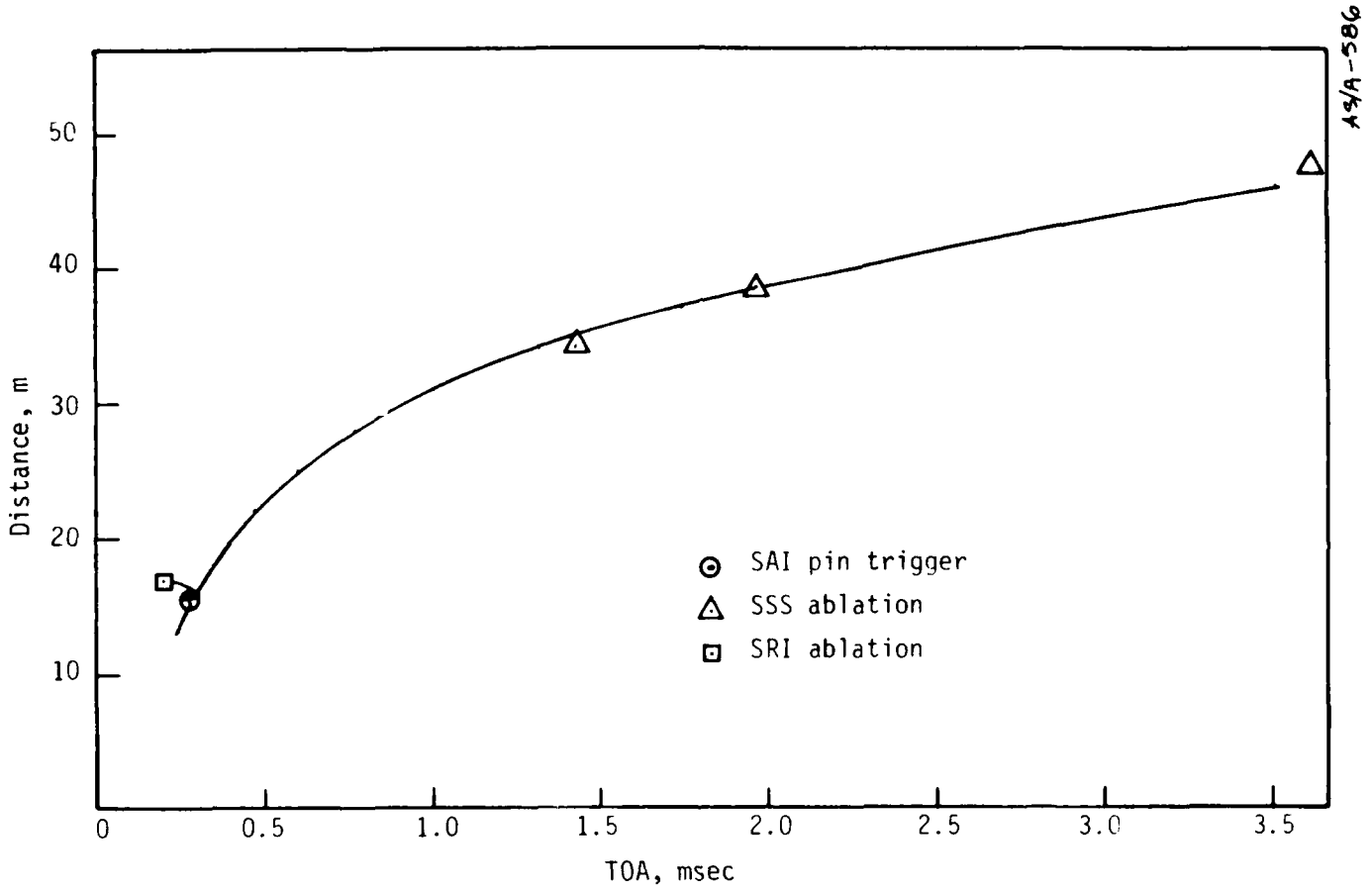

Figure 5-18. TOA data, 0.3 m smooth wall pipe.

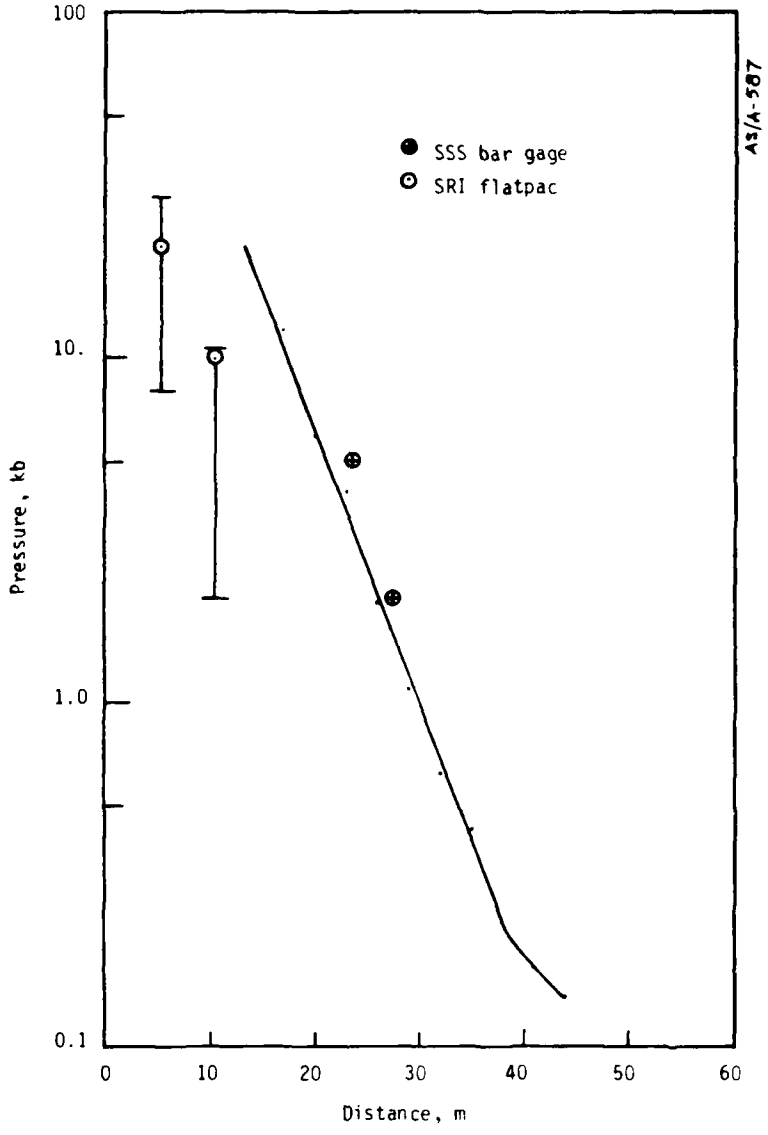

Figure 5-19. Calculated Hugoniot pressure vs distance compared to gage peak pressure data, 0.3 m smooth wall pipe.

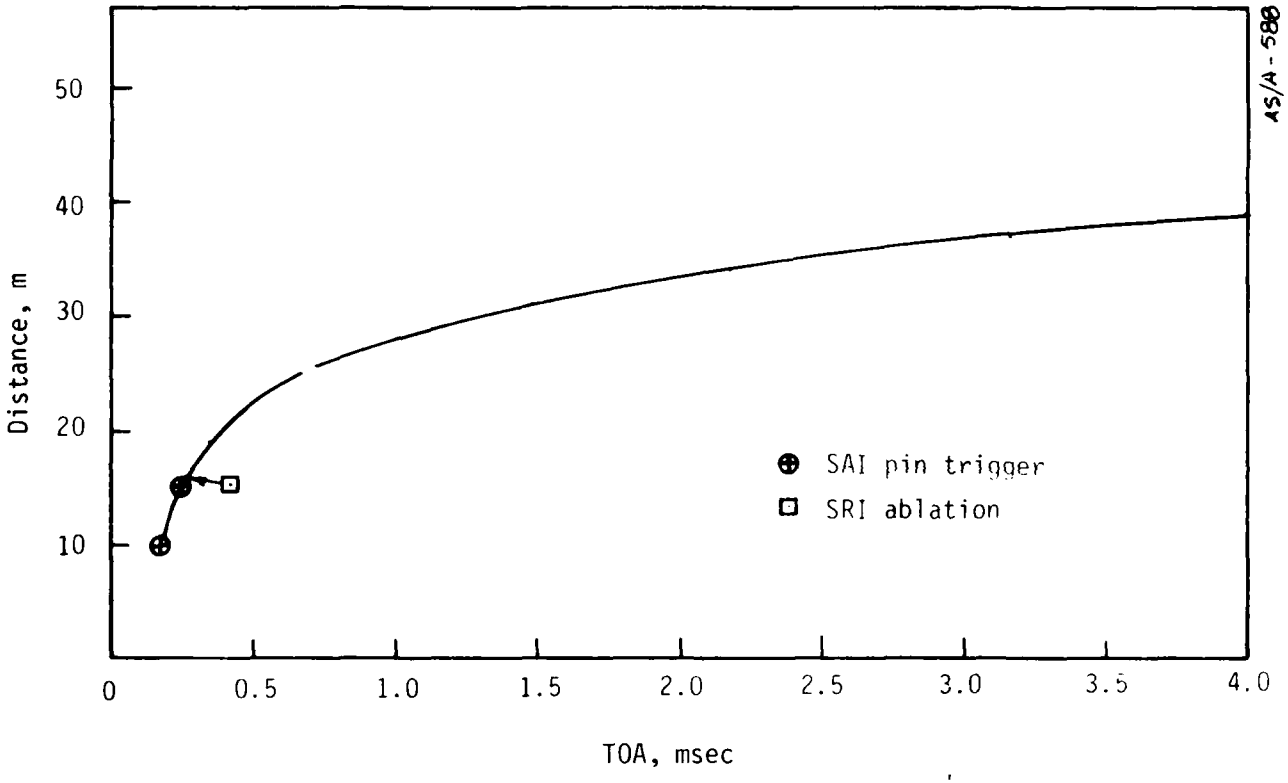

Figure 5-20. TOA data, 0.3 m ribbed wall pipe.

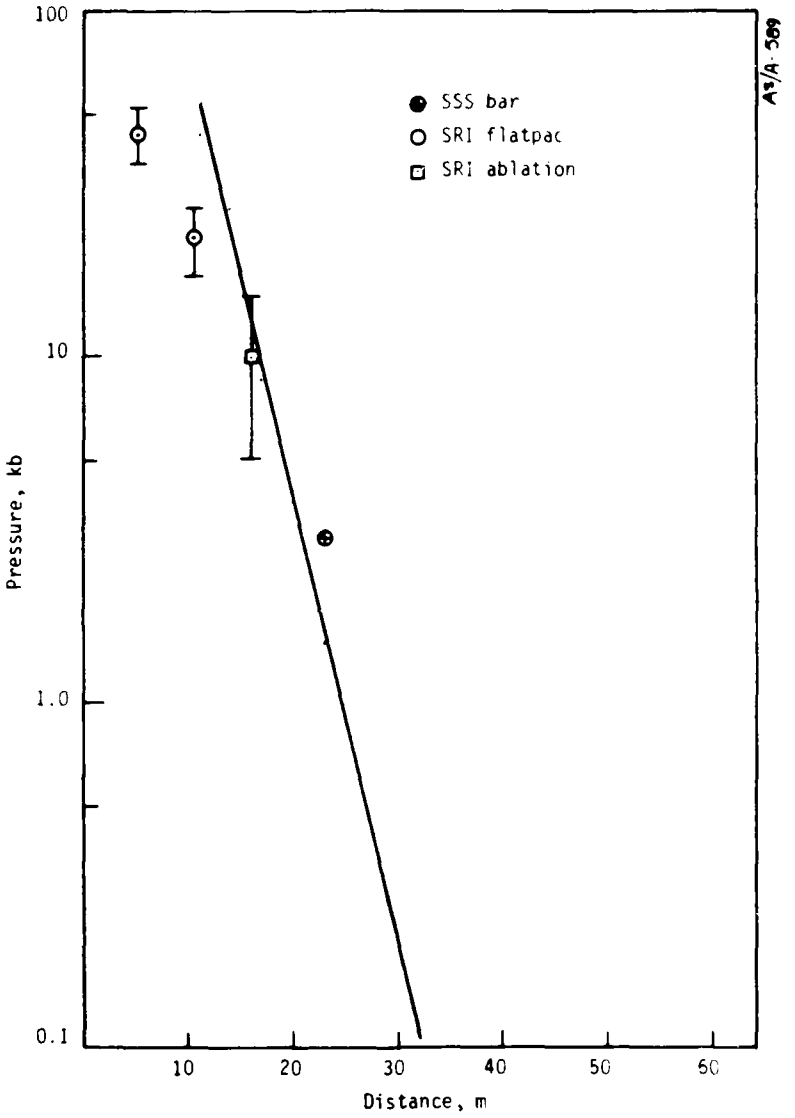

Figure 5-21. Calculated Hugoniot pressure vs distance compared to gage peak pressure data, 0.3 m rib wall pipe.

and bar gage peak pressure, the peak pressure measured by an SRI Mangagin ablation gage agrees quite well with the calculated Hugoniot pressure.

5.3.3 Water-Filled 0.3 m Pipe C

Remember that for the purpose of studying an alternate ablator, a third 0.3 m pipe containing approximately 7.5 cm of water was fielded in the HYBLA GOLD experiment. The TOA data available in the 0.3 m pipe C are shown in Figure 5-22, including the individual gage data. The apparent discrepancy between the TDR data and individual gage data has not been resolved. It is interesting to note, however, that this region is immediately behind the pipe section in which the water is located. Since the TDR cables are above the water line, and the measurement is continuous, it is thought that these are the more valid data in the water filled pipe. The calculated shock pressure for this 0.3 m pipe is depicted in Figure 5-23. There is reasonable agreement between the measured peak pressure data and the calculated shock pressure.

5.3.4 Comparison of 0.3 m Pipes

No data exists in the initial region where the 0.3 m pipes were all the same to check the similarity in the starting conditions for the pipe flow. It is of some interest, however, to note the data provided by the SRI flatpac gages at the pipe wall-grout interface. Table 5-3 (Reference 25) summarizes the data for all three 0.3 m pipes at the first two locations, which are approximately the same range for each pipe. This data tends to support the conclusion that the smooth-walled B pipe did not have the same initial conditions as the other two pipes (A and C). The shock moves slower in this region at a reduced peak pressure. A careful examination of the effects due to the geometry of the zero room might

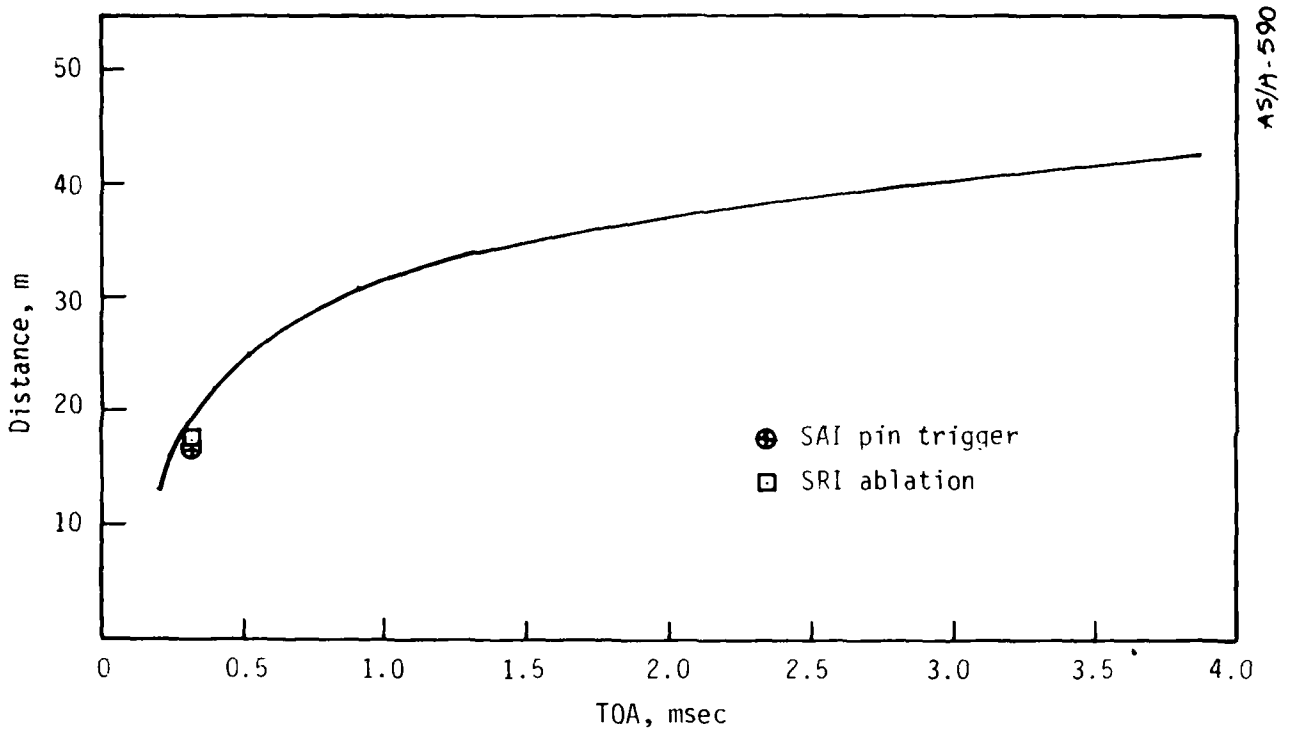

Figure 5-22. TOA data, 0.3 m water pipe.

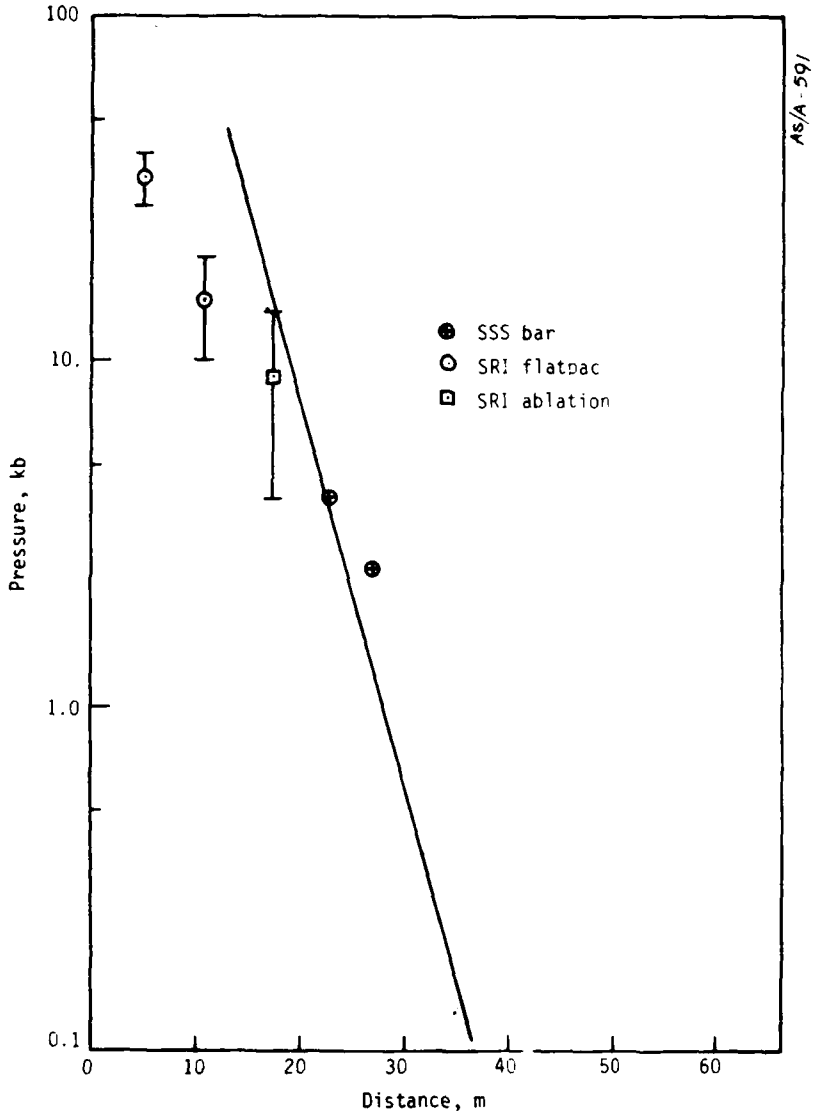

Figure 5-23. Calculated Hugonoit pressure vs distance compared to gage peak pressure data, 0.3 m water pipe.

TABLE 5-3. WALL PRESSURE DATA, 0.3 m PIPES

A Pipe, Ribbed			B Pipe, Smooth			C Pipe, H_2O		
Range, m	TOA, μs	Pressure, GPa	Range, m	TOA, μs	Pressure, GPa	Range, m	TOA, μs	Pressure, GPa
5.3	132	4.4 ± 0.8	5.3	152	1.6 ± 0.8	5.3	132	3.4 ± 0.6
10.4	216	2.2 ± 0.5	10.1	~250	1.0 + 0.0 - 0.8	10.9	198	1.5 ± 0.5

substantiate this conclusion. Since the A and C pipes are located in corners of the zero room, it has been postulated that the main shock and reflected shocks in the corners have converged to produce different driving conditions for the 0.3 m pipes. Neglecting this apparent discrepancy in driving conditions, the pressure attenuation in the 0.3 m pipes is of interest in evaluating the utility of various ablators and wall materials.

The calculated shock pressures from Figures 5-19, 5-21 and 5-23 are displayed in Figure 5-24. The following observations are made based on these curves:

- Pipes A (rib) and C (water) have similar initial driving conditions at ranges < 15m
- The attenuation in pipes A and C are very similar; if the ribbed pipe was offset by 3-5 m, the pressure attenuation would be nearly the same for these two alternate ablator pipes
- Even though the driving conditions are dissimiliar, the B (smooth) pipe appears to have a lesser pressure attenuation rate than the other two pipes at pressures less than a few kilobars
- All three pipes display a trend toward constant pressure flow conditions at ranges greater than 40 m

5.4 RESULTS OF SCALING PHENOMENA INVESTIGATION

As previously noted, three different size smooth wall pipes were fielded to investigate the scaling laws associated with the ablation dominated flow. Insufficient data were obtained to describe the pressure attenuation in the 0.15 m pipe. The ground shock from the expanding

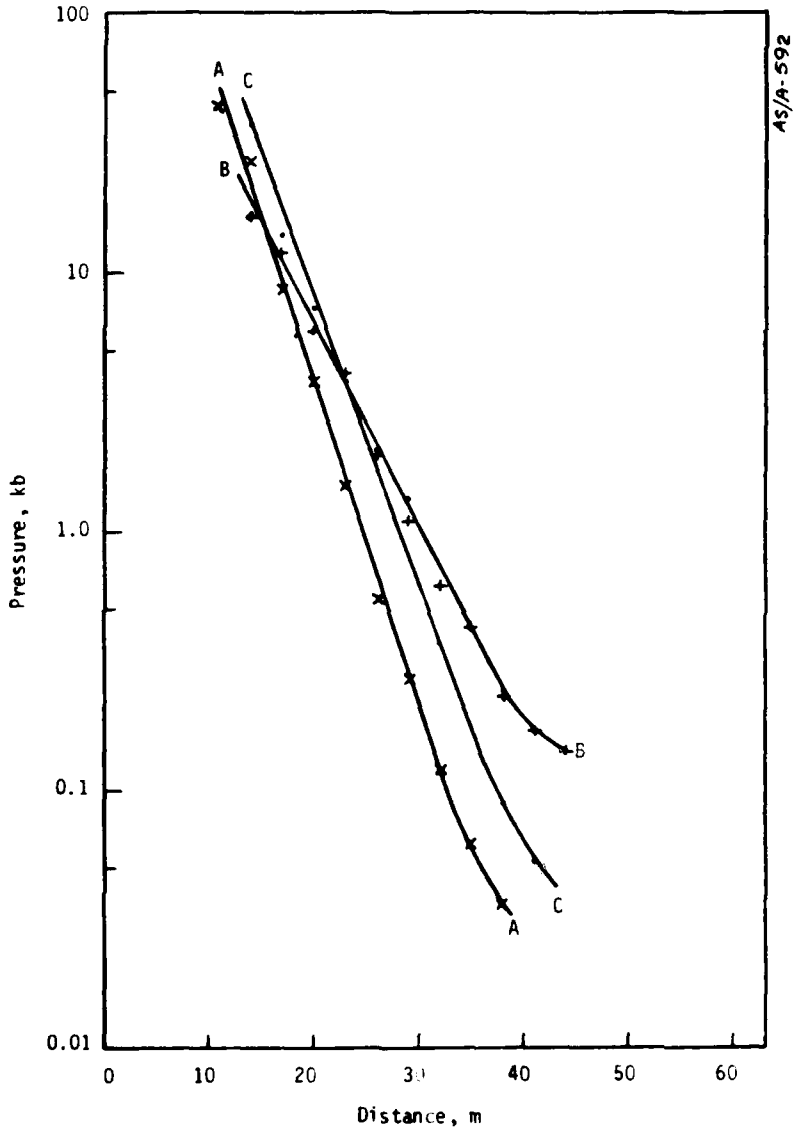

Figure 5-24. Calculated Hugoniot pressure for the three 0.3 m pipes.

0.91 m pipe arrived at the gage locations before the air shock in the 0.15 m arrived, thereby eliminating meaningful data regarding the pipe flow. Some individual gages at ranges < 20 m yielded valid data and are reported in the Project Officers' Report of each individual experimenter (References 25 and 29).

The validity of scaling can be illustrated by plotting the pressure attenuation in the smooth wall pipes as a function of range, where the range is expressed as the ratio of length (range) to pipe diameter (L/D). Figure 5-25 combines the result of Figures 5-7 and 5-19 in the above described manner. Although the two curves do not exactly overlay one another, the slopes (rate of attenuation) appear to be equal for the region L/D < 100. This would indicate that the results indeed do scale for the range of pipe diameters investigated. However, one should be cautioned about implying that these results are valid for significantly larger pipe diameters.

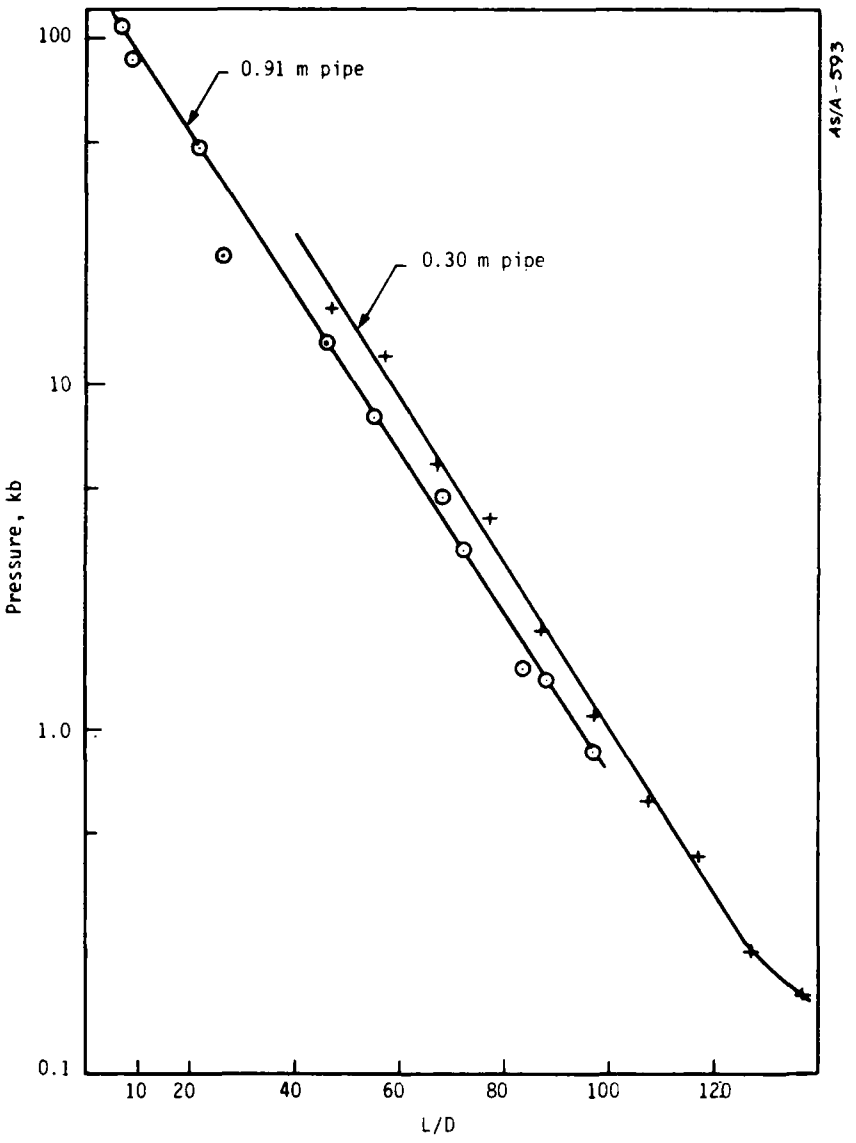

Figure 5-25. L/D scaling for smooth wall pipes.

SECTION 6

CONCLUSIONS AND RECOMMENDATIONS

The HYBLA GOLD experiment satisfied most of the original objectives. The final experiment design provided for the decoupling of the two basic plasma flow loss mechanisms, venting and wall ablation. Useful data were obtained for developing and validating instrumentation which might be required in future underground nuclear tests. In general, the instrumentation fielded to measure shock TOA, plasma static pressure versus time, and the shock front profile were successful. Although the wall ablation information obtained is somewhat difficult to interpret, it did provide sufficient data to establish upper bounds. The instrumentation systems designed to provide pipe wall expansion versus time were the least successful. However, since both systems employed were in the development stage, some useful information was obtained regarding the deficiencies and the corrective actions needed, which is valuable for future test applications.

The data obtained in the HYBLA GOLD experiment has already been used to develop new empirical models of the plasma flow. These models have been used in the current assessment of the survivability and vulnerability of the MX continuous buried trench concept. Specifically, a new empirical ablation model has been formulated. Since the observed attenuation of the maximum pressure in the plasma flow was more rapid than

originally predicted, this new model is one approach to achieving closer agreement between the calculated and measured pressure attenuation for the HYBLA GOLD experiment.

The effectiveness of ribs and alternate ablators was qualitatively evaluated. The test results would indicate that the rib wall pipe and water pipe were more effective flow attenuators than the smooth wall pipe at pressures less than 5 kb. Examination of the available TOA data in the 0.3 m pipes indicates that the water pipe was the most effective attenuator and the smooth-wall pipe was the least effective attenuator.

The results of HYBLA GOLD were inconclusive regarding the scaling issue. As discussed in the previous section, the pressure attenuation in the 0.3 m and 0.91 m smooth wall pipes appears to scale in a reasonable manner for $L/D \leq 100$. This does not imply that scaling laws will be valid for much larger diameter pipes (i.e., the MX trench) at distances greater than those observed.

These conclusions have been based primarily on peak pressure and TOA data without addressing some problems that exist in the data interpretation. The most important unresolved discrepancy is the plasma pressure profile (S^3 bar gage) and the resulting pressure pulses (SRI and SLA) measured at the pipe wall grout interface.

The slow rise times of the S^3 measured signals are not indicative of classical shock fronts. Gage anomalies might explain this problem, however, other measurements also observed long rise times. Laboratory experiments would be useful in understanding the importance of emplacement and operation of the bar gage system in a hostile environment, and the theory of wave propagation in a rod. Further details may be found in

Reference 27. It is possible that the bar gage profiles are correct, and the one-dimensional well-mixed flow models of the predictive theory are not appropriate. The data do not suggest a steadily attenuating waveform propagating with a relatively consistent character.

In addition, the disagreements among the results obtained by various experimenters have not been explained. The in-pipe pressure profiles (KSC and S^3) and the interface pressure profiles (SRI and SLA) differ substantially and cylindrical calculations of the in-pipe profile being transmitted through the pipe wall cannot resolve these differences. An indirect iterative calculational technique has been suggested by SRI (Reference 25) as a possible means to resolve uncertainties associated with the plasma pressure profile. These calculations would utilize the constitutive models for concrete and grout which were formulated during post-HYBLA GOLD experiments conducted at SRI.

The validity of applying the usual strong shock relationships to calculate the plasma shock pressure, based on measurements of shock velocity, may be questioned because of the uncertainty in our knowledge of the ambient gas conditions. For HYBLA GOLD, reasonable guesses have been made as to the temperature, pressure, and moisture content of the air ahead of the shock. Although no measurements were made, the uncertainties present in the data analysis indicate the need for such data in any future experiments.

Several research suggestions for future test instrumentation development have been made in the individual experimental Project Officers' Reports. In general, this author agrees with the proposed

research, especially regarding noise analysis and reduction, and new pressure measurement systems. This includes the recording equipment necessary to compliment the piezoresistant transducers themselves.

REFERENCES

1. Knowles, C. P., "A Discussion of Underground Nuclear Testing for the MX Trench Environment," R&D Associates Report RDA-TR-104804-001, March 1977.

2. Christensen, LCDR C., (1977) Private Communications, Field Command Defense Nuclear Agency.

3. Austin, M.G., "HYBLA GOLD SOC Calculations," Lawrence Livermore Laboratory memorandum UCON 77-73, 26 August 1977.

4. Knowles, C. P., (1977) Private Communication, R&D Associates.

5. Keller, C. F., Fisher, K. and Johnson, W., "2-D and 3-D Problems for HYBLA GOLD," Los Alamos Scientific Laboratory J-15 Quarterly Report to DNA -- April/June 1977, 26 July 1977.

6. Stockton, J. R., "HYBLA GOLD Configuration Meeting," R&D Asociates letter to Field Command DNA, 25 March 1977.

7. Duff, R. (2977) Private Communication, Systems, Science and Software.

8. Gage, Major D. (1977) Private Communications, Air Force Space and Missile Systems Organization.

9. Christensen, LCDR C., "HYBLA GOLD," Field Command, DNA memorandum, 20 May 1977.

10. Eilers, D. D., "Proposal for TDR Measurements on HYBLA GOLD," Los Alamos Scientific Laboratory Proposal No. P-762, February 1977.

11. "Summary of Sandia Participation -- HYBLA GOLD," Sandia Laboratories, Albuquerque letter to Field Command DNA, 23 February 1977.

12. "Proposal to Design and Field Instrumentation for Diagnostic Measurements on HYBLA GOLD," Systems, Science and Software Proposal No. P-77-8610263, 7 January 1977.

13. Sites, K. R., "Debris Detectors," Science Applications letter to Systems, Science and Software, 31 May 1977.

14. Keough, D. D. and DeCarli, P. S., "Stress and Ablation Measurements on HYBLA GOLD," Stanford Research Institute Proposal No. PYU 77-003, 17 January 1977.

15. Keough, D. D., "Stress and Ablation Measurements on HYBLA GOLD," SRI Bimonthly Progress Report to DNA, 31 May 1977.

16. DeCarli, P. S., "Stress and Ablation Measurements on HYBLA GOLD," SRI Bimonthly Progress Report to DNA, 31 July 1977.

17. "Instrumentation Support for HYBLA GOLD Event," KAMAN Sciences Corporation Technical Proposal No. K6-7-56-1001, 3 February 1977.

18. "Microwave Guide Instrumentation for HYBLA GOLD," TRW Unsolicited Proposal No. 31551.0 for DNA, 14 February 1977.

19. Liebermann, P., (1977) Private Communication, TRW, Inc.

20. Sites, K. R., (1977) Private Communication, Science Applications, Inc., Las Vegas, Nevada.

21. Plimpton, J. D. and Miller, H. M., "Pre-HYBLA GOLD HE Test," Sandia Laboratories Report to Field Command, Defense Nuclear Agency, 22 February 1978.

22. Plimpton, J. D., "Preliminary Calculations for the Pre-HYBLA GOLD HE Test," Sandia Laboratories Letter to Field Command, Defense Nuclear Agency, 14 June 1977.

23. Whitener, J., (1977) Private Communication, R&D Associates.

24. Scott, L., "Grounding and Shielding Recommendations for Underground Nuclear Tests and Other Simulators of Nuclear Environments," Science Applications, Inc. Report SAI-77-015-CS, 2 December 1977.

25. DeCarli, P. S., et. al, "Stress and Ablation Measurements on HYBLA GOLD," SRI International, August 1978, prepared for DNA under Contract DNA 001-77-C-0161 (to be published).

26. Christensen, LCDR C. L., "HUSSAR SWORD SERIES, HYBLA GOLD EVENT, Test Execution and Preliminary Results Report," DNA POR 6970, 8 February 1979.

27. Coleman, P. L. and Kratz, H. R., "HYBLA GOLD Measurements: Plasma Pressure, Ablation, and Pipe Expansion Results," Systems, Science and Software, DNA POR 6971, November 1978.

28. Sites, K. R. and Millonzi, L. A., "HUSSAR SWORD SERIES, HYBLA GOLD EVENT, Instrumentation Support," Science Applications, Inc., Las Vegas, Nevada, DNA POR 6972, 26 June 1978.

29. Dolce, S. and Plimpton, J. D., "HYBLA GOLD Final Report," Sandia Laboratories, Albuquerque letter report to Defense Nuclear Agency, 2 October 1978.

30. Hollister, H., et. al, "HUSSAR SWORD Series, HYBLA GOLD Event, HYBLA GOLD Results," KAMAN Sciences Corporation, Colorado Springs, Colorado, DNA POR 6975, 31 December 1978.

31. Lieberman, P. and Freeman, D., "Radial Wall Displacement History by Microwave Waveguide Measurements, "TRW Final Report on Project HYBLA GOLD, January 1978.

DISTRIBUTION LIST

DEPARTMENT OF DEFENSE

Defense Technical Information Center
12 cy ATTN: TC

Director
Defense Nuclear Agency
ATTN: STNA
ATTN: STRA
2 cy ATTN: STSP
4 cy ATTN: TITL

Field Command
Defense Nuclear Agency
ATTN: FCTMOF
ATTN: FCTMD
ATTN: FCTMC
ATTN: FCPR

Field Command
Defense Nuclear Agency
Livermore Branch
ATTN: FCPRL

Field Command
Defense Nuclear Agency
Los Alamos Branch
ATTN: FCPRA

Field Command Test Directorate
Test Construction Division
Defense Nuclear Agency
ATTN: FCTC

Undersecretary of Def for Rsch & Engrg
Department of Defense
ATTN: Strategic & Space Sys (OS)

DEPARTMENT OF THE ARMY

Harry Diamond Laboratories
Department of the Army
ATTN: Technical Library
ATTN: DRXDO-NP

Deputy Chief of Staff for Rsch Dev & Acq
Department of the Army
ATTN: DESRADA/CSM/N

Assistant Secretary of the Army
Research, Development and Acq
ATTN: Asst Secy for R&D

U.S. Army Engr Waterways Exper Station
ATTN: D. Day

DEPARTMENT OF THE NAVY

Office of the Chief of Naval Operations
ATTN: OP981

Naval Surface Weapons Center
ATTN: Technical Library
ATTN: Code WA 501

DEPARTMENT OF THE NAVY (Continued)

Asst Secretary of the Navy
Research & Development
ATTN: Asst Secy for R&D

DEPARTMENT OF THE AIR FORCE

Deputy Chief of Staff
Research & Development
Department of the Air Force
ATTN: RDQSM

Air Force Weapons Laboratory
Air Force Systems Command
ATTN: SUL Technical Library
2 cy ATTN: NT

Ballistic Missile Office
Air Force Systems Command
2 cy ATTN: MNNH

Research & Development
Department of the Air Force
ATTN: Asst Secy for R&D

DEPARTMENT OF ENERGY CONTRACTORS

Los Alamos National Scientific Lab
ATTN: J-DO, J. McQueen
ATTN: J-15, C. Keller
ATTN: Technical Library

Lawrence Livermore National Lab
ATTN: Technical Library

Sandia National Laboratories
ATTN: 1100, C. Broyles
ATTN: 1124, P. Nelson
ATTN: 1111, S. Dolce
ATTN: 1110, J. Kennedy
ATTN: 1112, J. Plimpton
ATTN: Technical Library

Sandia National Laboratories
Livermore Laboratory
ATTN: Technical Library

Nevada Operations Office
ATTN: Technical Library

DEPARTMENT OF DEFENSE CONTRACTORS

General Electric Company—TEMPO
ATTN: DASIAC

Kaman Sciences Corp
ATTN: F. Shelton
ATTN: F. Rich

Science Applications, Inc
ATTN: R. Miller

DEPARTMENT OF DEFENSE CONTRACTORS (Continued)

SRI International
ATTN: D. Keogh

Science Applications, Inc
ATTN: R. Parkinson

Systems, Science & Software, Inc
ATTN: C. Dismukes
ATTN: P. Coleman

Pacifica Technology
ATTN: G. Kent

Merritt CASES, Inc
ATTN: J. Merritt

R & D Associates
ATTN: J. Lewis
ATTN: Technical Library
ATTN: P. Haas

Mission Research Corp
ATTN: C. Longmire
ATTN: V. Vanlint

DEPARTMENT OF DEFENSE CONTRACTORS (Continued)

Science Applications, Inc
ATTN: K. Sites

TRW Defense & Space Sys Group
ATTN: P. Lieberman

Electromechanical Sys of New Mexico, Inc
ATTN: R. Shunk

H-Tech, Inc
ATTN: Hartenbaum

Science & Engineering Associates, Inc
ATTN: J. Stockton

Pacific-Sierra Research Corp
ATTN: H. Brode

Physics International Company
ATTN: R. Miller

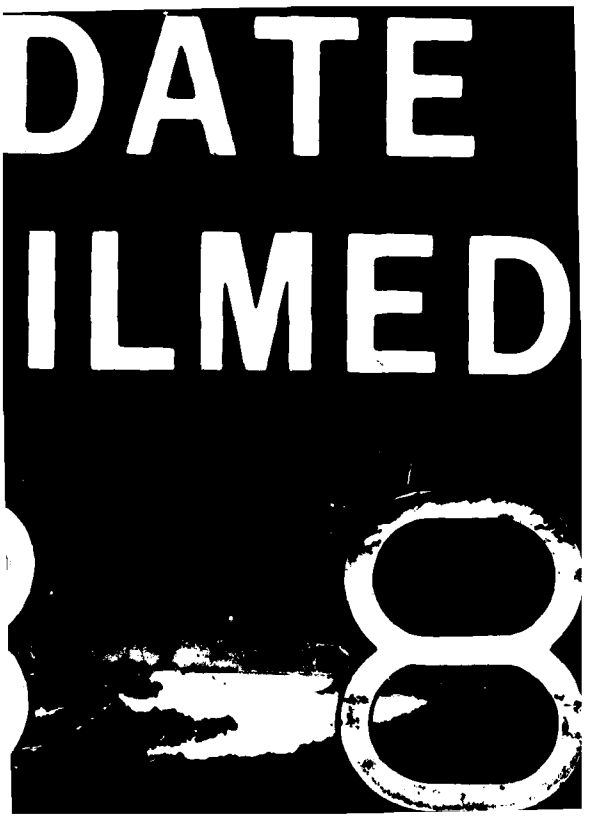
DATE
ILMED
8